

2013

# Novel Regulation of the Cell Cycle During Cell Fate Decisions in the Central Nervous System

Dorota D. Lubanska  
*University of Windsor*

Follow this and additional works at: <http://scholar.uwindsor.ca/etd>

---

## Recommended Citation

Lubanska, Dorota D., "Novel Regulation of the Cell Cycle During Cell Fate Decisions in the Central Nervous System" (2013). *Electronic Theses and Dissertations*. Paper 4903.

This online database contains the full-text of PhD dissertations and Masters' theses of University of Windsor students from 1954 forward. These documents are made available for personal study and research purposes only, in accordance with the Canadian Copyright Act and the Creative Commons license—CC BY-NC-ND (Attribution, Non-Commercial, No Derivative Works). Under this license, works must always be attributed to the copyright holder (original author), cannot be used for any commercial purposes, and may not be altered. Any other use would require the permission of the copyright holder. Students may inquire about withdrawing their dissertation and/or thesis from this database. For additional inquiries, please contact the repository administrator via email ([scholarship@uwindsor.ca](mailto:scholarship@uwindsor.ca)) or by telephone at 519-253-3000ext. 3208.

**Novel Regulation of the Cell Cycle During Cell Fate Decisions  
in the Central Nervous System**

By

**Dorota Lubanska**

A Dissertation  
Submitted to the Faculty of Graduate Studies  
through the Department of Biological Sciences  
in Partial Fulfillment of the Requirements for  
the Degree of Doctor of Philosophy at the  
University of Windsor

Windsor, Ontario, Canada

2013

© 2013 Dorota Lubanska

**Novel Regulation of the Cell Cycle During Cell Fate Decisions  
in the Central Nervous System**

by

**Dorota Lubanska**

APPROVED BY:

---

Susan Meakin, External Examiner

University of Western Ontario

---

Siyaram Pandey

Department of Chemistry and Biochemistry

---

Andrew Hubberstey

Department of Biological Sciences

---

Andrew Swan

Department of Biological Sciences

---

Lisa A. Porter, Advisor

Department of Biological Sciences

## DECLARATION OF CO-AUTHORSHIP / PREVIOUS PUBLICATION

### I. Co-Authorship Declaration

I hereby declare that this thesis incorporates material that is result of joint research, as follows:

**Chapter 2** incorporates the outcome of a joint research undertaken in collaboration with Brenna Market-Velker under the supervision of professor Porter. In all cases, the key ideas, primary contributions, experimental designs, data analysis and interpretation, were performed by the author, and the contribution of co-authors was primarily through performing preliminary experiments to the project including single repeat of western blot on tumour tissues and PC12 neuronal differentiation assay.

I am aware of the University of Windsor Senate Policy on Authorship and I certify that I have properly acknowledged the contribution of other researchers to my thesis, and have obtained written permission from each of the co-author(s) to include the above material(s) in my thesis.

I certify that, with the above qualification, this thesis, and the research to which it refers, is the product of my own work.

### II. Declaration of Previous Publication

This thesis includes one original paper that have been previously submitted for publication in peer reviewed journals, as follows:

Thesis Chapter	Publication title/full citation	Publication status
<i>Chapter 2</i>	The Cyclin-Like Protein Spyl Regulates Growth and Division Characteristics of the CD133+ Population in Human Glioma.	<i>submitted, in review</i>

I declare that, to the best of my knowledge, my thesis does not infringe upon anyone's copyright nor violate any proprietary rights and that any ideas, techniques, quotations, or any other material from the work of other people included in my thesis, published or otherwise, are fully acknowledged in accordance with the standard referencing practices. Furthermore, to the extent that I have included copyrighted material that surpasses the bounds of fair dealing within the meaning of the Canada Copyright Act, I certify that I have obtained a written permission from the copyright owner(s) to include such material(s) in my thesis.

I declare that this is a true copy of my thesis, including any final revisions, as approved by my thesis committee and the Graduate Studies office, and that this thesis has not been submitted for a higher degree to any other University or Institution

## ABSTRACT

Mitotically active cells at the sites of neurogenesis and primitive cells of the sympathetic nervous system are speculated to act as a source of stem-like tumor initiating cells (TICs) in neural cancers like glioma and neuroblastoma. Understanding how normal neural stem and progenitor cells regulate their growth and differentiation decisions throughout life is of high priority. Spy1 (Speedy, Spdya, RINGO) is a unique cyclin-like protein that enhances proliferation by activating the cyclin dependent kinase 2 (CDK2) and promoting the degradation of the CDK inhibitor p27<sup>Kip1</sup>. Spy1 levels are tightly regulated during developmental processes and Spy1 upregulation has been reported in several types of cancer including human glioma. Spy1 effectors, CDK2 and p27<sup>Kip1</sup>, play a regulatory role in many developmental events including neurogenesis and these effectors are aberrantly regulated in several aggressive forms of cancer. My study sought to investigate the role of Spy1 in regulating proliferation, self-renewal and differentiation processes of neural progenitors and to determine the implications of this protein in neural cancers. My work demonstrates that Spy1 is an important driver of the CD133+ brain tumour initiating cell (BTIC) population. Spy1 controls the ability of BTICs to symmetrically divide and the amplification of the *SPDYA* gene loci correlates with poor patient prognosis. We show that Spy1 is expressed at high levels in neurogenic regions of the adult brain and the overexpression of Spy1 significantly increases cell proliferation parameters including the number and longevity of neurospheres. These data demonstrate for the first time that the Spy1/RINGO family plays an important role in neural fate decisions and that overexpression of Spy1 is a driving factor in specific forms of neural cancer.

## **DEDICATION**

*This work is dedicated to my loving family. To my father who has always stimulated my fascination and interest in science and to my mother for her wisdom and inspiration. I dedicate this dissertation to my brother who has been always truly interested in my work and taught me how to explain complicated biology to computer science people. To my best friend Alicia who has always been my biggest cheerleader and to Rebecca for her supportive friendship, companionship and positive energy that made difficult times easier. Finally, I dedicate this work to my husband who has always challenged me to fulfill my dreams and has been my strength and motivation every step of the way.*

## ACKNOWLEDGEMENTS

*I would like to express my deepest gratitude to my advisor, Dr. Lisa Porter for her valuable expertise and guidance, continuous motivation and enthusiasm. Thank you so much for all the freedom, enlightening discussions and inspiration. I have been extremely lucky to have you as my supervisor.*

*I would like to extend my sincere thanks and appreciation to the committee members, Drs. A. Hubberstey, A. Swan and S. Pandey for their time, expertise and valuable advice through the course of this study. I thank Drs. M. Crawford, J. Hudson, D. Donoghue, B. Welm for plasmids or equipment use, Drs. L. Chen for the PC12 cell line and J. Rutka for U251 cells. J. Ritchie and A. Malysa for statistical analysis and K. Matthews and R. Hepburn for technical assistance. I extend special thanks to J. Maimaiti for the lentivirus production. I sincerely appreciate the time and feedback provided by Drs. D. Cavallo-Medved and A. Swan on the Chapter 2 and I thank Dr. Fidalgo da Silva for a valuable input. I thank the Brain Tumour Tissue Bank, and its funding agency the Brain Tumour Foundation of Canada, for donation of brain tumour tissue for this study as well as Children's Oncology Group for glioblastoma cell lines provided. I would like to thank my friends and colleagues, Ms. Bre-Anne Fifield, Ms. Rosa Ferraiuolo and Ms. Kaitlyn Matthews, Omar Davis as well as Dr. M. Al Sorkhy, Mrs. J. Dare, Mr. M. Crozier, Ms. Jalili, Ms. N. Lyons, Ms. I. Qemo and Ms. J. Tubman for their feedback, assistance and for making hard work enjoyable. This study is supported by different operating funds in addition to student funding through the Ontario Graduate Scholarship (OGS) program.*



## TABLE OF CONTENTS

• CO-AUTHORSHIP DECLARATION/ <i>PREVIOUS PUBLICATION</i> .....	iii
• ABSTRACT.....	v
• DEDICATION.....	vi
• ACKNOWLEDGEMENTS.....	vii
• LIST OF TABLES.....	xiii
• LIST OF FIGURES.....	xiv
• <i>LIST OF APENDICES</i> .....	xvi
• LIST OF ABBREVIATIONS/SYMBOLS.....	xvii
• CHAPTER 1: GENERAL INTRODUCTION	
• <i>Cell cycle regulation over cell fate decisions</i> .....	2
• <i>Putative function of G1 phase cyclins as fate determinants during neural development</i> .....	6
• <i>Embryonic stem cells (ESCs) and G1 phase regulators</i> .....	6
• <i>G1 phase and the adult neural stem cell (NSC) regulation</i> .....	8
• <i>G1 phase regulatory network in neural fate decisions</i> .....	9
• <i>D-type Cyclins in neural fate</i> .....	11
• <i>E-type Cyclins in neural fate</i> .....	12
• <i>Cell cycle regulation over mode of division during neural development</i> .....	16
• <i>D-type Cyclins in mode of division</i> .....	17
• <i>E-type Cyclins in mode of division</i> .....	18
• <i>Cell cycle inhibitors in neural development</i> .....	23
• <i>p21<sup>Cip1</sup></i> .....	23
• <i>p27<sup>Kip1</sup></i> .....	24

- *16<sup>Ink4</sup>* .....25
- *Brain tumours*.....26
- *Brain tumour subtypes and complexity*.....26
- *Molecular multiplicity of brain cancer*.....29
- *Classical subtype*.....29
- *Mesenchymal subtype*.....30
- *Proneural subtype*.....31
- *Neural subtype*.....32
- *The role of G1 phase in neural tumourigenesis*.....33
- *D-type Cyclins and gliomagenesis*.....33
- *Regulation of D-type Cyclins in glioma*.....33
- *Cyclin D1 and glioma invasion*.....35
- *Cyclin D and brain tumour initiating cells (BTIC)*.....37
- *Cyclin E1 and gliomagenesis*.....40
- *Cyclin E1 and genetic instability in glioma*.....40
- *Impaired degradation of Cyclin E1 in glioma*.....41
- *Cyclin E1 and p27<sup>Kip1</sup> in neural tumourigenesis*.....42
- *Cyclin E1 and BTIC*.....44
- *Spy1 family of cell cycle regulators*.....47
- *Speedy/RINGO family and human Spy1*.....47
- *Spy1-mediated cell cycle regulation and CDK2 substrate specificity*.....51
- *Spy1, DNA damage response and apoptosis*.....53
- *The role of Spy1 in normal development and tumourigenesis*.....54
- **HYPOTHESES AND OBJECTIVES**.....57

- REFERENCES.....58
- CHAPTER 2: THE CYCLIN-LIKE PROTEIN SPY1 REGULATES GROWTH AND DIVISION CHARACTERISTICS OF THE CD133+ POPULATION IN HUMAN GLIOMA
- INTRODUCTION.....76
- EXPERIMENTAL PROCEDURES.....79
- *Animals*.....79
- *Cell lines*.....79
- *Plasmid*.....79
- *Lentivirus production and infection*.....80
- *Protein isolation from Brain Tumour tissues*.....81
- *qRT-PCR*.....81
- *Tissue Microarray (TMA)* .....81
- *Primary cell harvest & Neurosphere Assays* ..... 82
- *Magnetic bead sorting*..... 83
- *Cell pair assay and immunofluorescence*..... 83
- *Statistical analysis*..... 84
- RESULTS
- *Spy1 Protein Levels are Elevated in Multiple Types of Glioma and Correlate with Increasing Tumour Grade*.....85
- *Amplification of the SPDYA Loci Correlates with Poor Patient Prognosis*.....97
- *Knockdown of Spy1 Reduces Proliferation and Stemness Properties in Human Glioma*.....98
- *Spy1 Regulates Stemness Properties of the CD133+ Glioma Population*.....102
- *Downregulation of Spy1 is Critical for Specific Differentiation Decisions*....108
- *Symmetric Division of CD133+ U87 Glioma Cells Relies Uniquely on Spy1117*

- DISCUSSION ..... 124
- REFERENCES..... 128
- CHAPTER 3: THE ROLE OF SPY1 IN ADULT NEUROGENESIS
- INTRODUCTION.....135
- EXPERIMENTAL PROCEDURES ..... 138
- *Animals*..... 138
- *Immunohistochemistry* ..... 138
- *Protein isolation from brain tissues* ..... 139
- *Western blotting* ..... 139
- *qRT-PCR*.....140
- *Statistical analysis*.....140
- RESULTS
- *Spy1 protein levels are tightly regulated during neural progenitor lineage commitment*.....141
- *Spy1 protein localizes to the neurogenic regions of the mammalian brain*....144
- *Spy1 is expressed in cells within the rostral migratory stream and SGZ of the hippocampus*.....148
- *Spy1 positive cells in the SVZ express markers of B-type cell subpopulation*.151
- DISCUSSION.....154
- REFERENCES.....158
- CHAPTER 4: THE ROLE OF SPY1 IN DIFFERENTIATION AND SELF-RENEWAL OF NEUROBLASTOMA
- INTRODUCTION.....163
- EXPERIMENTAL PROCEDURES.....166
- *Generation of stable cell lines*.....166
- *Differentiation assays*.....166

- *BrdU assay and fluorescent detection*.....167
- *Prolifeartion kinetics*.....167
- *MTT assay*.....168
- *Neurosphere formation assay*.....168
- *Western blotting*.....169
- *Immunoprecipitation and CDK2 kinase assay*.....169
- *qRT-PCR*.....170
- RESULTS
- *Endogenous levels of Spy1 are downregulated during Retinoic Acid-induced differentiation in Neuroblastoma*.....171
- *Stable overexpression of Spy1 causes delayed neural differentiation*.....174
- *Spy1 overexpression promotes neural stem cell self renewal in neuroblastoma cells*.....177
- *Spy1 regulation of stemness and neural lineage commitment is controlled by extracellular microenvironment*.....180
- DISCUSSION.....183
- REFERENCES.....186
- CHAPTER 5. FUTURE DIRECTIONS.....190
- REFERENCES.....196
- VITA AUCTORIS ..... 205

## LIST OF TABLES

### CHAPTER 1.

<i>Table 1. Collected data on G1 phase components manipulation during development and in the adult mouse and correlation between lengthening of G1 phase and differentiation</i> .....	15
<i>Table 2. WHO Grading of Tumours of the Central Nervous System.....</i>	28

## LIST OF FIGURES

- CHAPTER 1
- *Figure 1. The eukaryotic cell cycle and regulatory components of G1 phase..* .3
- *Figure 2. The cell cycle changes in ESCs during differentiation.....* 7
- *Figure 3. Cell cycle length and G1 changes during development.....*10
- *Figure 4. The link between cell cycle length and mode of division.....*22
- *Figure 5. Schematic representation of Speedy/RINGO structure and Speedy/RINGO isoforms.....*50
- CHAPTER 2
- *Figure 1. Spy1 Protein is Overexpressed in High-Grade Glioma.....*87
- *Figure 2. Spy1 Levels are Essential for Proliferation and Stem-Like Properties of Human Glioma Cells.....*100
- *Figure 3. Spy1 Expression Plays a Critical Role in the Stemness Properties of the CD133+ BTIC Population.....*104
- *Figure 4. Spy1 Protein Levels are Tightly Regulated During Neural Progenitor Fate ecisions.....*110
- *Figure 5. Spy1 Overexpression Abrogates Neuronal Differentiation and Promotes Neurosphere Clonal Growth.....* 112
- *Figure 6. Spy1 is Critical for Symmetric Division and Self-Renewal of CD133+ Cells.....*119
- *Figure S1. Spy1 protein levels are significantly elevated in patient brain tumour cores and peritumour compared to normal matched tissue.....*89
- *Figure S2. H&E stained sections from Human Normal and Brain Tumour TMA Cores.....*91
- *Figure S3. Immunofluorescent Detection of Spy1 Positive Cells in Human Normal and Brain Tumour TMA Cores.....*93
- *Figure S4. Spy1 is upregulated in malignant grades of OAC and ODG and its amplification correlates with reduced patient survival in ODG.....*95

- *Figure S5. Spyl expression plays a critical role in the stemness properties of the CD133+ BITC populations in diverse glioma cell lines.....*106
- *Figure S6. The SPDYA knockdown accelerates differentiation and decreases neurosphere forming capacity in primary neural cell populations.....*115
- *Figure S7.Spyl Sustains Viability of Glioma Tumourspheres in Long Term Culture and Supports CD133 Expression Upon Growth Factor Withdrawal.....*121
- CHAPTER 3
- *Figure 1. Spyl is tightly regulated in neurogenic regions of the developing brain.....*142
- *Figure 2. Spyl protein localizes to the neurogenic regions of a mammalian brain .....*146
- *Figure 3. Spyl positive populations of neural cells are found in the RMS, SGZ and SVZ of the LVs.....*149
- *Figure 4. Spyl colocalizes with glial and stemness markers in the SVZ .....* 152
- CHAPTER 4
- *Figure 1. Spyl protein levels are tightly regulated during neural progenitor fate decisions.....*172
- *Figure 2. Spyl overexpression abrogates neuronal differentiation.....*175
- *Figure 3. Elevated levels of Spyl protein promote neural progenitor self renew.....*178
- *Figure 4. Spyl regulation of stemness and neural lineage commitment is controlled by extracellular microenviroment.....*181



**LIST OF APENDICES**

APENDIX A. *Detailed protocols*.....198

## LIST OF ABBREVIATIONS/SYMBOLS

CAK.....	Cyclin activating kinase
bFGF.....	basic fibroblast growth factor
BTIC.....	brain tumour initiating cell
CD133.....	Prominin-1
CDK .....	Cyclin dependent kinase
CKI .....	cyclin dependent kinase inhibitor
CNS.....	central nervous system
DG.....	dentate gyrus
DMEM.....	Dulbecco's modified Eagle's medium
E3 .....	ubiquitin protein isopeptide ligase
ECM.....	extracellular matrix
EDTA.....	Ethylenediaminetetraacetic acid
EGF ... ..	epidermal growth factor
EGFR.....	epidermal growth factor receptor
EGFR vIII.....	variant III mutation of EGFR
EGTA.....	ethylene glycol tetraacetic acid
ERK.....	extracellular-signal-regulated kinase
ESC.....	embryonic stem cell
FAK.....	focal adhesion kinase
FBS.....	foetal bovine serum
G0 .....	Gap0
G1.....	Gap1
G2.....	Gap2

*GAP43*.....growth associated protein 43  
*GAPDH*..... Glyceraldehyde 3-phosphate dehydrogenase  
*GBM*.....glioblastoma multiforme  
*gcm*.....glial cell missing  
*GFAP*.....glial fibrillary acidic  
*GMC*.....ganglion mother cell  
*GSK3b*..... glycogen synthase kinase- $\beta$   
*H&E*.....hematoxylin and eosin  
*HBSS*..... Hank's Balanced Salt Solution  
*IDH 1*.....isocitrate dehydrogenase 1  
*Id4*..... Inhibitor of differentiation 4  
*LV*.....lateral ventricle  
*LIF*.....leukemia inhibitory factor  
*LOH*..... loss of heterozygosity  
*MCM2*.....mini chromosome maintenance 2  
*MMP*..... matrix metalloproteinase  
*MOI* ..... multiplicity of infection  
*Msi1*.....Musashi 1  
*MTT*..... 3-(4,5-Dimethylthiazol-2-yl)-2,5-diphenyltetrazolium bromide  
*NEDD4* .....neural precursor cell-expressed developmentally down regulated  
*NF1*.....neurofibromatosis 1  
*NSC*.....neural stem cell  
*NF $\kappa$ B*.....Nuclear Factor kappa-light-chain-enhancer of activated B cells

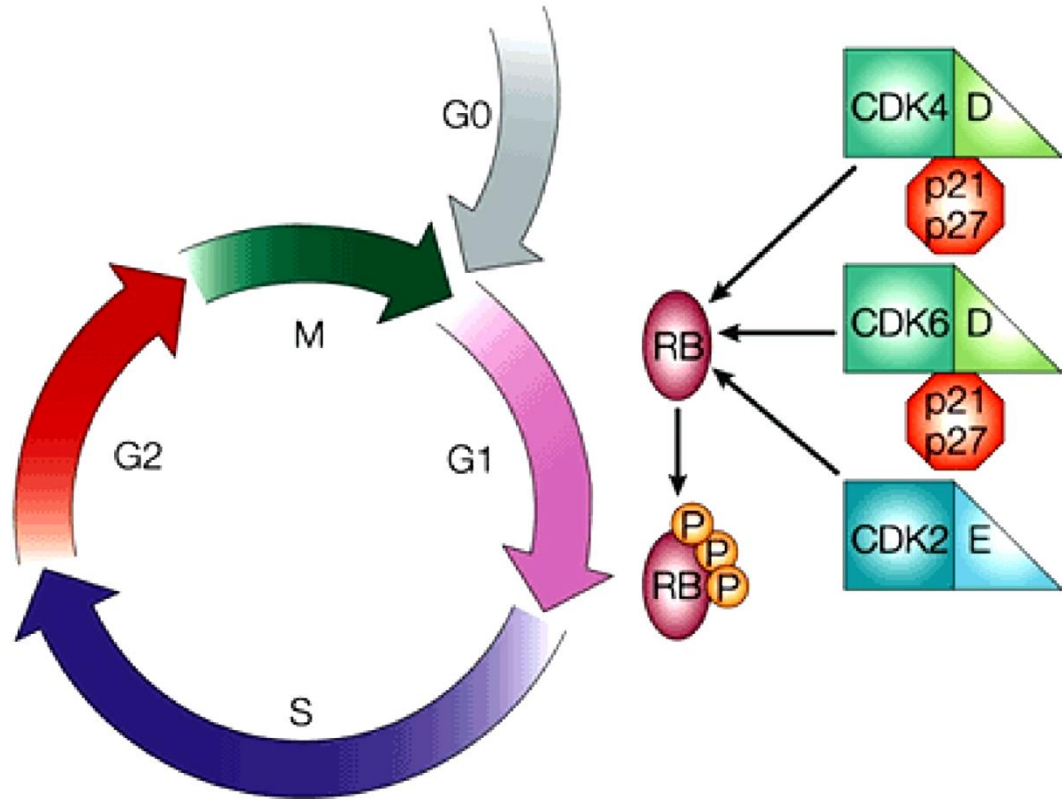
*OSVZ*.....*outer subventricular zone*  
*PAGE*..... *polyacrylamide gel electrophoresis*  
*PARK 2*..... *Parkinson protein 2*  
*PDGF*..... *platelet derived growth factor*  
*PDGFRA*..... *platelet-derived growth factor receptor  $\alpha$*   
*PI3K*..... *phosphatidylinositide 3-kinase*  
*PTEN*..... *phosphatase and tensin homolog*  
*p21*..... *CIP1*  
*p27*..... *KIP1*  
*PBS*.....*phosphate buffered saline*  
*PCR*.....*polymerase chain reaction*  
*pros*.....*Prospero*  
*PEI*..... *polyethylenimine*  
*QRT-PCR*.....*quantitative real time PC*  
*RA*.....*Retinoic Acid*  
*Rb*.....*Retinoblastoma Tumour Suppressor*  
*RINGO* ..... *Rapid Inducer of G2/M progression in Oocytes*  
*RMS*.....*rostral migratory strain*  
*RQ*.....*relative quantification*  
*SCF*.....*Skp1-Cullin1-F-box*  
*SDS*..... *sodium dodecyl sulfate*  
*SGZ*.....*subgranular zone*  
*shRNA*.....*small hairpin RNA*

<i>siRNA</i> .....	<i>small interference RNA</i>
<i>Spy1A</i> .....	<i>Spy1/RINGO A</i>
<i>SVZ</i> .....	<i>subventricular zone</i>
<i>TBST</i> .....	<i>Triss buffered saline and Tween 20</i>
<i>TCGA</i> .....	<i>The Cancer Genome Atlas</i>
<i>TMA</i> .....	<i>tissue micro array</i>
<i>3'UTR</i> .....	<i>3' untraslated regions</i>
<i>Ub</i> .....	<i>ubiquitin</i>
<i>VZ</i> .....	<i>ventricular zone</i>
<i>WT</i> .....	<i>wild type</i>
<i>WHO</i> .....	<i>World Health Organization</i>
<i>X-Spy1</i> .....	<i>Xenopus Spy1</i>

CHAPTER 1  
GENERAL INTRODUCTION

### *Cell Cycle regulation over cell fate decisions*

The cell cycle is the master network behind cell division that includes four distinct phases. Gap phase 1 (G1), DNA replication phase S and Gap phase 2 (G2) constitute the interphase that leads into mitotic division (M). During unfavourable growth conditions cells reside in G0 phase, a quiescent state, in which cells halt progression through S phase, remaining metabolically active and capable of cell cycle re-entry. Each individual stage is regulated by an ordered set of events driving movement from one phase to another. G1 phase represents an important stage capable of processing information from diverse environmental and developmental cues and external and internal stressors. These regulatory signals play a key role in the regulation of both proliferation and differentiation of mammalian progenitors (Orford and Scadden 2008; Salomoni and Calegari 2010; Zhang, Ran et al. 2011). Understanding the subtleties of this phase will reveal essential mechanisms responsible for the balance between stem and progenitor expansion and lineage commitment during development. The interplay between expansion and commitment in neural cells is indispensable for proper maturation of the nervous system. Furthermore, the inability to retain this balance is linked to many different clinical problems including neurodegenerative disease, brain injury and oncogenesis. To achieve a homeostatic environment, and ensure the appropriate neural cell maturation through development, G1 phase is equipped with several crucial proteins whose expression and function is set to occur at highly specified times (Fig. 1).



## Nature Reviews | Molecular Cell Biology

**Figure 1.** The eukaryotic cell cycle and regulatory components of G1 phase. Cell cycle consists of 4 distinct phases. Gap1 phase G1, DNA replication phase S, Gap2 phase G2 and mitotic division phase M. G0 phase is a quiescent state in which cells don't withdraw from the cell cycle permanently but do not divide either. The most important components of G1 phase machinery are D- and E-type Cyclins that drive the activity of CDK2 and CDK4/6 respectively. They all participate in the RB protein phosphorylation that is required for progression from G1 to S phase. Modified with permission: Nature Publishing Group© (license# 3126701221034) and Coleman, Marshall et al. 2004, Nature Reviews. Molecular Cell Biology, 2004 May; 5(5):355-66. doi:10.1038/nrm1365, 2004.



Cyclins serve as regulatory subunits of holoenzymes and control the activity of a family of serine/threonine kinases known as cyclin dependent kinases (CDKs) to regulate the phosphorylation processes on downstream proteins. CDKs are expressed at constant levels. Their enzymatically inactive state is terminated when bound to the cyclin subunit that not only facilitates the structural conformation of a more accessible catalytic cleft (Pacey, Stead et al. 2006) but also provides the CDK with a targeting domain essential for specific substrate selection (Schulman, Lindstrom et al. 1998). Besides the protein-protein interaction, activation of CDKs is regulated through posttranslational modification. CDK activating kinase (CAK) phosphorylates a conserved Thr residue of the CDK T-loop for full activation of the complex (Booher and Beach 1986; Gould, Moreno et al. 1991; Gu, Rosenblatt et al. 1992; Solomon, Lee et al. 1992). In turn, the inhibitory phosphorylation on the tyrosine residue, equivalent to CDK1 Tyr-15, is removed by Cdc25 phosphatases (Morgan 1996; Solomon and Kaldis 1998; Welburn, Tucker et al. 2007). G1 phase cyclins include D-type and E-type Cyclins that carry out their function by binding to CDK4/6 and CDK2 respectively. Although cyclins D1, D2 and D3 have been shown to have distinct roles in different cellular systems (Ciemerych, Kenney et al. 2002; Kong, Chua et al. 2002; Cooper, Sawai et al. 2006; Cole, Myant et al. 2010; Jirawatnotai, Hu et al. 2011), they share significant homology and are critical for G1 phase progression (Sherr 1994; Lukas, Bartkova et al. 1995). The expression inducing mechanism as well as the timing of the activation is distinct for D-type and E-type Cyclins. D-type cyclins are expressed in the early to mid portion of G1 phase and serve as functional linking elements between the cell cycle machinery and external mitogenic signals that regulate their expression. Several growth factors have been shown to stimulate Cyclin D1 levels including epithelial growth factor, insulin growth factor I and II and multiple hormones

(Albanese, D'Amico et al. 1999; Fu, Wang et al. 2002; Holnthoner, Pillinger et al. 2002). Once activated, Cyclin D binds to CDK4/6 and triggers phosphorylation of Rb, the product of the Retinoblastoma tumour suppressor gene, which subsequently leads to release of E2F transcription factors. Activation of E2F factors is an essential event for promoting the progression through G1 to S phase due to their ability to transcribe a battery of genes including Cyclin E (Ohtani, DeGregori et al. 1995; Botz, Zerfass-Thome et al. 1996; Geng, Eaton et al. 1996). The expression of Cyclins E1 and E2 starts in late period of G1 phase. Activation of CDK2 by Cyclin E (Koff, Cross et al. 1991; Koff, Giordano et al. 1992; Richardson, O'Keefe et al. 1993; Knoblich, Sauer et al. 1994) maintains the hyperphosphorylated state of Rb, abrogating its transcriptional repression. Multiple additional functions of Cyclin E-CDK2, including roles in centrosome duplication, histone biosynthesis and loading of the prereplication complex onto the DNA replication origins (Gladden and Diehl 2003), participate in the progression to S phase.

Importantly, the activity of the Cyclin E-CDK2 complex and S phase entry can be inhibited by a Cip/Kip family of cyclin dependent kinase inhibitors (CKIs). p21<sup>Cip1</sup>, p27<sup>Kip1</sup> and p57<sup>Kip1</sup> can inhibit a broad range of cyclin-CDK complexes (Nakayama, Ishida et al. 1996; Di Stefano, Giacca et al. 2011). p27<sup>Kip1</sup> has been shown to bind not only Cyclin E-CDK2 but also Cyclin A-CDK2 and Cyclin D-CDK4/6. The latter is known to sequester p27<sup>Kip1</sup> in a trimeric complex (Koh, Enders et al. 1995; Montagnoli, Fiore et al. 1999). Upon mitogen withdrawal the sequestered pool of p27<sup>Kip1</sup> is released and free to bind and inhibit Cyclin E-CDK2 activity (LaBaer, Garrett et al. 1997; Cheng, Olivier et al. 1999; Sherr and Roberts 2004). In turn, the Cyclin E-CDK2 complex can phosphorylate p27<sup>Kip1</sup> on Thr-187, a residue shown to target p27<sup>Kip1</sup> for degradation mediated by SCF<sup>Skp2</sup> ubiquitin ligase pathway (Pagano, Tam et al. 1995; Sheaff, Groudine

et al. 1997; Vlach, Hennecke et al. 1997). Another family of CKIs, Ink4 (p16<sup>Ink4a</sup> or its alternate reading frame (ARF) p14<sup>ARF</sup>, p15<sup>Ink4b</sup>, p18<sup>Ink4c</sup>, p19<sup>Ink4d</sup> or p19<sup>ARF</sup>), specifically inhibits CDK4 and CDK6.

### *Putative function of G1 phase cyclins as fate determinants during neural development*

#### *Embryonic stem cells (ESCs) and G1 phase regulators*

ESCs demonstrate unique cell cycle dynamics. The rapid division rate observed in ESCs is attributed to an extremely short cell cycle caused by a significant reduction in G1 phase. This unique regulation of the cell cycle is speculated to conserve the pluripotency of ESCs and prevent differentiation (White and Dalton 2005; Orford and Scadden 2008; Singh and Dalton 2009; Lange and Calegari 2010). Murine ESCs demonstrate very low levels of D-type Cyclin expression and CDK4 kinase activity (Orford and Scadden 2008). In human ESCs there is a constitutive high expression of D-type and E-type Cyclins, and elevated activity of G1 phase CDKs (Orford and Scadden 2008). While there are subtle mechanistic differences in murine and human ESCs both have a significant reduction in the mitogen dependent portion of G1 phase, thereby significantly shortening the cell cycle (Becker, Ghule et al. 2006) (Fig.2).

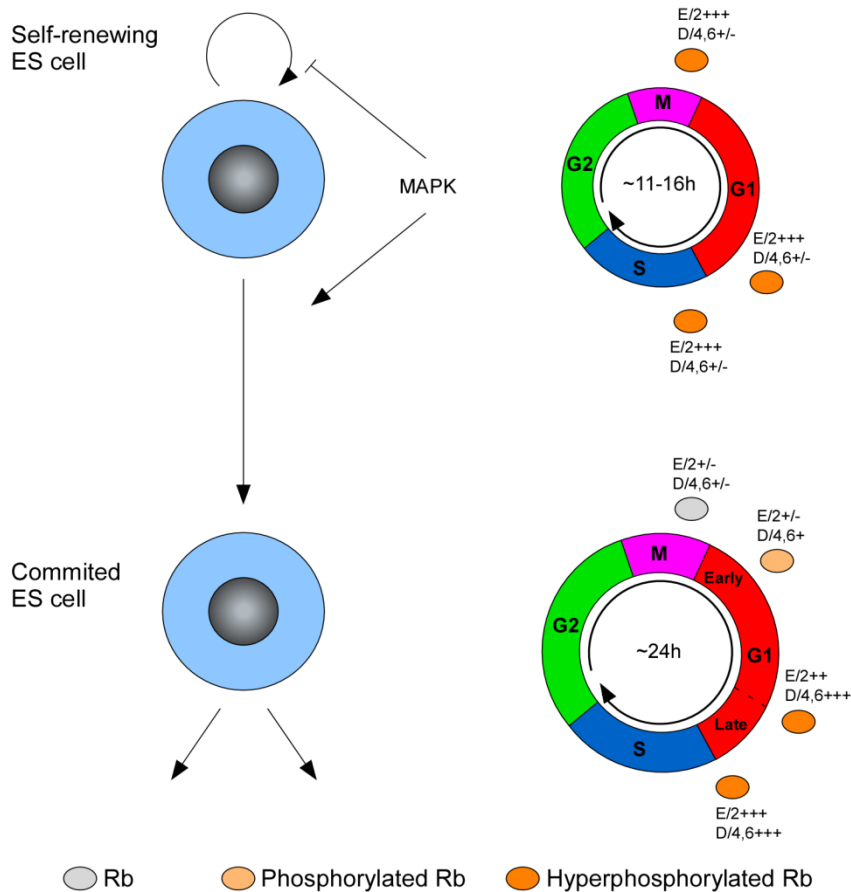


**Figure 2.** The cell cycle changes in ESCs during differentiation.

The cell cycle of ESCs is characterized by negligible levels and activity of the Cyclin D/CDK4 or Cyclin D/CDK6 (D/4,6) complexes and continuous overexpression of Cyclin E resulting in constitutively active CDK2. Cyclin E/CDK2 (E/2) overrides the early, mitogen-induced portion of G1 phase and shortens the overall length of G1 phase leading to decreased total cell cycle time. As ESCs commit to differentiation D/4,6 and hyperphosphorylated Rb gains control over Cyclin E, early G1 phase reconstitutes and cell cycle undergoes lengthening. + refers to cyclin-CDK activity: +/-, negligible; +, low; ++, intermediate; +++, high. Modified with permission: Nature Publishing Group© (license# 3126690068348) and Orford and Scadden 2008, Nature Reviews. Genetics. 2008. Feb;9(2):115-28. 2008

### *G1 phase and the adult neural stem cell (NSC) regulation*

In the adult mammalian brain, self-renewal and neurogenesis are dependent on populations of rarely dividing adult stem cells residing in quiescence (G0) within a discrete anatomical niche. The quiescent state remains under the control of an orchestrated network of CKIs, thus preserving the genomic integrity of the adult NSCs and preventing them from proliferative exhaustion. Interestingly, while in quiescence, NSCs infrequently re-enter the cell cycle to self-renew. Despite limitations in data on the G0 – G1 phase re-entry, the cell cycle components regulating G1 phase progression, as well as several oncogenes, are speculated to play a crucial role in the activation of quiescent cells (Geng, Yu et al. 2003; Wang, Plane et al. 2011). Powerful ultrastructural studies using transmission electron microscopy, contributed to the detailed data describing the quiescent cell population residing within neurogenic regions of the adult brain (Morshead, Reynolds et al. 1994; Doetsch, Garcia-Verdugo et al. 1997; Mirzadeh, Merkle et al. 2008). The forebrain subventricular zone (SVZ) of the lateral ventricles and the dentate gyrus of the hippocampus constitute the primary discrete regions of adult neurogenesis (Doetsch, Caille et al. 1999). In addition, the rostral migratory stream between the SVZ and olfactory bulb was also found to contain a minor population of adult NSCs (Gritti, Bonfanti et al. 2002).

In contrast to the abundant literature describing role of the cell cycle in ESCs, the critical cell cycle components responsible for maintaining self-renewing pools of neural progenitors during adulthood has yet to be determined. Nonetheless, the available data on cell cycle regulators essential for fate determination in neural systems through development is discussed in detail in this section.

### *G1 cyclin regulatory network in neural fate decisions*

During central nervous system (CNS) development coordination between the core cell cycle mechanisms regulating G1 phase progression and intrinsic and extrinsic signals delivering cues from the external environment lie at the heart of fate decisions. The embryonic neuroepithelium of the neural tube constitutes the original source of multipotent NSCs (Gotz and Huttner 2005; Takashima, Era et al. 2007; Ohtsuka, Shimojo et al. 2011). NSCs give rise to the gradually more committed progenitor cells including radial glia and basal progenitors and all neuronal and macroglial (astrocytes and oligodendrocytes) cells composing the mature mammalian brain (Doetsch, Caille et al. 1999; Gritti, Bonfanti et al. 2002; Bonaguidi, Wheeler et al. 2011; Guo, Patzlaff et al. 2012). The number of progenitor cells produced at embryonic stages of development, significantly exceeds the amount of neural precursors generated at the later stages, due to their short cell cycle and predominant expansive division (Gotz and Huttner 2005). It has been established that as embryogenesis progresses, the cell cycle of the neural progenitors undergoes lengthening mainly due to the stretching of G1 phase (Takahashi, Nowakowski et al. 1995) (Fig 3). Also, at postnatal stages the length of the G1 phase is speculated to affect fate determination by regulating the time when a neural progenitor leaves the cell cycle (Das, Choi et al. 2009). The different points in time when a progenitor is arrested are reflected by fate influencing changes that include altered progenitor potential and extrinsic stimuli/cues available at a certain stage of development, reviewed in (Livesey and Cepko 2001). Therefore, several studies attempt to investigate the key cell cycle regulators that participate in G1 phase progression and the S phase transit and how they regulate cell fate choices along the course of development.

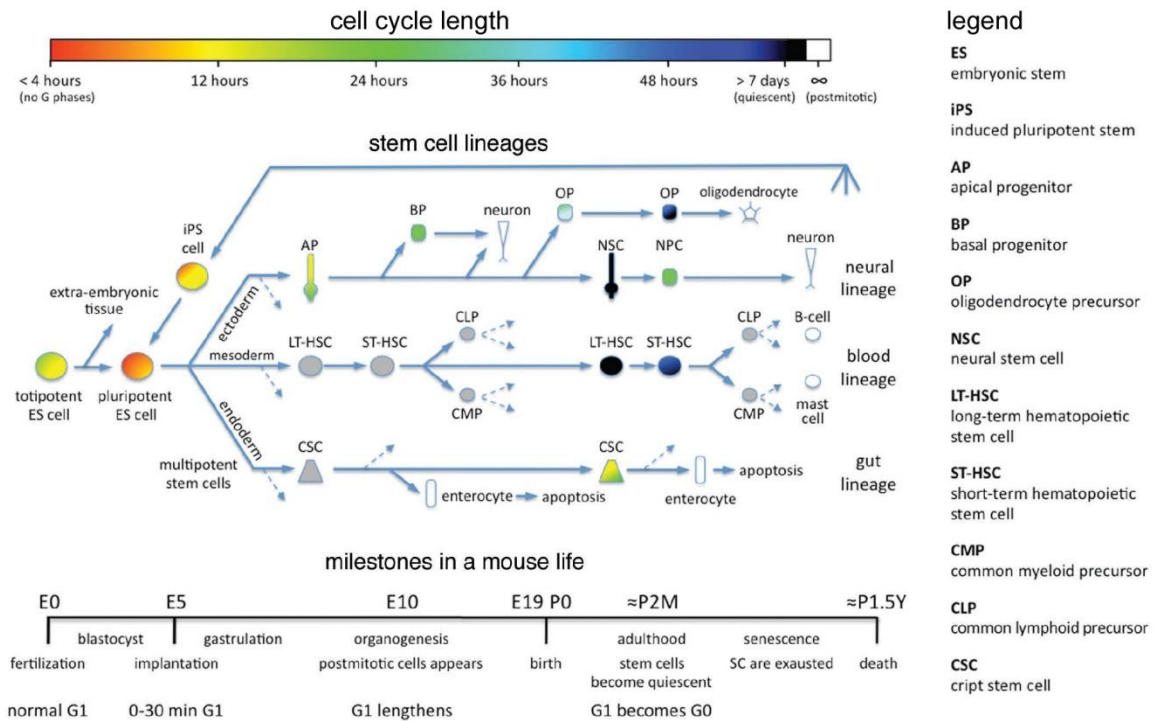


**Figure 3.** Cell cycle length and G1 changes during development.

Stem cells from each germ layer are presented. Cell cycle length (top) is marked in colour gradient and a timeline aligned to the cell cycle length indicated specific stages including embryonic (E), postnatal (P) in months (M) and years (Y). The diagram represents gradual lengthening of cell cycle G1 phase stretching through embryogenesis to postnatal quiescent state and postmitotic state of terminal differentiation. Modified with permission: Landes Bioscience Journals© and Lange and Calegari 2010, *Cell Cycle*. 2010 May 15;9(10):1893-900. doi.org/10.4161/cc.9.10.11598.

### *D-type Cyclins in neural fate*

D-type Cyclin function is essential in regulation of the early, mitogen dependent portion of G1 phase that is speculated to constitute a critical period during which cell fate decisions are made (Takahashi, Nowakowski et al. 1995; Sherr 2000; Calegari and Huttner 2003). Experiments involving electroporation of Cyclin D1-CDK4 or Cyclin E1-CDK2 into the lateral cortex of 13.5 day embryos (E13.5) revealed that only the Cyclin D1-CDK4 complex had the ability to prevent lengthening of G1 phase in the neural progenitors (Lange, Huttner et al. 2009). In these experiments overexpression of Cyclin D1 resulted in suppressed neurogenesis within the SVZ and an increased proportion of proliferating precursors. Interestingly, forced expression of Cyclin D1 shortens G1 phase during a window of embryogenesis, suggesting that downregulation of Cyclin D1 is essential in the natural lengthening of G1 phase but these overt phenotypes later in development are not apparent (Lange, Huttner et al. 2009). Alternatively, deletion of Cyclin D1 in progenitor cells within the embryonic ventricular zone was compensated by an endogenous increase of Cyclin D2 levels and its function (Glickstein, Monaghan et al. 2009; Lange and Calegari 2010). In contrary, Cyclin D2 deficient progenitors demonstrated precocious neurogenesis that was not rescued by endogenous accumulation of Cyclin D1 (Glickstein, Monaghan et al. 2009; Lange and Calegari 2010). These data imply cell-type dependent and redundant functions of D-type Cyclins in controlling the duration of G1 phase.

While all three D-type Cyclins are expressed during embryonic to early juvenile stages of CNS development, the neural stem cell populations within the adult brain were demonstrated to critically depend on the expression of Cyclin D2 (Kowalczyk, Filipkowski et al. 2004). The olfactory bulb region that constitutes one of the restricted



neurogenic zones within the adult brain requires a continual accumulation of progenitor cells as a source of neurons. The Cyclin D2<sup>-/-</sup> mouse model manifested a significant decrease in the number of proliferating progenitor cells within the adult brain including the olfactory bulb (Kowalczyk, Filipkowski et al. 2004; Imayoshi, Sakamoto et al. 2009). This indicates that Cyclin D2 deficiency at adult stages of development results in suppressed cell cycle progression and reduced pools of proneurogenic cells.

#### *E-type Cyclins in neural fate*

Manipulation of Cyclin E1-CDK2 expression in mouse embryonic cell lines demonstrated that decreased CDK2 activity in murine stem cells contributes to the gene expression and morphology modifications that are characteristic of differentiation (Koledova, Kafkova et al. 2010). Furthermore, the inhibition of CDK2 activity alone was sufficient to increase the frequency of cells residing in G1-phase and resulted in a subsequent switch to neurogenesis. The neurogenic shift was demonstrated to occur due to the prolonged G1 phase, suggesting that the Cyclin E1-CDK2-induced - cell cycle length may play a causal role in differentiation at embryonic stages of nervous system development (Koledova, Kafkova et al. 2010). Importantly, CDK2 activity in ESCs appears to be higher than that of CDK4 or CDK6, implying a crucial role for CDK2 in the dynamics of ESC G1 phase (Neganova et al. 2009). Consequently, the delivery of Cyclin E1 to the precursor cells lining the embryonic ventricular zone resulted in a shorter G1 phase and increased frequency of proliferative divisions (Pilaz, Patti et al. 2009). Cyclin E1 electroporation into cells of the germinal zone exhibited a significant increase in germinal zone thickness due to the expansion of the total precursor pool (Pilaz, Patti et al.

2009). These data demonstrate the importance of Cyclin E1 in controlling progenitor populations in the developing brain *in vivo*.

Although electroporation of Cyclin D1 produced analogous results to Cyclin E1 at embryonic stages, the overexpression of Cyclin E1 showed less effect on the reduction in the proportion of neurons produced in the postnatal brain. Consequently, Cyclin E1-CDK2 activity, but not the activity of Cyclin D1-CDK4, was demonstrated to rapidly decrease between postnatal day 15 and 30 of the development (Ghiani and Gallo 2001). These data point to some distinct differences in the expression, and potential functional importance, of Cyclin E1 and Cyclin D1 in the adult brain (Ghiani and Gallo 2001).

Both cyclins were found to be upregulated in proliferative neural populations versus those arrested or terminally differentiated (Ghiani and Gallo 2001). In contrast to this, decreasing levels of Cyclin E1-CDK2, but not Cyclin D1-CDK4/6, mediate reversible cell cycle withdrawal (Ghiani and Gallo 2001). These data demonstrate differences in cell cycle regulation in cases of permanent vs. transient cell cycle arrest. Upon application of mitogenic stimuli to quiescent progenitor cells, Cyclin E1-CDK2 is readily activated, confirming an important role in the cell cycle re-entry (Ghiani and Gallo 2001). As shown by Geng *et al.*, the inability to re-enter the cell cycle is among the most severe phenotypes of the double Cyclin E1/E2 knockout mouse model (Geng, Yu et al. 2003). The authors revealed that ablation of both E-type Cyclins caused impaired assembly of the origin of replication complex in quiescent cells, however, the origin loading and firing occurred without error in continuously proliferating double knockout cells. These results emphasize the role of the E-type Cyclins as a limiting factor in G0 - G1 progression (Geng, Yu et al. 2003). The data suggest that the timing of Cyclin E1/ E2 expression may be critical in the fate of quiescent cell populations.

In summary, the G1 phase cyclin components play an essential role in developmental processes and neuronal phenotype determination. These cyclins modulate the length of G1 phase, the timing of cell cycle arrest and the ability of quiescent cells to re-enter the cell cycle. Several studies on the key G1 phase regulators collectively indicate an exact correlation between G1 phase lengthening and differentiation (Lange and Calegari 2010) (Table 1). Consequently, G1 phase shortening reduces sensitivity to differentiation stimuli and may have other effects as well, such as reducing the time required for epigenetic remodelling of chromatin that may be required for differentiation to occur (Egli, Birkhoff et al. 2008). Despite well defined participation of certain G1 cyclins in timing and duration of G1 phase at diverse stages of development, how neural cells initiate exit from G0 stage and what are the required endogenous regulators of differentiation in diverse stem and progenitor cell pools remains to be determined.

	cell type	manipulated cell cycle regulator	type of manipulation	G1 length	differentiation	proliferation	reference
	ES cell	cdk2	Ph or RNAi ↓	↑	↑	↓	Koledova et al. 2009
	ES cell	cdk2	RNAi ↓	↑	↑	↓	Neganova et al. 2009
	ES cell	cdk2	Ph ↓	↑	↑	↓	Fillpczyk et al. 2009
development	retinal NSC	cyclin D1	KO ↓	↑	↑	↓	Das et al. 2009
	cortical NSC	cyclin D1	KO ↓	=	=	=	Glickstein et al. 2009
	cortical NSC	cyclin D1	OE ↑	N.D.	=	=	Lange et al. 2009
	cortical NSC	cyclin D2	KO ↓	↑	↑	↓	Glickstein et al. 2009
	cortical NSC	cdk4/cyclin D1	OE ↑	↓	↓	↑	Lange et al. 2009
	cortical NSC	cdk4/cyclin D1	RNAi ↓	↑	↑	↓	Lange et al. 2009
	cortical NSC	cdk2/cyclin E1	OE ↑	=	=	=	Lange et al. 2009
	cortical NSC	cdk2/cyclin E1	Ph ↓	↑	↑	↓	Calegari and Huttner 2003
	cortical NSC	cyclin D1 or cyclin E1	OE ↑	↓	↓	↑	Pilaz et al. 2009
	cortical NSC	cyclin D1 or cyclin E1	RNAi ↓	N.D.	↑	↓	Pilaz et al. 2009
	HSC	cyclin D1/D2/D3	KO ↓	↑	N.D.	↓	Kozar et al. 2004
	HSC	cdk4/cdk6	KO ↓	N.D.	N.D.	↓	Malumbres et al. 2004
	adulthood	NSC	cyclin D2	KO ↓	cell cycle block	N.A.	↓
HSC		cyclin D2	OE ↑	N.D.	N.D.	↑	Sasaki et al. 2009
B-cell progenitor		cyclin D3	KO ↓	N.D.	N.A.	↓	Cooper et al. 2006
T-cell progenitor		cyclin D3	KO ↓	N.D.	N.A.	↓	Sicinska et al. 2003
granulocyte progenitor		cyclin D3	KO ↓	N.D.	N.A.	↓	Sicinska et al. 2006
erythroid progenitor		non degradable Cyclin E1	KI ↑	N.D.	↓	↑	Minelli et al. 2008

**Table 1.** Collected data on G1 phase components manipulation during development and in the adult mouse and correlation between lengthening of G1 phase and differentiation. Red arrows indicate downregulation and green- upregulation in the columns 2-4 cyclin/cdk activity, G1 length, differentiation and proliferation respectively. Effects not observed/detected are marked as N.D. Manipulations are indicated as pharmacological (Ph), knockdown (RNAi), knockout (KO), overexpression (OE) and knockin (KI) types of manipulations are indicated. Modified with permission: Landes Bioscience Journals© and Lange and Calegari 2010, Cell Cycle. 2010 May 15;9(10):1893-900.

### *Cell cycle regulation over mode of division during neural development*

The self-renewing NSCs of the neuroepithelium are polarized along the apical-basal axis, exhibit high proliferative potential and form the most apical cell layer lining the ventricle referred to as the ventricular zone (Huttner and Brand 1997; Wodarz and Huttner 2003). In an early embryo prior to neurogenesis (E9- E11), the NSCs use symmetric division to self-renew and increase their pool of daughter cells with identical proliferative fate (McConnell 1995; Rakic 1995). From the onset of neurogenesis, asymmetric division becomes the predominant way to establish the pool of progressively more committed radial glial cells and basal progenitors capable of generating all of the brain tissues (Gotz and Huttner 2005). Although, radial glia represent several NSC characteristics including apical-basal polarity and expression of the neurofilament protein Nestin, they express astroglial markers such as glial fibrillary acidic protein (GFAP) or Vimentin and are more fate restricted in their potential (Kriegstein and Gotz 2003; Gotz 2003; Williams and Price 1995; (Fishell and Kriegstein 2003). Basal progenitors form the SVZ, a cell layer basal to the ventricular zone, and divide symmetrically to increase the number of neurons generated from ventricular zone precursors by providing an additional round of cell division in the SVZ, reviewed in (Gotz and Huttner 2005). Overall, from studies at the embryonic and postnatal level of CNS development the main principle arises that along the progression of developmental stages NSCs switch from using proliferative symmetric division to asymmetric division to form populations of progenitor cells capable of differentiating down various cell lineages. Asymmetric division of NSCs is characterized by the distribution of specific apical and basal cell structures that have been shown to function as cell fate determinants between the two daughter cells reviewed in (Gotz and Huttner 2005; Tsunekawa, Britto et al. 2012). Several characterized proteins,

including Numb, CD133 and Par complex proteins, are known to localize to the apical surface of dividing progenitors and serve as fate determinants (Wodarz and Huttner 2003). Moreover, as the cells divide asymmetrically along the course of development, the rate of their cell cycle progression decreases due to the gradual stretching of G1 phase (Takahashi, Nowakowski et al. 1995). The cell cycle machinery that regulates the length of G1 is speculated to affect the function of fate determinants (Caviness, Takahashi et al. 1995), suggesting the hypothesis that regulatory components of the G1-S transition may participate regulating the mode of division of stem cell populations.

#### *D-type Cyclins in mode of division*

Recently, a novel mechanism regarding Cyclin D2 distribution has been proposed by Tsunekawa *et al.* that involves active localization and at-the-site translation of Cyclin D2 mRNA to the basal progenitors during division (Tsunekawa, Britto et al. 2012). As a consequence, the basally positioned daughter cell acquires the self-renewing fate of an apical progenitor. The distribution of Cyclin D2 to the basal border is suggested to shorten G1 phase and consequently protect the progenitor from acquiring differentiation stimuli.

Cyclin D2 is found in the progenitor cells of the SVZ and its immunoreactivity appears to be higher than that of Cyclin D1 at the site (Glickstein, Alexander et al. 2007). This suggests a role for Cyclin D2, but not Cyclin D1, in regulating the mode of division and self-renewal of progenitor cells within the niche.

Although it is not known whether distribution of Cyclin D1 in dividing progenitors affects their behaviour, the studies using a knockout mouse model established that Cyclin D1 performs a unique role in maintaining the proper number of self-renewing progenitor

cells required for full maturation of the retina (Sicinski, Donaher et al. 1995). Cyclin D1, but not Cyclin D2 or D3, deficiency leads to neurological abnormalities and hypoplastic retinas resulting in small eyes in mouse and zebrafish models (Fantl, Stamp et al. 1995; Sicinski, Donaher et al. 1995; Rapaport, Wong et al. 2004; Duffy, McAleer et al. 2005; Das, Choi et al. 2009). The phenotypic manifestations were not found to be efficiently reversed by Cyclin D2 knock-in, suggesting that the roles of D-type Cyclins in regulating the mode of division and self-renewal are not fully redundant and are dependent on the system tested (Sicinski, Donaher et al. 1995). Furthermore, the observed retinal hypoplasia in Cyclin D1 deficient mice is attributed to the changes in cell cycle transit time and the high rate of retinal progenitors engaging in differentiation. Interestingly, the premature cell cycle exit followed by disturbed balance between the numbers of early retinal self-renewing progenitors and the birth of committed neuronal precursors can be corrected with overexpression of Cyclin E1 or depletion of p27 protein (Das, Choi et al. 2009).

Overall these data suggest that Cyclin D2 acts as a cell fate determinant during cell division and selectively regulates self-renewal of the SVZ progenitor cells. Conversely, Cyclin D1, but not Cyclin D2, affects cellular fate in retinal progenitors by regulating the duration of G1 phase. How Cyclin D1 is affecting cell fate, or if it can act as a direct fate determinant analogous to Cyclin D2, remains under investigation.

#### *E-type Cyclins in mode of division*

The most detailed information on the role of Cyclin E1/ E2 in the mode of division and their subsequent function in the mechanisms governing neural cell fate control comes from studies in *Drosophila*. The NSCs of the thoracic segment in the CNS of the

*Drosophila* embryo, referred to as neuroblasts, are characterized by expression of Cyclin E1 that localizes unequally during an initial self-renewing asymmetric division (Berger, Pallavi et al. 2005). In the daughter neuroblast, Cyclin E1 acts upstream of prospero (pros) and glial cell missing (gcm) proteins that lead to the generation of a neuron while the other daughter generates glia (Ragone, Bernardoni et al. 2001; Berger, Pallavi et al. 2005; Kannan, Berger et al. 2010). The neuroblasts in the abdominal segment however, use a specific mechanism involving Abdominal-A protein mediated downregulation of Cyclin E1 levels to restrict the multipotent character of the neuroblasts. The decrease in Cyclin E1 results in symmetric division and generation of two glial cells (Kannan, Berger et al. 2010).

In contrast to the asymmetrically self-renewing neuroblasts in the developing CNS of *Drosophila*, their progeny, ganglion mother cells (GMCs), undergo asymmetric terminal divisions (Thomas, Bastiani et al. 1984; Wai, Truong et al. 1999). According to Bhat *et al.* an uneven distribution of the Cyclin E1 protein confers self-renewing, asymmetric division potential to GMCs (Bhat and Apsel 2004). High levels of Cyclin E1, accumulating in one of the two descending progenitors, cause enhanced progression from G1 to S phase and a blockage in cell cycle exit in one daughter cell while the other commits to differentiation (Bhat and Apsel 2004). Although the question of whether Cyclin E1 distribution is a passive or an active process still remains to be answered, Cyclin E1 emerges as a key and direct component of fate decisions based on the mode of division control.

To date the mechanisms observed in *Drosophila* have not been reported in vertebrates. Nonetheless, the available studies suggest that Cyclin E1/ E2 participates in fate determination through regulation of division symmetry in the mammalian neural



system. An *ex vivo* study that investigated the cell cycle mechanisms behind the development of the primate cortex (corticogenesis) established that Cyclin E1 plays an essential role in cell fate decisions and self-renewal among a population of supragranular progenitors of the outer subventricular zone (OSVZ) (Lukaszewicz, Savatier et al. 2005). These results demonstrated that the levels of Cyclin E1 were upregulated in the region characterized by a high frequency of cell cycle re-entry, reduced G1 phase and an elevated proliferation rate (Lukaszewicz, Savatier et al. 2005). Furthermore, despite the developmental characteristics that are specific to primates, rodent corticogenesis demonstrates similar crucial features including patterning of the germinal zone and common expression of specific genes within the SVZ (Kennedy and Dehay 1993; Sestan, Rakic et al. 2001; Nieto, Monuki et al. 2004; Lukaszewicz, Savatier et al. 2005).

Data by Noctor *et al.* revealed that the SVZ of the mouse brain is characterized by predominant symmetric divisions in opposition to the ventricular zone where the majority of progenitor cells divide asymmetrically (Noctor, Martinez-Cerdeno et al. 2004). Interestingly, in this work the symmetric pattern of division in the SVZ includes both, a small population of cells that divide symmetrically to self-renew and a prevalent number of populations that undergo symmetric neurogenic divisions. Consistently, the regulation of Cyclin E1 in the primate OSVZ orchestrated the ongoing extensive neurogenesis within that region (Lukaszewicz, Savatier et al. 2005). These data suggest that Cyclin E1-mediated effects can regulate the mode of division in the SVZ and are important for sustained neurogenesis during development. To date there is insufficient evidence implying the role of Cyclin E1 as a direct fate determinant in the symmetry of division in the developing mammalian CNS. A careful redistribution analysis of Cyclin E1 to the

mitotic pairs of the progeny within the SVZ, followed by a study of the cell cycle mechanisms underlying fate determination are required for further conclusions.

As discussed previously, both D-type and E-type Cyclins regulate the duration of G1 phase and affect the window of time available for specific developmental cues acting at the indicated stage. Importantly, an analogous model has been proposed that involves changes in the timing of cell cycle transit and intrinsic fate determinant segregation (Calegari and Huttner 2003; Gotz and Huttner 2005; Dehay and Kennedy 2007) (Fig.4). The overexpression of cyclins is unequivocal for delaying the generation of post-mitotic cell populations. Cyclin upregulation will keep the competent precursor in the cell cycle, endorsing its self-renewal. Hence, the reduced expression of cyclins is expected to cause cell cycle exit and differentiation. According to the proposed model, the changes in cyclin expression can regulate the window of time sufficient for the intrinsic fate determinants to act effectively, thus affecting the symmetry of division. Hence it can be hypothesized that even in the face of uneven fate determinant segregation the overexpression of G1 phase cyclins may result in symmetric division due to insufficient time for the determinant to execute its effects (Calegari and Huttner 2003; Gotz and Huttner 2005; Dehay and Kennedy 2007). This hypothesis would indicate that G1 phase duration is closely associated with mode of division control, providing a mechanism by which cyclin dependent regulation of G1 phase lengthening can regulate neurogenesis.

In conclusion, the neurogenic switch in NSCs resulting in gradually more restricted progenitors along development is associated with stretching of their cell cycle predominantly due to cyclin regulated lengthening of G1 phase (Takahashi, Nowakowski et al. 1995). We hypothesize that this supports a mechanistic model whereby cyclin-CDK complexes can affect fate determinant function and control the symmetry of division.

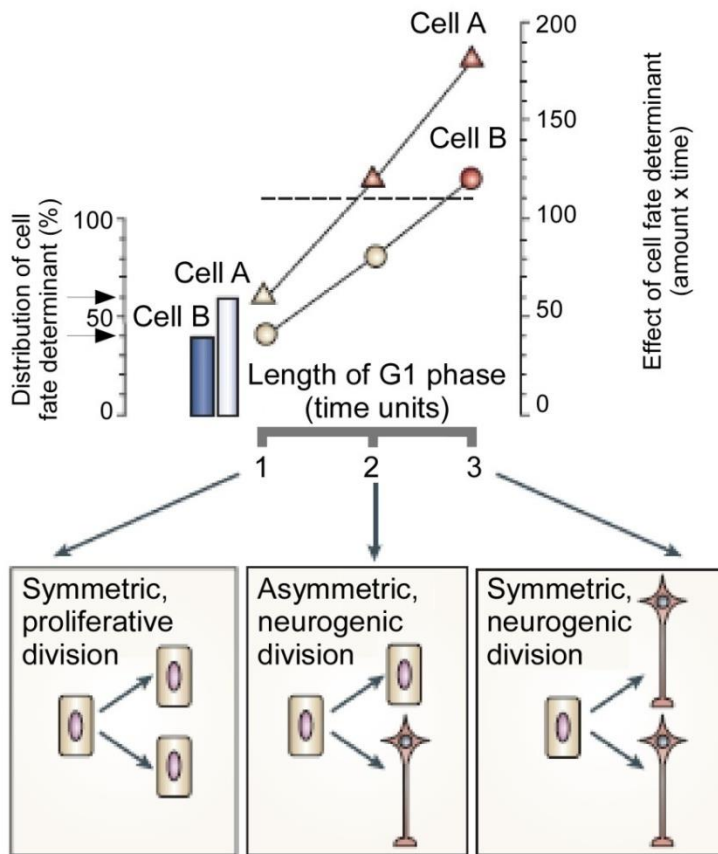


**Figure 4.** The link between cell cycle length and mode of division. Following mitosis the daughter cells A and B inherit uneven amount of a cell fate determinant (light and dark blue bar respectively). The fate determinant can induce neurogenesis depending on the G1 phase time sufficient for it to act. The G1 phase machinery can regulate the G1 phase duration so in the shortest time (1) none of the cells becomes a neuron. If the G1 phase gets longer (2) cell A becomes a neuron due sufficient time for the amount of the determinant to act. Further prolonged G1 phase allows both cells to differentiate as its duration is sufficient even for low amount of the fate determinant to exert its effect. Modified with permission: Nature Publishing Group© (license# 3126700971609) and Gotz and Huttner 2005, Nature Reviews. Molecular Cell Biology, 2005 Oct;6(10):777-88.

### *Cell cycle inhibitors in neural development*

The cell cycle can be negatively regulated by Ink4 and Cip/Kip groups of CDK inhibitors. Both families play an essential role in the development of the nervous system, reviewed in (Beukelaers, Vandenbosch et al. 2012). At the embryonic stages of development the expression of cell cycle inhibitors remains low to allow for high levels of proliferative expansion, reviewed in (Cheng 2004). The overexpression of p21<sup>Cip1</sup> or p27<sup>Kip1</sup> in embryonic stem cells results in the lengthening of G1 phase. This p21<sup>Cip1</sup>/p27<sup>Kip1</sup> driven mechanism is speculated to control the proper schedule of differentiation events along development (Li, Ballabeni et al. 2012). During postnatal development CDK inhibitors regulate entry into quiescence in early G1 phase (Blomen and Boonstra 2007) and their expression in the postmitotic neurons suggest that cell cycle inhibitors sustain mature neuronal phenotype (Herrup and Yang 2007).

#### *p21<sup>Cip1</sup>*

During adult neurogenesis p21<sup>Cip1</sup> plays an antiproliferative role in the neurogenic regions of the brain, maintaining cellular quiescence (Qiu, Takagi et al. 2004). The lifelong supply of neural progenitor cells and continual neurogenesis rely on p21<sup>Cip1</sup> expression as p21<sup>Cip1</sup> loss correlates with observed exhaustion of the neural stem cell pool (Kippin, Martens et al. 2005) *in vivo*. Importantly, p21<sup>Cip1</sup> deficient neural progenitor cells demonstrate an increased proliferation rate in neurosphere formation assays *in vitro* (Kippin, Martens et al. 2005). Alternatively, some groups reported no proliferation defects in p21<sup>Cip1</sup>- deficient animals at early stages of postnatal development (Qiu, Takagi et al. 2004; Kippin, Martens et al. 2005). This observation was attributed to the fact that p21<sup>Cip1</sup> specific expression is found to accumulate at late stages of development in the

most stem-like population of neural progenitor cells that reside within the neurogenic niche of the SVZ (type B cells) (Kippin, Martens et al. 2005). Recently, a p21<sup>Cip1</sup>-mediated molecular mechanism behind neural stem cell maintenance was proposed that involves direct regulation of the pluripotency inducing factor, Sox2 (Marques-Torrejon, Porlan et al. 2013). The study revealed that p21<sup>Cip1</sup> is capable of blocking Sox2 enhancer by a direct interaction thus reducing Sox2 expression in neural progenitors. Upregulation of Sox2 in p21<sup>Cip1</sup>- deficient neural progenitors resulted in increased entry into senescence due to accumulation of DNA damage and activation of p53 and p19<sup>ARF</sup> tumour suppressor genes (Marques-Torrejon, Porlan et al. 2013).

#### *p27<sup>Kip1</sup>*

p27<sup>Kip1</sup> overexpression in the populations of oligodendrocyte precursors at embryonic stages of development result in lower rates of proliferation (Lukaszewicz, Savatier et al. 2005). Consistently, in the adult SVZ p27<sup>Kip1</sup> deficient progenitor cells demonstrate an increase in proliferative potential. Indeed, p27<sup>Kip1</sup> is considered to act as an inhibitor of proliferation during neural development. p27<sup>Kip1</sup> was demonstrated to repress Sox2 during differentiation in a mechanism similar to the one presented for p21<sup>Cip1</sup> (Li, Ballabeni et al. 2012). In contrast to the type B cell specific expression of p21<sup>Cip1</sup>, p27<sup>Kip1</sup> deletion was demonstrated to selectively expand the transit amplifying precursor (type C cells) population followed by a decreased number of neuroblasts (type A cells) (Doetsch, Verdugo et al. 2002). Interestingly, since C-type cells give rise to A-type neuroblasts, it is speculated that the loss of p27<sup>Kip1</sup> results in a prolonged proliferative state of the amplifying precursors at the expense of the more committed neuroblast progenitors (Doetsch, Verdugo et al. 2002).

Studies on the role of  $p27^{Kip1}$  in neural commitment and differentiation established that  $p27^{Kip1}$  is a crucial component of the internal timer required for neural progenitors to differentiate at specific times during development (Durand, Gao et al. 1997). Experiments on oligodendrocyte populations revealed that  $p27^{Kip1}$  protein accumulates gradually in cells over time as they continue to proliferate (Durand, Gao et al. 1997). In addition, it has been demonstrated that  $p27^{Kip1}$  deficiency confers increased mitogen sensitivity to progenitor cells. Upon mitogen withdrawal,  $p27^{Kip1}$ -deficient cells demonstrate a delay in cellular arrest suggesting that  $p27^{Kip1}$  regulates the mitogen response in neural cells during development (Durand, Fero et al. 1998). Overall,  $p27^{Kip1}$  appears to play a crucial role in the orchestrated network of events regulating neural development.

### *p16<sup>Ink4a</sup>*

Aging of the CNS results in a significant decrease of the proliferative pool at neurogenic sites, most likely due to age progressive senescence (Campisi 2005; Lombard, Chua et al. 2005; Molofsky, Slutsky et al. 2006). The levels of  $p16^{Ink4a}$  cell cycle inhibitor are reported to increase with age in the SVZ and olfactory bulb, two main sites of proliferation and neurogenesis within the adult brain, respectively (Molofsky, Slutsky et al. 2006). Loss of  $p16^{Ink4a}$  prolongs self-renewal of multipotent progenitors in aging animals (Molofsky, Slutsky et al. 2006). Interestingly,  $p16^{Ink4a}$  deficiency-induced proliferation and neurogenesis were the most profound on the type B progenitors than the other lineage committed cells (Molofsky, Slutsky et al. 2006). These data suggest the hypothesis that cell cycle changes along lineage commitment render more restricted progenitors less dependent on the  $p16^{Ink4a}$  inhibitor (Molofsky, Slutsky et al. 2006). Moreover, the deletion of  $p16^{Ink4a}$  did not prolong proliferation in the dentate gyrus,

pointing to regional specific differences in cell cycle regulation of the adult neurogenic progenitors (Molofsky, Slutsky et al. 2006). Hence, p16<sup>Ink4a</sup> regulates senescence mechanisms that play a critical role in the aging brain.

### *Brain tumours*

A brain tumour is a mass of abnormal cells growing within the brain structures, or in the periphery of the brain (Louis, Ohgaki et al. 2007). Due to the organ's vitality brain tumour formation is devastating in nature. Tumours of the CNS are the leading cause of death among children and the third leading cause of death in young adults between 20 and 39 years of age. It is estimated that 27 Canadians are diagnosed with a brain tumour every day (<http://www.braintumour.ca/2494/brain-tumour-facts>).

### *Brain tumour subtypes and complexity*

Over 120 types of brain tumours are included into classification prepared by the World Health Organization (WHO) that distinguishes between histopathological entities, variants of entities and histological patterns of differentiation (Louis, Ohgaki et al. 2007). Every separate type or entity represents a distinct morphology, biological behavior, location and age distribution. Variants of a specific entity are defined by a certain, confirmed histological identity with a specific pathological significance.

Glioma is considered a brain tumour of a glial origin that encompasses all grades of WHO astrocytic tumours, oligodendrogliomas, ependymomas and mixed gliomas (Louis, Ohgaki et al. 2007). Histological grading included in the WHO brain tumour classification defines the malignancy scale and plays a role in the choice of therapy and proper chemotherapy protocol in the clinical setting. Across all tumour entities the WHO

established four grades of malignancy (Louis, Ohgaki et al. 2007). Grade I is characterized by low proliferative potential where the lesion can be cured following surgical resection. Grade II neoplasms (diffuse astrocytomas) are defined as a low proliferative lesion but can infiltrate and often recur with a propensity to progress to a higher grade of malignancy. The WHO grade III tumours (anaplastic astrocytomas) present with malignancy characteristics such as high mitotic index and nuclei atypia. The choice of therapy regimen in patients with grade III tumours usually includes adjuvant radiation and chemotherapy. Finally, grade IV glioma or glioblastoma multiforme (GBM) represents the most aggressive form of brain tumour due to its highly infiltrative nature, pre- and postoperative spread to surrounding tissues and very poor survival (Table 2). GBM demonstrate extreme heterogeneity when assessed by gross pathology (necrosis prone lesions or hemorrhage), microscopic assessment (microvascular proliferation, pleomorphic nuclei) and genetic diversity. At a molecular level glioma is characterized by a multitude of genetic amplifications, deletions and mutations; these characteristics contribute to the chemo- and radio- resistance of this disease.



	I	II	III	IV		I	II	III	IV
<b>Astrocytic tumours</b>									
Subependymal giant cell astrocytoma	•				Central neurocytoma		•		
Pilocytic astrocytoma	•				Extraventricular neurocytoma		•		
Pilomyxoid astrocytoma		•			Cerebellar liponeurocytoma		•		
Diffuse astrocytoma		•			Paraganglioma of the spinal cord	•			
<i>Pleomorphic xanthoastrocytoma</i>		•			Papillary glioneuronal tumour	•			
Anaplastic astrocytoma			•		Rosette-forming glioneuronal tumour of the fourth ventricle	•			
Glioblastoma				•					
Giant cell glioblastoma				•	<b>Pineal tumours</b>				
Gliosarcoma				•	Pineocytoma	•			
					Pineal parenchymal tumour of intermediate differentiation		•	•	
<b>Oligodendroglial tumours</b>					Pineoblastoma				•
Oligodendroglioma			•		Papillary tumour of the pineal region		•	•	
Anaplastic oligodendroglioma				•					
					<b>Embryonal tumours</b>				
<b>Oligoastrocytic tumours</b>					Medulloblastoma				•
Oligoastrocytoma			•		CNS primitive neuroectodermal tumour (PNET)				•
Anaplastic oligoastrocytoma				•	Atypical teratoid / rhabdoid tumour				•
<b>Ependymal tumours</b>					<b>Tumours of the cranial and paraspinal nerves</b>				
Subependymoma	•				Schwannoma	•			
Myxopapillary ependymoma	•				Neurofibroma	•			
Ependymoma		•			Perineurioma	•	•	•	
Anaplastic ependymoma			•		Malignant peripheral nerve sheath tumour (MPNST)		•	•	•
<b>Choroid plexus tumours</b>					<b>Meningeal tumours</b>				
Choroid plexus papilloma	•				Meningioma	•			
Atypical choroid plexus papilloma		•			Atypical meningioma		•		
Choroid plexus carcinoma			•		Anaplastic / malignant meningioma			•	
					Haemangiopericytoma		•		
<b>Other neuroepithelial tumours</b>					Anaplastic haemangiopericytoma			•	
Angiocentric glioma	•				Haemangioblastoma	•			
Chordoid glioma of the third ventricle		•							
					<b>Tumours of the sellar region</b>				
<b>Neuronal and mixed neuronal-glial tumours</b>					Craniopharyngioma	•			
Gangliocytoma	•				Pituicytoma	•			
Ganglioglioma	•				Granular cell tumour of the neurohypophysis	•			
Anaplastic ganglioglioma			•		Spindle cell oncocytoma of the adenohypophysis	•			
Desmoplastic infantile astrocytoma and ganglioglioma		•							
Dysembryoplastic neuroepithelial tumour	•								

**Table 2.** WHO Grading of Tumours of the Central Nervous System. Modified with permission: Springer© (license# 3150870813401) and Louis, D. N., H. Ohgaki, et al. 2007. Acta Neuropathol. 2007 Aug;114(2):97-109 .

### *Molecular multiplicity of brain cancer*

Genomic profiling leading to molecular classification of tumours is emerging as an indispensable tool in modern medicine. By sequencing 22,661 genes Parsons *et al.* established that on average over 45 different mutations characterize a single GBM tumour (Parsons, Jones et al. 2008). Work performed by The Cancer Genome Atlas (TCGA) Research Network (TCGA 2008), involving 91 GBM samples, established that 223 genes were affected by 453 non-silent somatic mutations (Verhaak, Hoadley et al. 2010). The high throughput and comprehensive analysis of next-generation sequencing technologies provides extensive data useful for molecular classification of GBM. The detailed analysis of 601 genes revealed a mutational spectrum within p53, Rb and tyrosine kinase pathways establishing the noted aberrations as the requirement in GBM pathogenesis (TCGA 2008). Based on the core gene expression, as well as copy number data, four GBM subtypes emerged that contribute to better understanding of molecular networks behind GBM pathology and potentially advance therapeutic strategies in a clinical setting. The specifics of these subtypes are outlined below:

#### *Classical subtype*

The Classical subtype is characterized by amplification of chromosome 7 and loss of chromosome 10. Epidermal growth factor receptor (*EGFR*) amplification was also observed in 97% of samples tested and was followed by a four-fold increase in *EGFR* expression. Point or variant III (vIII) mutations of *EGFR* accounted for 54% of the pool analysed (Verhaak, Hoadley et al. 2010). Interestingly, focal homozygous deletion of the 9p21.3 locus encoding for both *p16<sup>Ink4a</sup>* and *p14<sup>ARF</sup>* occurs frequently in this subtype and is correlated with *EGFR* amplification in almost 95% of samples tested. Furthermore,

mutations in the 9p21.3 locus exclusively affected the integrity of the Rb pathway. Notably, several marker proteins involved in stemness were upregulated in the Classical subtype including Notch and Sonic hedgehog signaling pathways. Although mutations to *p53* are the most common aberration among human brain tumours, the Classical subclass demonstrates lack of mutations in the gene. Moreover, the Classical subtype is strongly associated with the gene expression characteristic of mature astrocytes (Verhaak, Hoadley et al. 2010).

#### *Mesenchymal subtype*

Deletion of neurofibromatosis 1 (*NFI*) was observed to be the most significant and frequent mutation in the mesenchymal subclass of glioma, accounting for 53% of the samples tested. Interestingly, the *NFI* deletion frequently co-occurred with phosphatase and tensin homolog (*PTEN*) mutations indicating that the Akt pathway plays a crucial role in this subset. PTEN holds phosphatase activity and acts primarily through PI3K pathway inhibition but a role in cell cycle regulation has been reported as well (Koul 2008). The high activity of the super family of tumour necrosis factor and Nuclear Factor kappa-light-chain-enhancer of activated B cells (NF $\kappa$ B) pathway was demonstrated to occur in the mesenchymal subclass (Verhaak, Hoadley et al. 2010). This suggests that an elevated fraction of necrosis and presence of inflammatory infiltrates. In addition, characteristic expression of mesenchymal markers were noted and samples tested within the subclass expressed the signature of astroglial cultured cells, as well as elevated levels of microglial markers. Interestingly, the majority of immortalized cell lines analyzed represented the genetic signature of the mesenchymal subset of GBM (Verhaak, Hoadley et al. 2010).

### *Proneural subtype*

Focal 4q12 amplification of the platelet-derived growth factor receptor  $\alpha$  (*PDGFRA*) locus was found in all GBM samples tested, the proneural subset of glioma was characterized by a significant upregulation in the frequency of this aberration and subsequent overexpression of *PDGFRA* (Verhaak, Hoadley et al. 2010). In addition, several point mutations in the so called Ig-domain of *PDGFRA* are found, these mutations can potentially disrupt the binding of the PDGF ligand to the receptor (Verhaak, Hoadley et al. 2010). Another major feature of the proneural subtype is multiple point mutations in the isocitrate dehydrogenase 1 gene (*IDH1*) (Verhaak, Hoadley et al. 2010). The overall analysis showed that *p53* mutations and loss of heterozygosity (LOH) are more frequent in the proneural samples than in any other subtype of glioma. Interestingly, the proneural samples expressed oligodendrocytic but not astroglial markers and were characterized by upregulation of oligodendrocyte development related genes (Verhaak, Hoadley et al. 2010). Oligodendrocyte developmental genes have a pronounced downregulation of p21<sup>Cip1</sup> levels and an increase in markers indicative of proliferative potential in neural stem cells and glioma. Patients falling under the proneural subtype tend to be at an overall younger age distribution (Verhaak, Hoadley et al. 2010). Proneural-type tumours represented three out of four secondary GBMs tested (Verhaak, Hoadley et al. 2010). The secondary GBMs were originally derived from lower grade neoplasia or *IDH1* mutations. Importantly, unlike any other subtype, intensifying chemotherapy did not decrease mortality in patients with proneural tumours (Verhaak, Hoadley et al. 2010).

### *Neural subtype*

Neural subtypes are characterized by the expression of neuronal markers, including genes involved in neurite and axon outgrowth, synaptogenesis and synaptic transmission (Verhaak, Hoadley et al. 2010). The neural subclass samples expressed several genes reflecting differentiated neuronal phenotype but were positive for astrocytic and oligodendrocytic markers as well. Importantly, the gene expression signatures are very close to the ones obtained from normal brain tissue despite the fact that the samples analysed demonstrate typical GBM tumour morphology, multiple mutations as well as copy number alterations (Verhaak, Hoadley et al. 2010).

In conclusion, the genetic multiplicity of the proposed GBM subtypes indicates the importance and need for the development of therapeutically diverse strategies to achieve clinical success. Targeting the populations of cells responsible for GBM initiation, progression and resistance to therapy requires their prior identification. The work performed by the TCGA research network demonstrated a strong correlation between the established GBM classes and normal neural lineages suggesting that a common neural stem cell that undergoes aberrations at different levels of its commitment may constitute the source of glioma. Importantly, self-renewing neural cells found within the brain demonstrate expression of distinct markers including either EGFR or PDGFRA (Jackson, Garcia-Verdugo et al. 2006) indicating potential diversity among the populations, possibly correlating to their level of lineage commitment.

### *The role of G1 phase in neural tumourigenesis*

Compromised control of progression from G1 to S phase and reactivation from the quiescent state leading to inappropriate proliferation characterises virtually all malignant cells. As anticipated, disrupting the network of G1 phase regulation constitutes an important mechanistic basis behind neoplasia. Among extensive literature demonstrating distinct aberrant pathways behind cancer, several lines of evidence support the uncontrollable role of cyclins, CDKs and cell cycle inhibitors in multiple cancers including glioma.

### *D-type Cyclins and gliomagenesis*

#### *Deregulation of the D-type Cyclins in glioma*

Glioma cells gain proliferative benefit by evading the strict control of the G1-S cell cycle checkpoint. The Cyclin D-CDK4/ Rb axis is a primary mechanism controlling the checkpoint (Serrano, Hannon et al. 1993). Chakravarti *et al.* demonstrated that Rb control over E2F1 is lost or deregulated in 91% of the glial tumours tested (Chakravarti, Delaney et al. 2001). This occurs due to deactivating or deletion mutations in the Rb gene (Chakravarti, Delaney et al. 2001). Furthermore, amplification of the CDK4 and D-type Cyclin loci are also reported (2008; Koyama-Nasu, Nasu-Nishimura et al. 2012). G1 activators, Cyclin D1, Cyclin E1 and CDK4 have been reported to be upregulated in ~22% of human glioma (Chakravarti, Delaney et al. 2001). Furthermore, Cyclin D1 is elevated in progressively higher grades of glioma (Cavalla, Dutto et al. 1998; Hecker, Grammer et al. 2002). Several studies have reported that the overexpression of Cyclin D1 is associated with proliferative, antiapoptotic and proinvasive phenotypes correlating with

poor patient prognosis (Buschges, Weber et al. 1999; Sallinen, Sallinen et al. 1999; Wang, Wang et al. 2012).

An elegant study by Read *et al.* which utilized an organotypic and cell type specific glioma model in *Drosophila*, revealed that constitutive co-activation of EGFR and phosphatidylinositide 3-kinase (PI3K) - pathways contributes to the malignant transformation of normal glial cells and results in tumour-like masses (Read, Cavenee et al. 2009). In this study, overexpression of both pathways led to the suppression of cell cycle exit selectively in glia but not in neurons or neuronal precursor cells. Unconstrained cell cycle progression and entry resulted in unchecked proliferation and formation of transplantable, neoplastic growths that mimic human glioma. Importantly, the study established pivotal EGFR and PI3K downstream pathways that cooperate in glioma initiation and progression. Among these, the cell cycle regulatory axis emerged as a crucial component in the combinatorial network behind the glial neoplastic transformation. Specifically, the Cyclin D1-CDK4 complex was shown to play a critical role in c-Myc driven EGFR/ PI3K tumorigenesis which was mediated by Rb inactivation and inhibition of cell cycle exit (Read, Cavenee et al. 2009).

EGFR overexpression, amplification and frequent mutation, resulting in the truncated *EGFRvIII* form, are often observed in human glioma (Nishikawa, Ji et al. 1994; Huang, Nagane et al. 1997; Halatsch, Schmidt et al. 2006). Notably, EGFR inhibition was shown previously to correlate with reduced Cyclin D1 levels and concomitant cell cycle arrest in malignant glioblastoma (Ramis, Thomas-Moya et al. 2012). Furthermore, the regulation of Cyclin D1-mediated proliferation as a direct output of EGFR activity in glioma cells was demonstrated to function under the control of Notch1, which plays an important role in glioblastoma pathogenesis (Fan, Mikolaenko et al. 2004; Purow, Haque

et al. 2005; Fan, Khaki et al. 2010). Interestingly, Cyclin D1 was demonstrated previously to be a direct transcriptional target of activated Notch1 signalling (Ronchini and Capobianco 2001; Stahl, Ge et al. 2006), which is essential for Notch1-mediated transformation events (Stahl, Ge et al. 2006). In summary, Cyclin D1 expression and its cell cycle control in glioma cells can be regulated by mitogen activated transduction pathways or Notch, however their exact cooperation requires further investigation.

Interestingly a novel mechanism of Cyclin D1 regulation in glioma cells was described by Hui *et al.* that involved a micro RNA molecule that is significantly downregulated in both brain tumour cell lines and tissues obtained from glioma patients (Hui, Yuntao et al. 2013). miR195 overexpression was reported to decrease the G0 and G1 cell fraction, reduce anchorage independent growth and upregulate hyperphosphorylated Rb. The observed changes in glioblastoma cell characteristics were attributed to a decline in the protein levels of both Cyclin D1 and Cyclin E1. miR195 was revealed to downregulate the expression of both Cyclin D1 and E1 at the posttranscriptional level through targeting their 3' untranslated regions (3'UTRs) (Hui, Yuntao et al. 2013). Thus loss of miR195 in human glioma contributes to upregulation of Cyclin D1/ E1-mediated proliferation.

#### *Cyclin D1 and glioma invasion*

The aggressive character of glial tumours is associated with cellular invasion due to extracellular matrix (ECM) degradation and changes in cellular motility reviewed in (Hood and Cheresch 2002). Digestion of the ECM is performed by a family of enzymes known as matrix metalloproteinases (MMPs). The production of MMPs in higher but not in lower grades of glioma suggests their potential role in tumour progression (Sawaya,



Yamamoto et al. 1996; Arato-Ohshima and Sawa 1999). The function of Cyclin D1 in promoting glioma to more aggressive stages may depend on the ability of the D-type Cyclins to modulate the tumour microenvironment. Cyclin D1 overexpression is accompanied by an increased invasive phenotype that correlates with elevated levels and activity of MMPs. A Cyclin D1-mediated increase in MMP activity is speculated to involve extracellular-signal-regulated kinases (ERKs) (Gum, Wang et al. 1997). Cyclin D1 was reported previously to cause an elevation of ERK expression, whereas ERK dependent signalling is known to induce MMPs levels (Gum, Wang et al. 1997).

Cyclin D1 is suggested to play a role in cellular motility as its overexpression leads to a significant increase in the levels of Rac-1, one of the major regulators of cytoskeleton organization (Arato-Ohshima and Sawa 1999). The Cyclin D1-mediated upregulation of Rac-1 is followed by membrane ruffling, which is a typical characteristic of invasive cells (Arato-Ohshima and Sawa 1999). Moreover, Cyclin D1 was demonstrated to play an essential role in focal adhesion kinase (FAK) -mediated proliferation. FAK is a tyrosine kinase that plays a role in adhesion and mobility and its overexpression was previously shown to increase metastatic activity in breast cancer cells (Chan, Cortesio et al. 2009). FAK protein levels and activity are frequently elevated in anaplastic astrocytoma and GBM (Zagzag, Friedlander et al. 2000; Hecker, Grammer et al. 2002). Interestingly, the observed increase in cell cycle progression rate in FAK overexpressing glioma cells was suppressed upon downregulation of Cyclin D1 but not Cyclin E1 (Ding, Grammer et al. 2005). These data suggest a unique role for Cyclin D1 in FAK- driven invasion of glioma cells. Notably, Cyclin D1-CDK4 activity appears to be obligatory for glioma formation and progression in the platelet derived growth factor (PDGF)-induced tumour mouse model. Although Cyclin D1 knockout mice still develop brain tumours, the progression to

higher grades of malignancy is perturbed (Ciznadija, Liu et al. 2011). Interestingly, Cyclin D1 deficient mice fail to fully recruit and activate the tumour associated microglia that were previously implicated in promotion of gliomagenesis to higher stages. Thus, Cyclin D1 and CDK4 are required for the proper function of tumour activated microglia or for other populations of stromal cells that support their activation (Ciznadija, Liu et al. 2011). This suggests an essential role for Cyclin D1 in mediating the microenvironment effects in glioma progression.

In summary Cyclin D1 overexpression in glioma plays a role in cellular adhesion, degradation of the ECM and cellular motility through regulating key proteins involved in the invasive character of the GBM. The mechanistic details of this regulation remain to be determined.

#### *Cyclin D and Brain Tumour Initiating Cells (BTICs)*

A population of multipotent BTICs is speculated to reside within the brain tumour mass. BTICs express NSC markers, including CD133 and Musashi-1 (Toda, Iizuka et al. 2001; Hemmati, Nakano et al. 2003; Bao, Wu et al. 2006). Functionally BTICs self-renew and form tumours upon xenotransplantation to immunocompromised mice (Singh, Hawkins et al. 2004; Wang, Wang et al. 2008; Koyama-Nasu, Nasu-Nishimura et al. 2012). Moreover, BTICs contribute to glioma progression and to glioma resistance to chemo- and radiotherapy of the tumour (Barnes, Porter et al. 2003; Sakariassen, Immervoll et al. 2007; Beier, Schulz et al. 2011). Importantly, existence of stem-like cancer initiating cells has been reported in a broad variety of other tumours (Huntly and Gilliland 2005; Hassan, Wang et al. 2013; Zomer, Ellenbroek et al. 2013); however, the

characteristics of the cell cycle components that control the tumourigenicity of BTICs remain under investigation.

Recently, Cyclin D2 was demonstrated to play a crucial role in cell cycle progression and tumourigenic potential in BTICs (Koyama-Nasu, Nasu-Nishimura et al. 2012). In the proneural subtype of glioma, Cyclin D2 levels were upregulated in undifferentiated self-renewing BTICs whereas differentiated cells of the same type demonstrated almost no Cyclin D2 expression (Koyama-Nasu, Nasu-Nishimura et al. 2012). Additionally, both Cyclin D2-CDK4 and -CDK6 complexes were responsible for Rb phosphorylation in undifferentiated cells. In contrast, Cyclin D2 downregulation in self-renewing populations of glioma initiating cells led to a significant increase in the fraction of G1-arrested cells and decreased phosphorylation of Rb. Notably, Cyclin D2 knockdown effects were not mimicked by downregulation of Cyclins D1 or D3 (Koyama-Nasu, Nasu-Nishimura et al. 2012).

Cyclin D2 is not expressed in cells obtained from patients with the mesenchymal subtype of glioma and its expression is found to be significantly upregulated in higher grades of glioma in comparison to lower ones (Koyama-Nasu, Nasu-Nishimura et al. 2012). These data suggest a role for BTICs in the more aggressive subtypes of glioma. Indeed, self-renewing glioma cells transplanted into immunocompromised mice produce significantly more severe tumours than that seen with differentiated cells, and severity correlates with Cyclin D2 expression (Koyama-Nasu, Nasu-Nishimura et al. 2012). Xenografts of BTICs with knocked down Cyclin D2 result in increased survival of recipient mice in comparison to control cells (Koyama-Nasu, Nasu-Nishimura et al. 2012). Overall, Cyclin D2, but not Cyclin D1 or D3, is the most abundantly expressed D-type Cyclin in human glioma initiating cells contributing to their increased cell cycle

progression and tumourigenicity (Koyama-Nasu, Nasu-Nishimura et al. 2012). Owing to the fact that adult NSCs primarily express Cyclin D2, one can speculate that the presence of Cyclin D2 in BTICs could have conferred the tumourigenic potential to normal NSCs (Kowalczyk, Filipkowski et al. 2004; Walzlein, Synowitz et al. 2008; Koyama-Nasu, Nasu-Nishimura et al. 2012).

Surprisingly, it has been demonstrated that in opposition to Cyclin D2, Cyclin D1 levels are found to be higher in glioma cells that undergo differentiation, and consequently, the knockdown of Cyclin D1 in differentiated cells causes an increase in the number of tumour cells residing in G1 phase (Koyama-Nasu, Nasu-Nishimura et al. 2012). Interestingly, Cyclin D1, but not Cyclin D2 or E1, was previously suggested to regulate cell cycle progression in the CD133+ glioma cell populations as its levels were downregulated in c-Myc knockdown cells followed by a decline in self-renewal as well as decreased tumour formation capacity (Pacey, Stead et al. 2006; Wang, Wang et al. 2008). Since the expression of Cyclin D1 but not Cyclin D2 was reported in the mesenchymal group of glioma cells (Koyama-Nasu, Nasu-Nishimura et al. 2012), the observed discrepancy in the reported role of Cyclin D1 and D2 in glioma stem cells can be attributed to the different subtypes of glioma used for the studies. Moreover, the differences suggest that the role of Cyclin D1 might be restricted to a specific, CD133+ population of glioma initiating cells and so far Cyclin D2 function has been only addressed in a heterogeneous glioma populations.

In support of this, Cyclin D1 driven activity of CDK4 is known to play an essential role in the radiation resistance of the CD133+ glioma cells. The CD133 enriched population exhibits a significant decrease in radiosensitivity due to the upregulated Akt/ Cyclin D1 pathway. Akt suppresses glycogen synthase kinase-3 beta (GSK3 $\beta$ – mediated

degradation of Cyclin D1 and thus promotes its function (Shimura, Noma et al.). Importantly, besides its role in promoting G1 phase progression, Cyclin D1 plays a critical role in DNA damage repair as shown previously by Jirawatnotai *et al.*, indicating its high importance in BTIC targeting therapies. Depletion of Cyclin D1 was demonstrated to reduce homologous recombination repair in radioresistant cells (Kao, Jiang et al. 2007; Shimura, Kakuda et al. 2011). To execute this particular function Cyclin D1 cooperates with Rad51, a recombinase responsible for the homologues repair processes (Kao, Jiang et al. 2007; Jirawatnotai, Hu et al. 2011).

To summarize, both Cyclin D1 and D2 emerge as key players promoting proliferation and self-renewal in BTICs. Furthermore, the specific expression of D-type Cyclins in different subsets of glioma and the role of Cyclin D1 in radio-resistance suggest their potential advantage not only as prognostic markers but also in improving the efficacy of radiotherapy.

#### *Cyclin E1 and gliomagenesis*

#### *Cyclin E1 and genetic instability in glioma*

Accumulation of Cyclin E1 in cancer cells occurs due to an amplification of the gene (Akama, Yasui et al. 1995; Kitahara, Yasui et al. 1995; Courjal, Louason et al. 1996; Marone, Scambia et al. 1998) as well as posttranscriptional modifications responsible for increased protein levels (Porter, Malone et al. 1997). In addition there are known splice variants of Cyclin E1 that do not appear in conditions of normal cell cycle function (Sewing, Ronicke et al. 1994; Mumberg, Wick et al. 1997). It has been established that Cyclin E1-mediated tumorigenesis is attributed to genetic instability (Loeb, Kostner et al. 2005). Cyclin E1 overexpression alone or with a disabled p53 dependent checkpoint

causes aneuploidy in human cancer and primary cells (Spruck, Won et al. 1999; Minella, Swanger et al. 2002; Hwang and Clurman 2005). This aneuploidy is speculated to arise from defects in S-phase progression caused by faulty MCM loading, resulting in a stalled replication fork and subsequent breakage of the DNA (Hwang and Clurman 2005). This results in overridden checkpoint and defects in chromosome condensation and pairing. Moreover, although centrosome function defects are not observed upon Cyclin E1 depletion, centrosome amplification and aneuploidy were reported when Cyclin E1 was overexpressed following loss of p53 (Kawamura, Izumi et al. 2004; Hwang and Clurman 2005). Multiple studies suggest that Cyclin E1 takes part in, or contributes to a neoplastic event, rather than initiating tumorigenesis (Geisen and Moroy 2002; Martins and Berns 2002); (Haas, Johannes et al. 1997). Importantly, double Cyclin E1 and E2 knockout mice demonstrate resistance to oncogenic transformation with overexpression of Ras, c-Myc and a dominant negative mutant of p53 in different combinations (Geng, Yu et al. 2003). Consistently, several lines of evidence show that excess of Cyclin E1 in human brain cancer contributes to more aggressive presentation and poor patient survival (Tamiya, Mizumatsu et al. 2001).

#### *Impaired degradation of Cyclin E1 in glioma*

Cyclin E1 degradation is known to play a crucial role in glioblastoma (Hagedorn, Delugin et al. 2007) as the forced expression of its non-degradable mutant contributes to an increase in chromosomal aberration events (Hwang and Clurman 2005). The ubiquitination and subsequent proteasomal degradation of Cyclin E1 in human glioma cells is frequently impaired due to the reduced levels or loss of function mutations in the Parkinson protein 2 (PARK 2) E3 ubiquitin ligase (Veeriah, Morris et al. 2010; Veeriah,

Taylor et al. 2010; Vlachostergios, Voutsadakis et al. 2012; Yeo, Ng et al. 2012). Cancer specific mutations analyzed by Veeriah *et al.* showed an attenuated interaction between PARK 2 and Cyclin E1 in glioblastoma cells (Veeriah, Morris et al. 2010). In addition, PARK 2 knockdown results in stabilization and accumulation of Cyclin E1 followed by an increased fraction of cells in S and G2/M phases, multipolar spindles and abnormal mitoses associated with genetic anomalies (Veeriah, Morris et al. 2010).

Interestingly, a tumour suppressor FBXW7/ hCDC4 (Akhoondi, Sun et al. 2007), known to be responsible for Cyclin E1 targeted proteolysis, was shown to be significantly reduced in human astroglial tumours (Hagedorn, Delugin et al. 2007). FBXW7/ hCDC4 genetic inactivation, followed by loss of function, was demonstrated previously to attenuate cell cycle control of Cyclin E1 and result in genetic alternations prior to malignant transformation (Ekholm-Reed, Spruck et al. 2004; Rajagopalan, Jallepalli et al. 2004). According to Hedegorn *et al.*, hCDC4 levels are significantly reduced in grade IV gliomas in comparison to lower grades (Hagedorn, Delugin et al. 2007). The decrease in FBXW7/ hCDC4 expression levels correlates with accumulation of Cyclin E1 levels and corresponds with defective chromosome segregation at mitosis (Hagedorn, Delugin et al. 2007). In summary, mutations or defects in protein degradation that lead to an increase in Cyclin E1 levels play a significant role in human gliomagenesis.

#### *Cyclin E1 and p27 in neural tumourigenesis*

The role of Cyclin E1 in the initiation and progression of CNS malignancies is known to cooperate with the attenuated role of the p27<sup>Kip1</sup> cell cycle inhibitor (Tamiya, Mizumatsu et al. 2001). Consequently, it has been established that patients with low Cyclin E1 and high p27<sup>Kip1</sup> levels have the best survival prognosis, whereas the worst

survival is observed in patients with high Cyclin E1 and low p27<sup>Kip1</sup> levels (Tamiya, Mizumatsu et al. 2001). These data suggest that the ratio of Cyclin E1: p27<sup>Kip1</sup> could serve as a potential prognostic marker for at least subsets of glioma.

Moreover, pituitary brain tumours are known to rely on defects in p27 function (Roussel-Gervais, Bilodeau et al. 2010). Conditional expression of Cyclin E1 into the corticotroph cells of the pituitary gland causes cell cycle re-entry of quiescent cells and subsequent hyperplasia (Roussel-Gervais, Bilodeau et al. 2010). Although the cells exhibit defects in centrosome structure and number, the occurrence of hyperplasia and pituitary brain tumours is low and suggests a limited effect of Cyclin E1 function. Interestingly, forced expression of Cyclin E1 in p27<sup>Kip1</sup><sup>-/-</sup> cells results in a higher frequency and larger size of pituitary brain tumours (Roussel-Gervais, Bilodeau et al. 2010).

PTEN loss of function has been widely described in glioma (Brat, Castellano-Sanchez et al. 2002; Hill, Hunter et al. 2003; Mischel and Cloughesy 2003). Its overexpression in different glioblastoma cell lines causes G0/G1 cell cycle arrest due to suppressed activity of CDK2, but not CDK4, and accumulation of hypophosphorylated Rb (Cheney, Neuteboom et al. 1999). Interestingly, PTEN upregulation has no effect on Cyclin E1 expression levels but significantly increases the amount of p27<sup>Kip1</sup> protein bound to Cyclin E1-CDK2 immunocomplexes (Cheney, Neuteboom et al. 1999). PTEN was demonstrated to selectively stimulate p27<sup>Kip1</sup> transcription by the induction of forkhead transcription factors (Medema, Kops et al. 2000; Nakamura, Ramaswamy et al. 2000). PTEN can also reduce the ubiquitin-mediated degradation of p27<sup>Kip1</sup> (Mamillapalli, Gavrilova et al. 2001). Each of these examples ensure there are sufficient levels of p27<sup>Kip1</sup> to suppress Cyclin E1-CDK2 activity and keep cell cycle progression in



check. Hence, it can be speculated that this mechanism is frequently lost in glioblastoma due to *PTEN* mutations allowing cells to proliferate out of control.

Skp2 is a substrate targeting subunit of the Skp2, Cullin, F-box containing E3 ubiquitin ligase complex ( $SCF^{Skp2}$ ) that participates in p27<sup>Kip1</sup> proteolytic degradation (Carrano, Eytan et al. 1999; Tsvetkov, Yeh et al. 1999) and is often overexpressed in cancer (Gstaiger, Jordan et al. 2001). Skp2 was shown to be significantly upregulated in *PTEN*<sup>-/-</sup> embryonic cells whereas PTEN overexpression in glioma cells causes a decline in Skp2 levels and PTEN-mediated p27<sup>Kip1</sup> upregulation, resulting in Cyclin E1-CDK2 suppression (Mamillapalli, Gavrilova et al. 2001). Cyclin E1-CDK2 has the ability to phosphorylate p27<sup>Kip1</sup> on Thr-187 residue to target it for degradation (Sheaff, Groudine et al. 1997; Vlach, Hennecke et al. 1997). Interestingly, although Cyclin E1 overexpression restores CDK2 activity it does not downregulate p27<sup>Kip1</sup> levels, suggesting that Cyclin E1 expression in the absence of Skp2 is not sufficient to rescue a PTEN-induced cell cycle arrest in glioma cells; however, coexpression of Cyclin E1 and Skp2 results in a greater effect on cell cycle progression than Skp2 alone (Mamillapalli, Gavrilova et al. 2001).

In summary, Cyclin E1-induced cell cycle progression is not sufficient to drive gliomagenesis alone but Cyclin E1-CDK2 does participate in the multistep gliomagenesis process. This multistep process depends on many changes, including downregulation of cell cycle inhibitors.

### *Cyclin E1 and BTIC*

The Cyclin E1-mediated hyperproliferative potential and ability to recover the cell cycle from a quiescent state can be useful in activation and driving of populations of human glioblastoma initiating cells. Several studies suggesting that Cyclin E1 expression

contributes to gliomagenesis address their questions in heterogeneous populations of glioma cells and little is known about the role of Cyclin E1 in the self-renewing BTICs.

Inhibitor of differentiation 4 (Id4) plays role in fate determination of NSCs and was demonstrated to drive transformation and induce a dedifferentiated and self-renewing phenotype in *Ink4/Arf<sup>-/-</sup>* glia (Jeon, Jin et al. 2008). Cell cycle analysis of the transformed astrocytes revealed significant upregulation of Cyclin E1 and hyperphosphorylation of Rb. Consequently, Cyclin E1 knockdown resulted in a significant decrease in proliferation. Tumour formation from Cyclin E1 overexpressing *Ink4/Arf<sup>-/-</sup>* xenografts was not as pronounced as the tumour growth from Id4 *Ink4/Arf<sup>-/-</sup>* astrocytes. Moreover, Cyclin E1 knockdown significantly reduced the size of the Id4 *Ink4/Arf<sup>-/-</sup>* tumours and tumour cell proliferation, confirming that Id4-induced gliomagenesis depends on Cyclin E1-mediated proliferation (Jeon, Jin et al. 2008). Notably, self-renewal analysis, including stem cell marker expression and neurosphere formation capacity, showed that neither Cyclin E1 overexpression nor Cyclin E1 downregulation had any effect on the functional parameters of the stem cell population (Jeon, Jin et al. 2008). Cyclin E1 levels were also demonstrated to increase in human glioma upon Id4 overexpression, the above data suggests that the role of Cyclin E1 is important at the level of proliferation in the self-renewing populations of glioma cells; however its function is dispensable for clonal growth in this particular system studied. Consequently, whether BTIC self-renewal is coupled to cell cycle machinery through Cyclin E1 remains elusive.

Cyclin E1 was demonstrated previously to act as a limiting factor in G0 arrest (Geng, Yu et al. 2003). Additionally, Groszer *et al.* suggested that the regulation of self-renewal is tightly associated with G0/G1 cell cycle entry control in *PTEN<sup>-/-</sup>* neural stem cells (Groszer, Erickson et al. 2006). *PTEN* mutations that are extremely common in

human glioblastoma (Brat, Castellano-Sanchez et al. 2002; Hill, Hunter et al. 2003; Mischel and Cloughesy 2003) are found to result in enhanced cell cycle progression due to unchecked activity of CDK2 driven by Cyclin E1 (Groszer, Erickson et al. 2001). Interestingly, the loss of PTEN function in NSCs correlates with increased proliferative potential due to shortened cell cycle time (Groszer, Erickson et al. 2001). Furthermore, *PTEN* deficiency was demonstrated to confer sustained self-renewal and multilineage differentiation potential in long-term cultures of NSCs suggesting a potential mechanism involving PTEN and G1 regulation in glioma stem cells. *PTEN*<sup>-/-</sup>-induced self-renewal was demonstrated to rely on enhanced quiescent state arrest and cell cycle re-entry which is accompanied by increased levels of Cyclin E1 and Cyclin D1.

Given the importance of Cyclin E1-CDK2 suppression in PTEN-mediated pathways, the crucial question remains if the molecular mechanism underlying self-renewal and proliferation of *PTEN*<sup>-/-</sup> NSCs shares similarity with *PTEN*-loss dependent tumourigenic behaviour of glioblastoma cells. Since Cyclin E1-CDK2 activity control is lost in *PTEN*-deficient glioma cells, one can speculate that the observed shortened G1 phase contributes to a decreased growth factor dependence, one established hallmark of cancer (Hanahan and Weinberg 2000).

To summarize, the available literature suggests that Cyclin E1 functions in the crosstalk between multiple tumour suppressors and oncogenes and constitutes an important link between cell cycle and gliomagenesis. Cyclin E1 overexpression alone is not sufficient to drive transformation in the neural systems studied, however its role contributes to uncontrolled S-phase entry, excessive proliferation and genetic instability.

The role of the main G1 phase cyclin components discussed in this section reflects close collaboration between cell cycle machinery and frequently disrupted pathways in

human glioblastoma. Mutations in *EGFR* and *PTEN*, corrupted Rb pathway and perturbations in proper degradation of crucial proteins drive tumourigenesis in neural systems. The genetic instability and deregulation of signal transduction pathways conferred by Cyclin E1 and D-type Cyclins respectively are known hallmarks of cancer. All of the aberrant events presented in this section use the G1 cyclin network components to execute their function. Furthermore, the mechanisms underlying changes in the brain tumour microenvironment as well as extensively studied self-renewing populations of BTICs can be addressed in a cell cycle dependent manner as several of them require G1 cyclin function.

#### *Spy1 family of cell cycle regulators*

##### *Speedy/RINGO family and human Spy1*

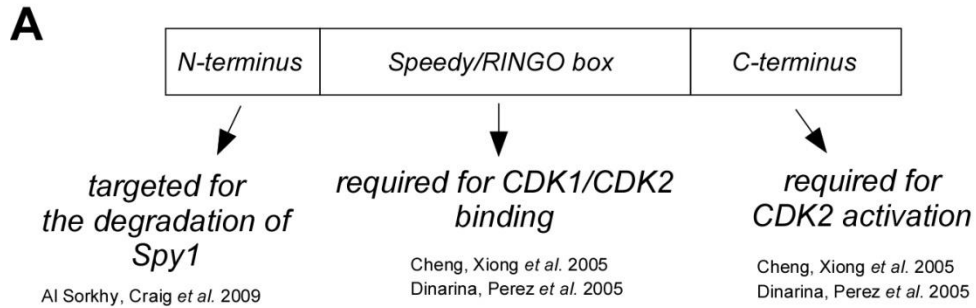
Spy1 or Speedy/RINGO (Rapid Inducer of G2/M progression in Oocytes) protein was initially identified in a genetic screen of a *Xenopus laevis* ovarian cDNA library (Lenormand, Dellinger et al. 1999), in the fission yeast cell line. The cell line used was deficient for cell cycle checkpoint gene *rad1* allowing for isolation of cell cycle regulatory genes that override the G2/M checkpoint and confer resistance to radiation-induced DNA damage (Lenormand, Dellinger et al. 1999). The isolated X-Spy1 clone was able to partially rescue UV sensitivity and provided resistance to ionizing radiation, suggesting that the newly found X-Spy1 regulates the G2/M checkpoint in *Xenopus* oocytes (Lenormand, Dellinger et al. 1999). Furthermore, X-Spy1 mRNA levels were expressed during oogenesis and at early embryogenesis, and microinjection of X-Spy1 mRNA into stage VI oocytes resulted in activation of mitogen-activated protein kinase (MAPK) and CDK1. This occurred at a much faster rate than progesterone-mediated

oocyte maturation with subsequent germinal vesicle breakdown (GVBD). These data indicated that X-Spy1 contributes to oocyte release from a G2 arrest. Despite having no sequence homology to any known proteins, including cell cycle regulators, X-Spy1 was found to associate with CDK2 and cause its precocious activity in Spy1 stimulated oocyte maturation (Lenormand, Dellinger et al. 1999).

To date, no X-Spy1 homologues have been found in yeast, worms, flies or plants (Cheng, Xiong et al. 2005; Dinarina, Perez et al. 2005). There are six mammalian X-Spy1 homologues that constitute the Speedy/RINGO family of proteins (Porter, Dellinger et al. 2002). Interestingly, RINGO/Speedy proteins share a conserved ~100 residue core of a predicted  $\alpha$ -helical structure referred to as Speedy/RINGO box that is crucial for the interaction with a CDK (Cheng, Xiong et al. 2005) (Fig. 5A). Besides the 79- amino acid stretch within the RINGO box that confers 51-67% similarity to all RINGO mammalian proteins, the family members exhibit significant sequence diversity within the flanking termini (Dinarina, Perez et al. 2005). This diversity may reflect differences within the family in the specificity of association with different CDKs and potentially in substrate specificity. Importantly, mammalian RINGO family members were shown to bind to CDK1 and CDK2 but failed to activate CDK4 and CDK6 (Cheng, Xiong et al. 2005; Dinarina, Perez et al. 2005) (Fig. 5B).

The first human Spy1 identified, Spy1A (often referred to as Spy1), was isolated from a human testis cDNA library and shares 40% overall homology with X-Spy1 (Porter, Dellinger et al. 2002). Spy1A has two splice variants, Spy1A1 and Spy1A2, that are both found in mouse and human (Porter, Dellinger et al. 2002; Cheng, Xiong et al. 2005). The Spy1A gene, *SPDYA*, is ubiquitously expressed in most mammalian tissues

with high levels found in the testis and elevated levels found in hormonally sensitive tissues and some fetal tissues including the fetal brain and cerebellum (Porter, Dellinger et al. 2002; Cheng, Xiong et al. 2005). *SPDYA* expression was also found to be cell cycle dependent and occurred specifically at the G1/S transition. Furthermore, consistent with X-Spy1, Spy1A was shown to bind CDK1 and CDK2 and stimulate its activity (Al Sorkhy, Ferraiuolo et al. 2012).



**B**

<b>Name</b>	<b>Species</b>	<b>CDK2 preference</b>	<b>Length (aa)</b>	<b>References</b>
X-RINGO	<i>Xenopus laevis</i>	Cdc2/CDK2	299	Ferby, Blazquez <i>et al.</i> 1999
X-Spy1	<i>Xenopus laevis</i>	Cdc2/CDK2	298	Ferby, Blazquez <i>et al.</i> 1999 Lenormand, Dellinger <i>et al.</i> 1999
Speedy/ RINGO A1 (Spy1A1)	<i>Homo sapiens</i>	Cdc2/CDK2	286	Porter, Dellinger <i>et al.</i> 2002 Dinarina, Perez <i>et al.</i> 2005 Chauhan, Zheng <i>et al.</i> 2012
	<i>Mus musculus</i>		283	
	<i>Pan troglodytes</i>		313	
	<i>Danio rerio</i>		289	
Speedy/ RINGO A2 (Spy1A2)	<i>Homo sapiens</i>	Cdc2/CDK2	313	Kume, Endo <i>et al.</i> 2007 Cheng, Xiong <i>et al.</i> 2005
	<i>Mus musculus</i>		310	
	<i>Sus scrofa</i>		311	
Speedy/ RINGO B	<i>Mus musculus</i>	Cdc2	268	Dinarina, Perez <i>et al.</i> 2005 Cheng, Xiong <i>et al.</i> 2005
Speedy/ RINGO C	<i>Homo sapiens</i>	Cdc2/CDK2	293	Dinarina, Perez <i>et al.</i> 2005
	<i>Sus scrofa</i>			
Speedy/ RINGO D	<i>Mus musculus</i>	?	339	Cheng, Xiong <i>et al.</i> 2005
Speedy/ RINGO E	<i>Homo sapiens</i>	Cdc2/CDK2/ CDK5	336	Cheng, Xiong <i>et al.</i> 2005 Dinarina, Perez <i>et al.</i> 2005
Speedy	<i>Ciona intestinalis</i>	?	302	Chauhan, Zheng <i>et al.</i> 2012

Figure 5. Schematic representation of Speedy/RINGO structure and Speedy/RINGO isoforms. (A) A simplified schematic of Speedy/RINGO protein domains. (B) Table demonstrating Speedy/RINGO family members.

*Spy- mediated cell cycle regulation and CDK2 substrate specificity*

Several lines of evidence demonstrate that mammalian Spy1 proteins are essential for mitotic cell cycle progression. Spy1A, herein referred to as Spy1, overexpression results in an overall increased proliferation characterized by more rapid divisions (Porter, Dellinger et al. 2002, (Golipour, Myers et al. 2008). Furthermore, the upregulation of Spy1 causes a significant reduction in the frequency of cells residing in G1 phase (Porter, Dellinger et al. 2002). Consistently, the decline in endogenous levels of Spy1 results in decreased mitotic index and a higher percentage of cells in late G1/early S phase. The Spy1-mediated increase in cellular replication is attributed to its ability to induce CDK2 activity. Moreover, CDK2 inhibitor treatment attenuates Spy1 stimulated proliferation (Porter, Dellinger et al. 2002), suggesting that Spy1-induced cell cycle progression depends on CDK2 activity. Although mutation analysis of CDK2 shows that the residues responsible for binding to Spy1 are comparable with the ones interacting with canonical cyclins, proteins from the Speedy/RINGO family exhibit surprising differences in CDK activation (Dinarina, Perez et al. 2005). The stimulation of CDK activity by Spy1 does not require the CAK-mediated T-loop Thr-161 and Thr-160 phosphorylation on CDK1 and CDK2 respectively (Cheng, Xiong et al. 2005; Dinarina, Perez et al. 2005). Importantly, Spy1-CDK complexes are less sensitive to the inhibitory phosphorylation on Thr-14/Tyr-15 on human CDK1 and CDK2-mediated by Wee1 and Myt1 kinases and are less susceptible to p21<sup>Cip1</sup> cell cycle inhibitor action (Karaïskou, Perez et al. 2001).

In addition, the mechanism behind Spy1-mediated cell cycle progression was demonstrated to occur, at least in part, through Spy1 binding directly to the cell cycle inhibitor p27<sup>Kip1</sup> (Porter, Kong-Beltran et al. 2003; McAndrew, Gastwirt et al. 2007). The Spy1-CDK2 interaction was enhanced when p27<sup>Kip1</sup> was overexpressed, supporting the



hypothesis that these proteins can exist in a trimeric complex (Porter, Kong-Beltran et al. 2003; McAndrew, Gastwirt et al. 2007). Interestingly, Spy1 overexpression overrides the ability of p27<sup>Kip1</sup> to inhibit CDK2 kinase activity (Porter, Kong-Beltran et al. 2003; McAndrew, Gastwirt et al. 2007). Spy1 thereby overrides a p27<sup>Kip1</sup>-induced cell cycle arrest, activating CDK2 and stimulating proliferation. Importantly, the Spy1-mediated proliferative pathway was shown to be p27<sup>Kip1</sup> dependent, as Spy1 was unable to stimulate proliferation in p27<sup>Kip1</sup><sup>-/-</sup> fibroblasts (Porter, Kong-Beltran et al. 2003). The G1/S phase transition is facilitated by p27<sup>Kip1</sup> SCF<sup>Skp2</sup> dependent proteolysis that is initiated by the phosphorylation of p27<sup>Kip1</sup> on Thr-187 (Pagano, Tam et al. 1995). This modification occurs by Cyclin E-CDK2 (Sheaff, Groudine et al. 1997; Vlach, Hennecke et al. 1997). How p27<sup>Kip1</sup> is phosphorylated by the kinase it inhibits was previously not known. McAndrew *et. al.* demonstrated that Spy1-CDK2 prevents p27<sup>Kip1</sup> from interacting with CDK2, allowing for CDK activation and subsequent phosphorylation and degradation of p27<sup>Kip1</sup> (McAndrew, Gastwirt et al. 2007). The reported mechanism explains one mechanism by which Spy1-CDK2 can regulate S phase transition.

In addition to profound differences in the regulation of CDK activity between known cyclins and Speedy/RINGO proteins, the substrate specificity conferred by both was demonstrated to be quite diverse (Cheng, Gerry et al. 2005). It has been established that the canonical Cyclin A-CDK2 complex has a defined ((S/T)PX(K/R)) consensus target site and demonstrates strong affinity for the Lys at the +3 position of the substrate (Cheng, Gerry et al. 2005). In contrast, Spy1 bound to CDK2 displays broad substrate specificity with a preference to phosphorylate noncanonical substrates (Cheng, Gerry et al. 2005). Furthermore phosphorylation of the CDK within the T-loop was not required for Spy1 activation of the CDK (Cheng, Gerry et al. 2005). It is speculated that in analogy

to cyclins, Speedy/RINGO proteins may have their own specific substrate interacting motifs that would further explain the observed divergence in substrate specificity.

*Spy1, DNA damage response and apoptosis*

The regulation of CDK activity by Speedy/RINGO proteins represents a novel and unconventional model of cell cycle control. The importance of CDK stimulation independent of T-loop modification and altered substrate specificity imply an activating mechanism that can be utilized when CDKs are held in an inactive state due to p21<sup>Cip1</sup> or Wee-like kinases inhibition. The circumstances that show a need for such activation may include DNA damage repair or inhibition of apoptosis required in normal development; however if set out of control, can lead to cell cycle deregulation and potential oncogenesis.

Checkpoint activation is characterized by tight regulation of CDK2 activity. In the face of DNA damage, published and unpublished data support that Spy1 levels must be tightly regulated to allow for inhibition of CDK2 activity (Barnes, Porter et al. 2003). When Spy1 levels are elevated Spy1-CDK2-mediated phosphorylation of Cdc25, and insensitivity of the complex to p21<sup>Cip1</sup>, bypasses the S and G2/M checkpoints promoting DNA synthesis and division of damaged cells (Barnes, Porter et al. 2003; Gastwirt, McAndrew et al. 2007). In addition, Spy1 was reported to regulate the intrinsic DNA damage response and confer resistance to apoptosis in a p53 and p21<sup>Cip1</sup> dependent manner (Gastwirt, Slavin et al. 2006). These data suggest that Spy1-mediated pro-survival effects may rely on p53 pathway inhibition. Overall, Spy1-CDK2- mediated resistance to genotoxic agents and radiation confers survival and subversion of apoptosis to damaged cells (Barnes, Porter et al. 2003). Heightened resistance to chemotherapy and radiation-

induced programmed cell death are established hallmarks of cancer stem cells. Hence, targeting Spy1 overexpression in self-renewing populations of cells within a tumour can potentially contribute to novel strategies in cancer therapy.

#### *The role of Spy1 in normal development and tumourigenesis*

The initial report on the role of Spy1 in the development of the mammary gland demonstrated that Spy1 levels are tightly regulated during development in this system (Golipour, Myers et al. 2008). The upregulation of Spy1 was shown to be characteristic of the proliferative stages in the gland, followed by the reduction of Spy1 levels during terminal differentiation. When Spy1 was overexpressed however, premature development and an increase in ductal morphogenesis was observed. Moreover, Spy1 was demonstrated to be regulated downstream of the c-Myc and MAPK pathways frequently activated in many breast cancers. Overexpression of Spy1 in mouse models resulted in rapid and invasive tumourigenesis (Golipour, Myers et al. 2008). Notably, Spy1 was found among the most upregulated genes in metastatic ductal breast carcinoma (Zucchi, Mento et al. 2004) and recent data shows that Spy1 levels are indicated in the majority of the most common breast cancer types (Al Sorkhy, Ferraiuolo et al. 2012).

Although the role of Spy1 in the development of the nervous system is still under investigation, the studies addressing the behavior of Spy1 in neural regeneration shed some light on its potential functions in the nervous system. Under physiological conditions Spy1 is found to be expressed in both neurons and astrocytes of the lumbar spinal cord region (Huang, Liu et al. 2009). The sciatic nerve injury model revealed that Spy1 levels were readily upregulated after the nerve crush mainly in Schwann cells, astrocytes and microglia and its levels correlated with enhanced proliferation. In Schwann

cells, Spy1 localized mainly to axons and was expressed in an opposite manner to the growth associated protein 43 (GAP43), neuronal marker (Cao, Yang et al. 2013). Moreover, a corresponding increase of CDK2 activity and decline of p27<sup>Kip1</sup> levels was reported, suggesting that Spy1-mediated cell cycle effects play a role in the glial response to injury (Huang, Liu et al. 2009). Collectively these data support that Spy1 may induce the regenerative processes within the nervous system. Zhang *et al* demonstrated that Spy1 was selectively expressed in the glial but not in the neuronal cells, and its overexpression correlated with the highest stages of glioma (Zhang, Shen et al. 2012). The downregulation of Spy1 in glioma cell lines resulted in decreased proliferation, downregulated CDK2 activity and upregulation of p27<sup>Kip1</sup> levels. Spy1 expression correlated negatively with patient prognosis indicating that Spy1 may serve as a valuable prognostic marker for patients with glioma.

Recently, Spy1 was also indicated as a prognostic marker in human Non Hodgkin's Lymphoma (NHL) as levels correlated with poor patient prognosis (Hang, Fei et al. 2012). Upregulated levels of Spy1 in human NHL specimens were demonstrated to correspond with increased Thr-187 phosphorylation on p27<sup>Kip1</sup> and enhanced proliferation. The knockdown of Spy1 in leukemia cells resulted in decreased phosphorylation of p27<sup>Kip1</sup> and cell cycle arrest (Hang, Fei et al. 2012). These data support that Spy1-mediated proliferation in human NHL depends on its ability to induce p27<sup>Kip1</sup> Thr-187 phosphorylation followed by its degradation.

Spy1 overexpression was also suggested to play a role in the pathogenesis of hepatocellular carcinoma (Ke, Ji et al. 2009). The increase in histological grade was characterized by upregulated levels of Spy1 and Ki67 proliferation marker expression (Ke, Ji et al. 2009). The overexpression of Spy1 in a wide variety of human cancers

suggests the importance of Spy1-mediated cell cycle effects in malignant transformation. Despite the significant cancer type diversity observed, common features included positive correlation between Spy1 levels, the stage of malignancy and poor patient prognosis. These data collectively suggest a role for Spy1 as a prognostic marker, and potential therapeutic target, in a vast number of human cancers.

## **HYPOTHESIS AND OBJECTIVES**

This work aims to determine the role of the novel cell cycle regulator Spy1 in neural proliferation and commitment. We will address the potential implications of Spy1-mediated effects in tumours of neural origin.

This study will test the hypothesis that: *Spy1 is a key player in neural cell fate, playing a role in the self-renewal and differentiation of neural stem and progenitor populations.* Furthermore we hypothesize *that Spy1-mediated molecular mechanisms drive tumour initiating cell decisions and regulate potential neural malignancies.*

To address this hypothesis we have the following objectives:

- To elucidate the role of Spy1 in proliferation and self-renewal of neural stem cells and tumour initiating cells in human glioma
- To determine the expression and localization of Spy1 during development of the central nervous system and in adult neurogenesis
- To elucidate the role of Spy1 in the differentiation of human neuroblastoma progenitor populations

The data obtained during the course of this study will contribute to advancing our understanding of cell cycle mechanisms behind fate determination in neural systems. This work may reveal novel diagnostic and therapeutic avenues for brain cancer therapy.

## REFERENCES

- Akama, Y., W. Yasui, et al. (1995). "Frequent amplification of the cyclin E gene in human gastric carcinomas." *Jpn J Cancer Res* **86**(7): 617-21.
- Akhoondi, S., D. Sun, et al. (2007). "FBXW7/hCDC4 is a general tumor suppressor in human cancer." *Cancer Res* **67**(19): 9006-12.
- Al Sorkhy, M., R. M. Ferraiuolo, et al. (2012). "The cyclin-like protein Spy1/RINGO promotes mammary transformation and is elevated in human breast cancer." *BMC Cancer* **12**: 45.
- Albanese, C., M. D'Amico, et al. (1999). "Activation of the cyclin D1 gene by the E1A-associated protein p300 through AP-1 inhibits cellular apoptosis." *J Biol Chem* **274**(48): 34186-95.
- Arato-Ohshima, T. and H. Sawa (1999). "Over-expression of cyclin D1 induces glioma invasion by increasing matrix metalloproteinase activity and cell motility." *Int J Cancer* **83**(3): 387-92.
- Bao, S., Q. Wu, et al. (2006). "Glioma stem cells promote radioresistance by preferential activation of the DNA damage response." *Nature* **444**(7120): 756-60.
- Barnes, E. A., L. A. Porter, et al. (2003). "Human Spy1 promotes survival of mammalian cells following DNA damage." *Cancer Res* **63**(13): 3701-7.
- Becker, K. A., P. N. Ghule, et al. (2006). "Self-renewal of human embryonic stem cells is supported by a shortened G1 cell cycle phase." *J Cell Physiol* **209**(3): 883-93.
- Beier, D., J. B. Schulz, et al. (2011). "Chemoresistance of glioblastoma cancer stem cells - much more complex than expected." *Mol Cancer* **10**: 128.
- Berger, C., S. K. Pallavi, et al. (2005). "A critical role for cyclin E in cell fate determination in the central nervous system of *Drosophila melanogaster*." *Nat Cell Biol* **7**(1): 56-62.
- Beukelaers, P., R. Vandenbosch, et al. (2012). "Cycling or not cycling: cell cycle regulatory molecules and adult neurogenesis." *Cell Mol Life Sci* **69**(9): 1493-503.
- Bhat, K. M. and N. Apsel (2004). "Upregulation of Mitimere and Nubbin acts through cyclin E to confer self-renewing asymmetric division potential to neural precursor cells." *Development* **131**(5): 1123-34.

- Blomen, V. A. and J. Boonstra (2007). "Cell fate determination during G1 phase progression." *Cell Mol Life Sci* **64**(23): 3084-104.
- Bonaguidi, M. A., M. A. Wheeler, et al. (2011). "In vivo clonal analysis reveals self-renewing and multipotent adult neural stem cell characteristics." *Cell* **145**(7): 1142-55.
- Booher, R. and D. Beach (1986). "Site-specific mutagenesis of *cdc2+*, a cell cycle control gene of the fission yeast *Schizosaccharomyces pombe*." *Mol Cell Biol* **6**(10): 3523-30.
- Botz, J., K. Zerfass-Thome, et al. (1996). "Cell cycle regulation of the murine cyclin E gene depends on an E2F binding site in the promoter." *Mol Cell Biol* **16**(7): 3401-9.
- Brat, D. J., A. Castellano-Sanchez, et al. (2002). "Genetic and biologic progression in astrocytomas and their relation to angiogenic dysregulation." *Adv Anat Pathol* **9**(1): 24-36.
- Buschges, R., R. G. Weber, et al. (1999). "Amplification and expression of cyclin D genes (*CCND1*, *CCND2* and *CCND3*) in human malignant gliomas." *Brain Pathol* **9**(3): 435-42; discussion 432-3.
- Calegari, F. and W. B. Huttner (2003). "An inhibition of cyclin-dependent kinases that lengthens, but does not arrest, neuroepithelial cell cycle induces premature neurogenesis." *J Cell Sci* **116**(Pt 24): 4947-55.
- Campisi, J. (2005). "Senescent cells, tumor suppression, and organismal aging: good citizens, bad neighbors." *Cell* **120**(4): 513-22.
- Cao, J., J. Yang, et al. (2013). "Temporal-spatial expressions of *spyl* in rat sciatic nerve after crush." *Cell Mol Neurobiol* **33**(2): 213-21.
- Carrano, A. C., E. Eytan, et al. (1999). "SKP2 is required for ubiquitin-mediated degradation of the CDK inhibitor p27." *Nat Cell Biol* **1**(4): 193-9.
- Cavalla, P., A. Dutto, et al. (1998). "Cyclin D1 expression in gliomas." *Acta Neuropathol* **95**(2): 131-5.
- Caviness, V. S., Jr., T. Takahashi, et al. (1995). "Numbers, time and neocortical neuronogenesis: a general developmental and evolutionary model." *Trends Neurosci* **18**(9): 379-83.



- Chakravarti, A., M. A. Delaney, et al. (2001). "Prognostic and pathologic significance of quantitative protein expression profiling in human gliomas." *Clin Cancer Res* **7**(8): 2387-95.
- Chan, K. T., C. L. Cortesio, et al. (2009). "FAK alters invadopodia and focal adhesion composition and dynamics to regulate breast cancer invasion." *J Cell Biol* **185**(2): 357-70.
- Cheney, I. W., S. T. Neuteboom, et al. (1999). "Adenovirus-mediated gene transfer of MMAC1/PTEN to glioblastoma cells inhibits S phase entry by the recruitment of p27Kip1 into cyclin E/CDK2 complexes." *Cancer Res* **59**(10): 2318-23.
- Cheng, A., S. Gerry, et al. (2005). "Biochemical characterization of Cdk2-Speedy/Ringo A2." *BMC Biochem* **6**: 19.
- Cheng, A., W. Xiong, et al. (2005). "Identification and comparative analysis of multiple mammalian Speedy/Ringo proteins." *Cell Cycle* **4**(1): 155-65.
- Cheng, T. (2004). "Cell cycle inhibitors in normal and tumor stem cells." *Oncogene* **23**(43): 7256-66.
- Ciemerych, M. A., A. M. Kenney, et al. (2002). "Development of mice expressing a single D-type cyclin." *Genes Dev* **16**(24): 3277-89.
- Ciznadija, D., Y. Liu, et al. (2011). "Cyclin D1 and cdk4 mediate development of neurologically destructive oligodendroglioma." *Cancer Res* **71**(19): 6174-83.
- Cole, A. M., K. Myant, et al. (2010). "Cyclin D2-cyclin-dependent kinase 4/6 is required for efficient proliferation and tumorigenesis following Apc loss." *Cancer Res* **70**(20): 8149-58.
- Cooper, A. B., C. M. Sawai, et al. (2006). "A unique function for cyclin D3 in early B cell development." *Nat Immunol* **7**(5): 489-97.
- Courjal, F., G. Louason, et al. (1996). "Cyclin gene amplification and overexpression in breast and ovarian cancers: evidence for the selection of cyclin D1 in breast and cyclin E in ovarian tumors." *Int J Cancer* **69**(4): 247-53.
- Das, G., Y. Choi, et al. (2009). "Cyclin D1 fine-tunes the neurogenic output of embryonic retinal progenitor cells." *Neural Dev* **4**: 15.

- Di Stefano, V., M. Giacca, et al. (2011). "Knockdown of cyclin-dependent kinase inhibitors induces cardiomyocyte re-entry in the cell cycle." *J Biol Chem* **286**(10): 8644-54.
- Dinarina, A., L. H. Perez, et al. (2005). "Characterization of a new family of cyclin-dependent kinase activators." *Biochem J* **386**(Pt 2): 349-55.
- Ding, Q., J. R. Grammer, et al. (2005). "p27Kip1 and cyclin D1 are necessary for focal adhesion kinase regulation of cell cycle progression in glioblastoma cells propagated in vitro and in vivo in the scid mouse brain." *J Biol Chem* **280**(8): 6802-15.
- Doetsch, F., I. Caille, et al. (1999). "Subventricular zone astrocytes are neural stem cells in the adult mammalian brain." *Cell* **97**(6): 703-16.
- Doetsch, F., J. M. Garcia-Verdugo, et al. (1997). "Cellular composition and three-dimensional organization of the subventricular germinal zone in the adult mammalian brain." *J Neurosci* **17**(13): 5046-61.
- Duffy, K. T., M. F. McAleer, et al. (2005). "Coordinate control of cell cycle regulatory genes in zebrafish development tested by cyclin D1 knockdown with morpholino phosphorodiamidates and hydroxypropyl-phosphono peptide nucleic acids." *Nucleic Acids Res* **33**(15): 4914-21.
- Durand, B., M. L. Fero, et al. (1998). "p27Kip1 alters the response of cells to mitogen and is part of a cell-intrinsic timer that arrests the cell cycle and initiates differentiation." *Curr Biol* **8**(8): 431-40.
- Durand, B., F. B. Gao, et al. (1997). "Accumulation of the cyclin-dependent kinase inhibitor p27/Kip1 and the timing of oligodendrocyte differentiation." *Embo J* **16**(2): 306-17.
- Egli, D., G. Birkhoff, et al. (2008). "Mediators of reprogramming: transcription factors and transitions through mitosis." *Nat Rev Mol Cell Biol* **9**(7): 505-16.
- Ekholm-Reed, S., C. H. Spruck, et al. (2004). "Mutation of hCDC4 leads to cell cycle deregulation of cyclin E in cancer." *Cancer Res* **64**(3): 795-800.
- Fan, X., L. Khaki, et al. (2010). "NOTCH pathway blockade depletes CD133-positive glioblastoma cells and inhibits growth of tumor neurospheres and xenografts." *Stem Cells* **28**(1): 5-16.

- Fan, X., I. Mikolaenko, et al. (2004). "Notch1 and notch2 have opposite effects on embryonal brain tumor growth." *Cancer Res* **64**(21): 7787-93.
- Fantl, V., G. Stamp, et al. (1995). "Mice lacking cyclin D1 are small and show defects in eye and mammary gland development." *Genes Dev* **9**(19): 2364-72.
- Ferby, I., M. Blazquez, et al. (1999). "A novel p34(cdc2)-binding and activating protein that is necessary and sufficient to trigger G(2)/M progression in *Xenopus* oocytes." *Genes Dev* **13**(16): 2177-89.
- Fishell, G. and A. R. Kriegstein (2003). "Neurons from radial glia: the consequences of asymmetric inheritance." *Curr Opin Neurobiol* **13**(1): 34-41.
- Fu, M., C. Wang, et al. (2002). "Acetylation in hormone signaling and the cell cycle." *Cytokine Growth Factor Rev* **13**(3): 259-76.
- Gastwirt, R. F., C. W. McAndrew, et al. (2007). "Speedy/RINGO regulation of CDKs in cell cycle, checkpoint activation and apoptosis." *Cell Cycle* **6**(10): 1188-93.
- Gastwirt, R. F., D. A. Slavin, et al. (2006). "Spy1 expression prevents normal cellular responses to DNA damage: inhibition of apoptosis and checkpoint activation." *J Biol Chem* **281**(46): 35425-35.
- Geisen, C. and T. Moroy (2002). "The oncogenic activity of cyclin E is not confined to Cdk2 activation alone but relies on several other, distinct functions of the protein." *J Biol Chem* **277**(42): 39909-18.
- Geng, Y., E. N. Eaton, et al. (1996). "Regulation of cyclin E transcription by E2Fs and retinoblastoma protein." *Oncogene* **12**(6): 1173-80.
- Geng, Y., Q. Yu, et al. (2003). "Cyclin E ablation in the mouse." *Cell* **114**(4): 431-43.
- Ghiani, C. and V. Gallo (2001). "Inhibition of cyclin E-cyclin-dependent kinase 2 complex formation and activity is associated with cell cycle arrest and withdrawal in oligodendrocyte progenitor cells." *J Neurosci* **21**(4): 1274-82.
- Glickstein, S. B., S. Alexander, et al. (2007). "Differences in cyclin D2 and D1 protein expression distinguish forebrain progenitor subsets." *Cereb Cortex* **17**(3): 632-42.
- Glickstein, S. B., J. A. Monaghan, et al. (2009). "Cyclin D2 is critical for intermediate progenitor cell proliferation in the embryonic cortex." *J Neurosci* **29**(30): 9614-24

- Golipour, A., D. Myers, et al. (2008). "The Spy1/RINGO family represents a novel mechanism regulating mammary growth and tumorigenesis." *Cancer Res* **68**(10): 3591-600.
- Gotz, M. and W. B. Huttner (2005). "The cell biology of neurogenesis." *Nat Rev Mol Cell Biol* **6**(10): 777-88.
- Gould, K. L., S. Moreno, et al. (1991). "Phosphorylation at Thr167 is required for *Schizosaccharomyces pombe* p34cdc2 function." *Embo J* **10**(11): 3297-309.
- Gritti, A., L. Bonfanti, et al. (2002). "Multipotent neural stem cells reside into the rostral extension and olfactory bulb of adult rodents." *J Neurosci* **22**(2): 437-45.
- Groszer, M., R. Erickson, et al. (2006). "PTEN negatively regulates neural stem cell self-renewal by modulating G0-G1 cell cycle entry." *Proc Natl Acad Sci U S A* **103**(1): 111-6.
- Groszer, M., R. Erickson, et al. (2001). "Negative regulation of neural stem/progenitor cell proliferation by the Pten tumor suppressor gene in vivo." *Science* **294**(5549): 2186-9.
- Gstaiger, M., R. Jordan, et al. (2001). "Skp2 is oncogenic and overexpressed in human cancers." *Proc Natl Acad Sci U S A* **98**(9): 5043-8.
- Gu, Y., J. Rosenblatt, et al. (1992). "Cell cycle regulation of CDK2 activity by phosphorylation of Thr160 and Tyr15." *Embo J* **11**(11): 3995-4005.
- Gum, R., H. Wang, et al. (1997). "Regulation of 92 kDa type IV collagenase expression by the jun aminoterminal kinase- and the extracellular signal-regulated kinase-dependent signaling cascades." *Oncogene* **14**(12): 1481-93.
- Guo, W., N. E. Patzlaff, et al. (2012). "Isolation of multipotent neural stem or progenitor cells from both the dentate gyrus and subventricular zone of a single adult mouse." *Nat Protoc* **7**(11): 2005-12
- Haas, K., C. Johannes, et al. (1997). "Malignant transformation by cyclin E and Ha-Ras correlates with lower sensitivity towards induction of cell death but requires functional Myc and CDK4." *Oncogene* **15**(21): 2615-23.
- Hagedorn, M., M. Delugin, et al. (2007). "FBXW7/hCDC4 controls glioma cell proliferation in vitro and is a prognostic marker for survival in glioblastoma patients." *Cell Div* **2**: 9.

- Halatsch, M. E., U. Schmidt, et al. (2006). "Epidermal growth factor receptor inhibition for the treatment of glioblastoma multiforme and other malignant brain tumours." *Cancer Treat Rev* **32**(2): 74-89.
- Hanahan, D. and R. A. Weinberg (2000). "The hallmarks of cancer." *Cell* **100**(1): 57-70.
- Hang, Q., M. Fei, et al. (2012). "Expression of Spyl protein in human non-Hodgkin's lymphomas is correlated with phosphorylation of p27 Kip1 on Thr187 and cell proliferation." *Med Oncol* **29**(5): 3504-14.
- Hassan, K. A., L. Wang, et al. (2013). "Notch pathway activity identifies cells with cancer stem cell-like properties and correlates with worse survival in lung adenocarcinoma." *Clin Cancer Res*.
- Hecker, T. P., J. R. Grammer, et al. (2002). "Focal adhesion kinase enhances signaling through the Shc/extracellular signal-regulated kinase pathway in anaplastic astrocytoma tumor biopsy samples." *Cancer Res* **62**(9): 2699-707.
- Hemmati, H. D., I. Nakano, et al. (2003). "Cancerous stem cells can arise from pediatric brain tumors." *Proc Natl Acad Sci U S A* **100**(25): 15178-83.
- Herrup, K. and Y. Yang (2007). "Cell cycle regulation in the postmitotic neuron: oxymoron or new biology?" *Nat Rev Neurosci* **8**(5): 368-78.
- Hill, C., S. B. Hunter, et al. (2003). "Genetic markers in glioblastoma: prognostic significance and future therapeutic implications." *Adv Anat Pathol* **10**(4): 212-7.
- Holnthoner, W., M. Pillinger, et al. (2002). "Fibroblast growth factor-2 induces Lef/Tcf-dependent transcription in human endothelial cells." *J Biol Chem* **277**(48): 45847-53.
- Hood, J. D. and D. A. Cheresh (2002). "Role of integrins in cell invasion and migration." *Nat Rev Cancer* **2**(2): 91-100.
- Huang, H. S., M. Nagane, et al. (1997). "The enhanced tumorigenic activity of a mutant epidermal growth factor receptor common in human cancers is mediated by threshold levels of constitutive tyrosine phosphorylation and unattenuated signaling." *J Biol Chem* **272**(5): 2927-35.
- Huang, Y., Y. Liu, et al. (2009). "Peripheral nerve lesion induces an up-regulation of Spyl in rat spinal cord." *Cell Mol Neurobiol* **29**(3): 403-11.

- Hui, W., L. Yuntao, et al. (2013). "MicroRNA-195 inhibits the proliferation of human glioma cells by directly targeting cyclin D1 and cyclin E1." *PLoS One* **8**(1): e54932.
- Huntly, B. J. and D. G. Gilliland (2005). "Leukaemia stem cells and the evolution of cancer-stem-cell research." *Nat Rev Cancer* **5**(4): 311-21.
- Huttner, W. B. and M. Brand (1997). "Asymmetric division and polarity of neuroepithelial cells." *Curr Opin Neurobiol* **7**(1): 29-39.
- Hwang, H. C. and B. E. Clurman (2005). "Cyclin E in normal and neoplastic cell cycles." *Oncogene* **24**(17): 2776-86.
- Imayoshi, I., M. Sakamoto, et al. (2009). "Continuous neurogenesis in the adult brain." *Dev Growth Differ* **51**(3): 379-86.
- Jackson, E. L., J. M. Garcia-Verdugo, et al. (2006). "PDGFR alpha-positive B cells are neural stem cells in the adult SVZ that form glioma-like growths in response to increased PDGF signaling." *Neuron* **51**(2): 187-99.
- Jeon, H. M., X. Jin, et al. (2008). "Inhibitor of differentiation 4 drives brain tumor-initiating cell genesis through cyclin E and notch signaling." *Genes Dev* **22**(15): 2028-33.
- Jirawatnotai, S., Y. Hu, et al. (2011). "A function for cyclin D1 in DNA repair uncovered by protein interactome analyses in human cancers." *Nature* **474**(7350): 230-4.
- Kannan, R., C. Berger, et al. (2010). "Abdominal-A mediated repression of Cyclin E expression during cell-fate specification in the Drosophila central nervous system." *Mech Dev* **127**(1-2): 137-45.
- Kao, G. D., Z. Jiang, et al. (2007). "Inhibition of phosphatidylinositol-3-OH kinase/Akt signaling impairs DNA repair in glioblastoma cells following ionizing radiation." *J Biol Chem* **282**(29): 21206-12.
- Karaiskou, A., L. H. Perez, et al. (2001). "Differential regulation of Cdc2 and Cdk2 by RINGO and cyclins " *J Biol Chem* **276**(38): 36028-34.
- Kawamura, K., H. Izumi, et al. (2004). "Induction of centrosome amplification and chromosome instability in human bladder cancer cells by p53 mutation and cyclin E overexpression." *Cancer Res* **64**(14): 4800-9.

- Ke, Q., J. Ji, et al. (2009). "Expression and prognostic role of Spy1 as a novel cell cycle protein in hepatocellular carcinoma." *Exp Mol Pathol* **87**(3): 167-72.
- Kennedy, H. and C. Dehay (1993). "Cortical specification of mice and men." *Cereb Cortex* **3**(3): 171-86.
- Kippin, T. E., D. J. Martens, et al. (2005). "p21 loss compromises the relative quiescence of forebrain stem cell proliferation leading to exhaustion of their proliferation capacity." *Genes Dev* **19**(6): 756-67.
- Kitahara, K., W. Yasui, et al. (1995). "Concurrent amplification of cyclin E and CDK2 genes in colorectal carcinomas." *Int J Cancer* **62**(1): 25-8.
- Knoblich, J. A., K. Sauer, et al. (1994). "Cyclin E controls S phase progression and its down-regulation during *Drosophila* embryogenesis is required for the arrest of cell proliferation." *Cell* **77**(1): 107-20.
- Koff, A., F. Cross, et al. (1991). "Human cyclin E, a new cyclin that interacts with two members of the CDC2 gene family." *Cell* **66**(6): 1217-28.
- Koff, A., A. Giordano, et al. (1992). "Formation and activation of a cyclin E-cdk2 complex during the G1 phase of the human cell cycle." *Science* **257**(5077): 1689-94.
- Koledova, Z., L. R. Kafkova, et al. (2010). "Cdk2 inhibition prolongs G1 phase progression in mouse embryonic stem cells." *Stem Cells Dev* **19**(2): 181-94.
- Kong, G., S. S. Chua, et al. (2002). "Functional analysis of cyclin D2 and p27(Kip1) in cyclin D2 transgenic mouse mammary gland during development." *Oncogene* **21**(47): 7214-25.
- Koul, D. (2008). "PTEN signaling pathways in glioblastoma." *Cancer Biol Ther* **7**(9): 1321-5.
- Kowalczyk, A., R. K. Filipkowski, et al. (2004). "The critical role of cyclin D2 in adult neurogenesis." *J Cell Biol* **167**(2): 209-13.
- Koyama-Nasu, R., Y. Nasu-Nishimura, et al. (2012). "The critical role of cyclin D2 in cell cycle progression and tumorigenicity of glioblastoma stem cells." *Oncogene*.
- Kriegstein, A. R. and M. Gotz (2003). "Radial glia diversity: a matter of cell fate." *Glia* **43**(1): 37-43.

- Kume, S., T. Endo, et al. (2007). "Porcine SPDYA2 (RINGO A2) stimulates CDC2 activity and accelerates meiotic maturation of porcine oocytes." *Biol Reprod* **76**(3): 440-7.
- LaBaer, J., M. D. Garrett, et al. (1997). "New functional activities for the p21 family of CDK inhibitors." *Genes Dev* **11**(7): 847-62.
- Lange, C., W. B. Huttner, et al. (2009). "Cdk4/cyclinD1 overexpression in neural stem cells shortens G1, delays neurogenesis, and promotes the generation and expansion of basal progenitors." *Cell Stem Cell* **5**(3): 320-31.
- Lenormand, J. L., R. W. Dellinger, et al. (1999). "Speedy: a novel cell cycle regulator of the G2/M transition." *Embo J* **18**(7): 1869-77.
- Li, V. C., A. Ballabeni, et al. (2012). "Gap 1 phase length and mouse embryonic stem cell self-renewal." *Proc Natl Acad Sci U S A* **109**(31): 12550-5.
- Li, H., M. Collado, et al. (2012). "p27(Kip1) directly represses Sox2 during embryonic stem cell differentiation." *Cell Stem Cell* **11**(6): 845-52.
- Livesey, F. J. and C. L. Cepko (2001). "Vertebrate neural cell-fate determination: lessons from the retina." *Nat Rev Neurosci* **2**(2): 109-18.
- Loeb, K. R., H. Kostner, et al. (2005). "A mouse model for cyclin E-dependent genetic instability and tumorigenesis." *Cancer Cell* **8**(1): 35-47.
- Louis, D. N., H. Ohgaki, et al. (2007). "The 2007 WHO classification of tumours of the central nervous system." *Acta Neuropathol* **114**(2): 97-109.
- Louis DN, Ohgaki H, Wiestler OD, Cavenee WK (eds) (2007)WHO Classification of tumours of the central nervous system. IARC, Lyon.
- Lukaszewicz, A., P. Savatier, et al. (2005). "G1 phase regulation, area-specific cell cycle control, and cytoarchitectonics in the primate cortex." *Neuron* **47**(3): 353-64.
- Mamillapalli, R., N. Gavrilova, et al. (2001). "PTEN regulates the ubiquitin-dependent degradation of the CDK inhibitor p27(KIP1) through the ubiquitin E3 ligase SCF(SKIP2)." *Curr Biol* **11**(4): 263-7.
- Marone, M., G. Scambia, et al. (1998). "Analysis of cyclin E and CDK2 in ovarian cancer: gene amplification and RNA overexpression." *Int J Cancer* **75**(1): 34-9.



- Marques-Torrejon, M. A., E. Porlan, et al. (2013). "Cyclin-dependent kinase inhibitor p21 controls adult neural stem cell expansion by regulating Sox2 gene expression." *Cell Stem Cell* **12**(1): 88-100.
- Martins, C. P. and A. Berns (2002). "Loss of p27(Kip1) but not p21(Cip1) decreases survival and synergizes with MYC in murine lymphomagenesis." *Embo J* **21**(14): 3739-48.
- McAndrew, C. W., R. F. Gastwirt, et al. (2007). "Spy1 enhances phosphorylation and degradation of the cell cycle inhibitor p27." *Cell Cycle* **6**(15): 1937-45.
- Medema, R. H., G. J. Kops, et al. (2000). "AFX-like Forkhead transcription factors mediate cell-cycle regulation by Ras and PKB through p27kip1." *Nature* **404**(6779): 782-7.
- Minella, A. C., J. Swanger, et al. (2002). "p53 and p21 form an inducible barrier that protects cells against cyclin E-cdk2 deregulation." *Curr Biol* **12**(21): 1817-27.
- Mirzadeh, Z., F. T. Merkle, et al. (2008). "Neural stem cells confer unique pinwheel architecture to the ventricular surface in neurogenic regions of the adult brain." *Cell Stem Cell* **3**(3): 265-78.
- Mischel, P. S. and T. F. Cloughesy (2003). "Targeted molecular therapy of GBM." *Brain Pathol* **13**(1): 52-61.
- Molofsky, A. V., S. G. Slutsky, et al. (2006). "Increasing p16INK4a expression decreases forebrain progenitors and neurogenesis during ageing." *Nature* **443**(7110): 448-52.
- Montagnoli, A., F. Fiore, et al. (1999). "Ubiquitination of p27 is regulated by Cdk-dependent phosphorylation and trimeric complex formation." *Genes Dev* **13**(9): 1181-9.
- Morshead, C. M., B. A. Reynolds, et al. (1994). "Neural stem cells in the adult mammalian forebrain: a relatively quiescent subpopulation of subependymal cells." *Neuron* **13**(5): 1071-82.
- Mumberg, D., M. Wick, et al. (1997). "Cyclin ET, a new splice variant of human cyclin E with a unique expression pattern during cell cycle progression and differentiation." *Nucleic Acids Res* **25**(11): 2098-105.

- Nakamura, N., S. Ramaswamy, et al. (2000). "Forkhead transcription factors are critical effectors of cell death and cell cycle arrest downstream of PTEN." *Mol Cell Biol* **20**(23): 8969-82.
- Nakayama, K., N. Ishida, et al. (1996). "Mice lacking p27(Kip1) display increased body size, multiple organ hyperplasia, retinal dysplasia, and pituitary tumors." *Cell* **85**(5): 707-20.
- Nieto, M., E. S. Monuki, et al. (2004). "Expression of Cux-1 and Cux-2 in the subventricular zone and upper layers II-IV of the cerebral cortex." *J Comp Neurol* **479**(2): 168-80.
- Nishikawa, R., X. D. Ji, et al. (1994). "A mutant epidermal growth factor receptor common in human glioma confers enhanced tumorigenicity." *Proc Natl Acad Sci U S A* **91**(16): 7727-31.
- Noctor, S. C., V. Martinez-Cerdeno, et al. (2004). "Cortical neurons arise in symmetric and asymmetric division zones and migrate through specific phases." *Nat Neurosci* **7**(2): 136-44.
- Ohtani, K., J. DeGregori, et al. (1995). "Regulation of the cyclin E gene by transcription factor E2F1." *Proc Natl Acad Sci U S A* **92**(26): 12146-50.
- Ohtsuka, T., H. Shimojo, et al. (2011). "Gene expression profiling of neural stem cells and identification of regulators of neural differentiation during cortical development." *Stem Cells* **29**(11): 1817-28.
- Orford, K. W. and D. T. Scadden (2008). "Deconstructing stem cell self-renewal: genetic insights into cell-cycle regulation." *Nat Rev Genet* **9**(2): 115-28.
- Pacey, L., S. Stead, et al. (2006). "Neural Stem Cell Culture: Neurosphere generation, microscopical analysis and cryopreservation."
- Pagano, M., S. W. Tam, et al. (1995). "Role of the ubiquitin-proteasome pathway in regulating abundance of the cyclin-dependent kinase inhibitor p27." *Science* **269**(5224): 682-5.
- Parsons, D. W., S. Jones, et al. (2008). "An integrated genomic analysis of human glioblastoma multiforme." *Science* **321**(5897): 1807-12.

- Pilaz, L. J., D. Patti, et al. (2009). "Forced G1-phase reduction alters mode of division, neuron number, and laminar phenotype in the cerebral cortex." *Proc Natl Acad Sci U S A* **106**(51): 21924-9.
- Porter, L. A., R. W. Dellinger, et al. (2002). "Human Speedy: a novel cell cycle regulator that enhances proliferation through activation of Cdk2." *J Cell Biol* **157**(3): 357-66.
- Porter, L. A., M. Kong-Beltran, et al. (2003). "Spy1 interacts with p27Kip1 to allow G1/S progression." *Mol Biol Cell* **14**(9): 3664-74.
- Porter, P. L., K. E. Malone, et al. (1997). "Expression of cell-cycle regulators p27Kip1 and cyclin E, alone and in combination, correlate with survival in young breast cancer patients." *Nat Med* **3**(2): 222-5.
- Purow, B. W., R. M. Haque, et al. (2005). "Expression of Notch-1 and its ligands, Delta-like-1 and Jagged-1, is critical for glioma cell survival and proliferation." *Cancer Res* **65**(6): 2353-63.
- Qiu, J., Y. Takagi, et al. (2004). "Regenerative response in ischemic brain restricted by p21cip1/waf1." *J Exp Med* **199**(7): 937-45.
- Rajagopalan, H., P. V. Jallepalli, et al. (2004). "Inactivation of hCDC4 can cause chromosomal instability." *Nature* **428**(6978): 77-81.
- Rakic, P. (1995). "A small step for the cell, a giant leap for mankind: a hypothesis of neocortical expansion during evolution." *Trends Neurosci* **18**(9): 383-8.
- Ramis, G., E. Thomas-Moya, et al. (2012). "EGFR inhibition in glioma cells modulates Rho signaling to inhibit cell motility and invasion and cooperates with temozolomide to reduce cell growth." *PLoS One* **7**(6): e38770.
- Rapaport, D. H., L. L. Wong, et al. (2004). "Timing and topography of cell genesis in the rat retina." *J Comp Neurol* **474**(2): 304-24.
- Read, R. D., W. K. Cavenee, et al. (2009). "A drosophila model for EGFR-Ras and PI3K-dependent human glioma." *PLoS Genet* **5**(2): e1000374.
- Richardson, H. E., L. V. O'Keefe, et al. (1993). "A Drosophila G1-specific cyclin E homolog exhibits different modes of expression during embryogenesis." *Development* **119**(3): 673-90.

- Ronchini, C. and A. J. Capobianco (2001). "Induction of cyclin D1 transcription and CDK2 activity by Notch(ic): implication for cell cycle disruption in transformation by Notch(ic)." *Mol Cell Biol* **21**(17): 5925-34.
- Roussel-Gervais, A., S. Bilodeau, et al. (2010). "Cooperation between cyclin E and p27(Kip1) in pituitary tumorigenesis." *Mol Endocrinol* **24**(9): 1835-45.
- Sakariassen, P. O., H. Immervoll, et al. (2007). "Cancer stem cells as mediators of treatment resistance in brain tumors: status and controversies." *Neoplasia* **9**(11): 882-92.
- Sallinen, S. L., P. K. Sallinen, et al. (1999). "Cyclin D1 expression in astrocytomas is associated with cell proliferation activity and patient prognosis." *J Pathol* **188**(3): 289-93.
- Salomoni, P. and F. Calegari (2010). "Cell cycle control of mammalian neural stem cells: putting a speed limit on G1." *Trends Cell Biol* **20**(5): 233-43.
- Sawaya, R. E., M. Yamamoto, et al. (1996). "Expression and localization of 72 kDa type IV collagenase (MMP-2) in human malignant gliomas in vivo." *Clin Exp Metastasis* **14**(1): 35-42.
- Schulman, B. A., D. L. Lindstrom, et al. (1998). "Substrate recruitment to cyclin-dependent kinase 2 by a multipurpose docking site on cyclin A." *Proc Natl Acad Sci U S A* **95**(18): 10453-8.
- Serrano, M., G. J. Hannon, et al. (1993). "A new regulatory motif in cell-cycle control causing specific inhibition of cyclin D/CDK4." *Nature* **366**(6456): 704-7.
- Sestan, N., P. Rakic, et al. (2001). "Independent parcellation of the embryonic visual cortex and thalamus revealed by combinatorial Eph/ephrin gene expression." *Curr Biol* **11**(1): 39-43.
- Sewing, A., V. Ronicke, et al. (1994). "Alternative splicing of human cyclin E." *J Cell Sci* **107** ( Pt 2): 581-8.
- Sheaff, R. J., M. Groudine, et al. (1997). "Cyclin E-CDK2 is a regulator of p27Kip1." *Genes Dev* **11**(11): 1464-78.
- Sherr, C. J. (2000). "The Pezcoller lecture: cancer cell cycles revisited." *Cancer Res* **60**(14): 3689-95.

- Sherr, C. J. and J. M. Roberts (2004). "Living with or without cyclins and cyclin-dependent kinases." *Genes Dev* **18**(22): 2699-711.
- Shimura, T., S. Kakuda, et al. (2011). "Targeting the AKT/GSK3beta/cyclin D1/Cdk4 survival signaling pathway for eradication of tumor radioresistance acquired by fractionated radiotherapy." *Int J Radiat Oncol Biol Phys* **80**(2): 540-8.
- Shimura, T., N. Noma, et al. "Activation of the AKT/cyclin D1/Cdk4 survival signaling pathway in radioresistant cancer stem cells." *Oncogenesis* **1**: e12.
- Sicinski, P., J. L. Donaher, et al. (1995). "Cyclin D1 provides a link between development and oncogenesis in the retina and breast." *Cell* **82**(4): 621-30.
- Singh, A. M. and S. Dalton (2009). "The cell cycle and Myc intersect with mechanisms that regulate pluripotency and reprogramming." *Cell Stem Cell* **5**(2): 141-9
- Singh, S. K., C. Hawkins, et al. (2004). "Identification of human brain tumour initiating cells." *Nature* **432**(7015): 396-401.
- Solomon, M. J. and P. Kaldis (1998). "Regulation of CDKs by phosphorylation." *Results Probl Cell Differ* **22**: 79-109.
- Spruck, C. H., K. A. Won, et al. (1999). "Deregulated cyclin E induces chromosome instability." *Nature* **401**(6750): 297-300.
- Stahl, M., C. Ge, et al. (2006). "Notch1-induced transformation of RKE-1 cells requires up-regulation of cyclin D1." *Cancer Res* **66**(15): 7562-70.
- Takahashi, T., R. S. Nowakowski, et al. (1995). "The cell cycle of the pseudostratified ventricular epithelium of the embryonic murine cerebral wall." *J Neurosci* **15**(9): 6046-57.
- Takashima, Y., T. Era, et al. (2007). "Neuroepithelial cells supply an initial transient wave of MSC differentiation." *Cell* **129**(7): 1377-88.
- Tamiya, T., S. Mizumatsu, et al. (2001). "High cyclin E/low p27Kip1 expression is associated with poor prognosis in astrocytomas." *Acta Neuropathol* **101**(4): 334-40.
- (TCGA 2008). "Comprehensive genomic characterization defines human glioblastoma genes and core pathways." *Nature* **455**(7216): 1061-8.
- Thomas, J. B., M. J. Bastiani, et al. (1984). "From grasshopper to *Drosophila*: a common plan for neuronal development." *Nature* **310**(5974): 203-7.

- Toda, M., Y. Iizuka, et al. (2001). "Expression of the neural RNA-binding protein Musashi1 in human gliomas." *Glia* **34**(1): 1-7.
- Tsunekawa, Y., J. M. Britto, et al. (2012). "Cyclin D2 in the basal process of neural progenitors is linked to non-equivalent cell fates." *Embo J* **31**(8): 1879-92.
- Tsvetkov, L. M., K. H. Yeh, et al. (1999). "p27(Kip1) ubiquitination and degradation is regulated by the SCF(Skp2) complex through phosphorylated Thr187 in p27." *Curr Biol* **9**(12): 661-4.
- Veeriah, S., L. Morris, et al. (2010). "The familial Parkinson disease gene PARK2 is a multisite tumor suppressor on chromosome 6q25.2-27 that regulates cyclin E." *Cell Cycle* **9**(8): 1451-2.
- Veeriah, S., B. S. Taylor, et al. (2010). "Somatic mutations of the Parkinson's disease-associated gene PARK2 in glioblastoma and other human malignancies." *Nat Genet* **42**(1): 77-82.
- Verhaak, R. G., K. A. Hoadley, et al. (2010). "Integrated genomic analysis identifies clinically relevant subtypes of glioblastoma characterized by abnormalities in PDGFRA, IDH1, EGFR, and NF1." *Cancer Cell* **17**(1): 98-110.
- Vlach, J., S. Hennecke, et al. (1997). "Phosphorylation-dependent degradation of the cyclin-dependent kinase inhibitor p27." *Embo J* **16**(17): 5334-44.
- Vlachostergios, P. J., I. A. Voutsadakis, et al. (2012). "The ubiquitin-proteasome system in glioma cell cycle control." *Cell Div* **7**(1): 18.
- Wai, P., B. Truong, et al. (1999). "Cell division genes promote asymmetric interaction between Numb and Notch in the Drosophila CNS." *Development* **126**(12): 2759-70.
- Walzlein, J. H., M. Synowitz, et al. (2008). "The antitumorigenic response of neural precursors depends on subventricular proliferation and age." *Stem Cells* **26**(11): 2945-54.
- Wang, Y. Z., J. M. Plane, et al. (2011). "Concise review: Quiescent and active states of endogenous adult neural stem cells: identification and characterization." *Stem Cells* **29**(6): 907-12.

- Wang, J., H. Wang, et al. (2008). "c-Myc is required for maintenance of glioma cancer stem cells." *PLoS One* **3**(11): e3769.
- Wang, J., Q. Wang, et al. (2012). "Knockdown of cyclin D1 inhibits proliferation, induces apoptosis, and attenuates the invasive capacity of human glioblastoma cells." *J Neurooncol* **106**(3): 473-84.
- White, J. and S. Dalton (2005). "Cell cycle control of embryonic stem cells." *Stem Cell Rev* **1**(2): 131-8.
- Wodarz, A. and W. B. Huttner (2003). "Asymmetric cell division during neurogenesis in *Drosophila* and vertebrates." *Mech Dev* **120**(11): 1297-309.
- Yeo, C. W., F. S. Ng, et al. (2012). "Parkin pathway activation mitigates glioma cell proliferation and predicts patient survival." *Cancer Res* **72**(10): 2543-53.
- Zagzag, D., D. R. Friedlander, et al. (2000). "Molecular events implicated in brain tumor angiogenesis and invasion." *Pediatr Neurosurg* **33**(1): 49-55.
- Zhang, X., Q. Ran, et al. (2011). "Cell cycle arrest of Jurkat cells by leukemic bone marrow stromal cells: possible mechanisms and involvement of CRIF1." *Transplant Proc* **43**(7): 2770-3.
- Zhang, L., A. Shen, et al. (2012). "Spy1 is frequently overexpressed in malignant gliomas and critically regulates the proliferation of glioma cells." *J Mol Neurosci* **47**(3): 485-94.
- Zomer, A., S. I. Ellenbroek, et al. (2013). "Brief report: intravital imaging of cancer stem cell plasticity in mammary tumors." *Stem Cells* **31**(3): 602-6.
- Zucchi, I., E. Mento, et al. (2004). "Gene expression profiles of epithelial cells microscopically isolated from a breast-invasive ductal carcinoma and a nodal metastasis." *Proc Natl Acad Sci U S A* **101**(52): 18147-52.

## CHAPTER 2

### THE CYCLIN-LIKE PROTEIN SPY1 REGULATES GROWTH AND DIVISION CHARACTERISTICS OF THE CD133+ POPULATION IN HUMAN GLIOMA



## INTRODUCTION

Primary brain tumours can be driven by a population of brain tumour-derived cells with stem-like characteristics, or brain tumour initiating cells (BTICs) (Hemmati, Nakano et al. 2003; Singh, Hawkins et al. 2004). Whether these cells arise through dedifferentiation of lineage specified progenitors or through malignant transformation of endogenous neural stem cells (NSCs) is a subject of much debate. Regardless of the origin, understanding how BTICs regulate growth and development is of utmost importance for future treatment strategies (Dean, Fojo et al. 2005). Analogous to the hematopoietic system, neural markers are emerging which correlate primitive neural cells with BTICs (Hemmati, Nakano et al. 2003). One such example is the pentaspan transmembrane glycoprotein CD133 (Prominin1). CD133 is found in undifferentiated NSCs as well as in invasive glioma populations harboring stem-like properties (Yan, Lu et al. 2011 ). Ultimately the growth of BTICs correlates with high levels of positive cell cycle regulators and reduced levels of cell cycle inhibitors (Hidaka, Hama et al. 2009). Despite this the essentiality of core cell cycle machinery has yet to be fully elucidated.

Spy1 (Spdya; Speedy; Spy1A; RINGO) is a cyclin-like protein highly conserved in all vertebrates and some invertebrates, that is implicated in several cancers including glioblastoma (Porter, Dellinger et al. 2002; Cheng, Xiong et al. 2005; Golipour, Myers et al. 2008; Al Sorkhy, Ferraiuolo et al. 2012; Zhang, Shen et al. 2012). Spy1 can directly bind and activate the cyclin dependent kinases (CDK) independent of phosphorylation within the T-loop of the CDK, and with decreased dependency on dephosphorylation by the Cdc25 phosphatases (Porter, Dellinger et al. 2002; Cheng, Xiong et al. 2005). This unique manner of activating CDKs implies a mechanism by which Spy1 can bypass

classically defined cell cycle checkpoints. Indeed Spy1 is required for cell cycle re-entry in maturing vertebrate oocytes (Lenormand, Dellinger et al. 1999; Arumugam, MacNicol et al. 2012). The Spy1 gene, *SPDYA*, was initially isolated as a gene that conferred resistance to UV damage in a *rad1* deficient strain of *S. pombe* (Lenormand, Dellinger et al. 1999). Since this time Spy1 protein has been shown to override a number of cell cycle checkpoints, and is capable of directly binding and promoting degradation of the CDK inhibitor p27<sup>Kip1</sup> (p27) (Porter, Kong-Beltran et al. 2003; McAndrew, Gastwirt et al. 2007). The implication of this in the molecular processes regulating development and aging is also interesting. In mammary progenitor cells Spy1 levels are tightly regulated through normal development and accumulated protein levels abrogate differentiation and promote precocious development (Golipour, Myers et al. 2008). In the acute sciatic injury model Spy1 levels are dramatically upregulated in populations of proliferating astrocytes and microglia of the lumbar spinal cord, consequently implicating Spy1 in the regenerative processes of this system (Huang, Liu et al. 2009). Interestingly, upregulation of Spy1 is accompanied by an increase in CDK2 activity and downregulation of p27 in this system. The Spy1 effectors CDK2 and p27 are known mediators of normal neurogenesis (Dobashi, Shoji et al. 2000; Jablonska, Aguirre et al. 2007; Li, Tang et al. 2009). Stimulating neuronal differentiation in cell culture leads to the consequent downregulation of levels and activity of CDK2, as well as an increase in the protein levels of p27 (Kranenburg, Scharnhorst et al. 1995; Dobashi, Shoji et al. 2000). *CDK2* knockout mice have marked defects in the proliferative capabilities and self-renewal of adult neural progenitors in the subventricular zone (SVZ) (Jablonska, Aguirre et al. 2007). Indeed, enhanced CDK2 activity and downregulation of p27 are observed in many cases of brain cancer (Narita, Nagane et al. 2002; Fiano, Ghimenti et al. 2003; Hemmati, Nakano et al.

2003). CDK inhibitors have shown efficacy in human glioma *in vitro* (Jane, Premkumar et al. 2006); however, many biological questions remain to be elucidated before this approach can be reliably used *in vivo*. One important question is whether the cyclin partner of the CDK2 confers specificity in the decisions of NSCs or BTICs.

Recently, Zhang *et al.* demonstrated that Spy1 protein levels are elevated in malignant human glioma and protein levels correlate with poor prognosis (Zhang, Shen et al. 2012). Our work confirms this result and further quantifies Spy1 levels in increasing stage of glioma. We demonstrate that amplification of the *SPDYA* gene loci is an indicator of poor prognosis for glioma patients. Herein we show for the first time that endogenous levels of *SPDYA* decrease as NSCs differentiate. We also show that elevated levels of *SPDYA* expand the population of cells expressing BTIC markers and promote a BTIC phenotype. Furthermore, knockdown of *SPDYA* decreases stemness parameters and symmetric division of the CD133+ population. These effects are not seen with knockdown of classic G1/S cyclin, *CCNE1*, indicating that the observed changes are unique to Spy1. These data demonstrate that the Spy1/RINGO family of CDK regulators plays an important role in neural fate decisions. Abrogation of these decisions may promote the initiation and/or progression of human glioma.

## **EXPERIMENTAL PROCEDURES**

### **Animals**

Balb/c mice (Jackson Labs) were maintained and cared for following Canadian Council for Animal Care guidelines, under the University of Windsor AUPP# 10-08.

### **Cell Lines**

Rat pheochromocytoma PC12 cells and human GBM U-87 MG cells were obtained from ATCC. U251 cell line was a kind gift from Dr. James Rutka (The Hospital for Sick Children Research Institute, University of Toronto, Canada). The SJ-GBM2 cell line was obtained from The Children's Oncology Group repository (Arcadia, CA, USA). PC12 cells were grown in Dulbecco's modified Eagle's medium (DMEM; Sigma, USA, St. Luis, MO) containing 10% heat inactivated horse serum, 5% FBS, 1% L-glutamine and 1% penicillin/streptomycin. PC12 DMEM differentiation media contained 5% horse serum and 1% FBS. U-87 MG and U251 cells were cultured in Eagle's Minimum Essential Medium (*EMEM*; Sigma) and DMEM ,respectively, supplemented with 10% FBS and 1% penicillin/streptomycin. SJGBM2 cells were cultured in Iscove's Modified Dulbecco Medium (IMDM) supplemented with 20% of FBS, 5µg Insulin, 5µg Transferrin and 5ng Sodium Selenite. All cells were maintained at 37°C in 5% CO<sub>2</sub>. Cell proliferation and viability were measured using trypan blue exclusion assay. Cell numbers were quantified using TC100 Automated Cell Counter (BioRad).

### **Plasmids**

Vectors pJT0013 and pEIZ were generously donated from Drs. D. Donoghue and B. Welm respectively. Spy1 (*SPDYA*) was inserted into the *EcoRI* and *XbaI* sites of pEIZ to

create pEIZ-Spy1. Spy1-pLXSN (described previously (Porter, Kong-Beltran et al. 2003)) was modified to remove the polyA tail and renamed pBAM04. pLKO-scrambled control (#8453) and lentiviral constructs: pLB (#11619), pMD.G (#12259), pMDLg/pRE (#12251) and pRSV-Rev (#12253) were all obtained from Addgene. pLKO-*SPDYA* was cloned to express the short hairpin previously described in place of the scrambled sequence (Porter, Dellinger et al. 2002). pLB vector was cloned to express either shRNA specific to target murine *SPDYA* or scrambled control.

### **Lentivirus Production and Infection**

VSV-G pseudotyped lentivirus was produced by transient transfection of HEK293 LentiX cells with transfer vector plasmid (pEIZ, pLKO or pLB) and the multi-deleted packaging plasmids (pMDG, pMDL2, pRSV) using Polyethylenimine (PEI) (408719, Sigma) reagent with 1:3 DNA to PEI ratio and incubation for 5 hours at 37°C, 5% CO<sub>2</sub>. The virus was collected on the next day and concentrated for 3 hours at 4°C using and ultracentrifuge. The titer for pEIZ and pLB was determined by transducing 293T cells and analysis of eGFP protein expression by flowcytometry at 72 hours post transduction. The titer for pLKO lentivirus was assessed by puromycin selection followed by crystal violet staining and quantification of resistant colonies. The titered virus was filter sterilized and stored at -80°C. Cells were seeded into 96 well plate in serum and antibiotic free media containing 4-8 µg/ml of Polybrene. PEIZ- vector or pEIZ-*SPDYA* viral particles at MOI-2, pLKO- vector or pLKO-sh*SPDYA* viral particles at MOI-3 and pLB- vector or pLB-sh*SPDYA* at MOI-3 were incubated on cells overnight at 37°C, 5% CO<sub>2</sub>. The media containing virus were changed and cells were left to recover. After 72 hours the expression of pEIZ or pLB constructs was confirmed by the expression of eGFP

fluorescent protein. All the experiments utilizing pLKO vectors were performed under 1 µg/ml Puromycin selection.

### **Protein Isolation from Brain Tumour Tissues**

Flash frozen brain samples were thawed quickly and cut into 0.03-0.13 g pieces. Tissue pieces were weighed and 250 µl of NP40 Extraction Buffer (50 mM Tris-HCl pH 7.5, 1% NP40, 1 mM EGTA pH 8.0, 0.2% SDS, 150 mM NaCl, 0.25% sodium deoxycholate, 1.5% antifoam A) with protease inhibitors (leupeptin 2 µg/mL, aprotinin 5 µg/mL, sodium fluoride 50 mM, pepstatin A 1 µg/mL and PMSF 100 µg/mL) was used per 0.1 g of tissue. Tissues and extraction buffer were homogenized on ice (3x10 sec.). Samples were then centrifuged at 13,000 rpm for 15 min at 4°C. Supernatant was collected and stored at -20°C until use.

### **qRT-PCR**

Total RNA was extracted using the RNeasy Plus Mini Kit (Qiagen) and reverse transcribed using 200U Superscript II (Invitrogen), 0.5 µg OligodT's and 0.5 µg random nanomers (Sigma) according to the manufacturer instructions. Primers were designed using Primer Express software (Applied Biosystems). Real time PCR was carried out using SYBR green detection (Applied Biosystems) with 200-400 nM of each primer (Table 1; Suppl. Mat.) and was performed and analyzed using ViiA™ 7 Real-Time PCR system (Life Technologies) or ABI Prism 7300 thermocycler and software. Data represented log<sub>10</sub> relative quantification (RQ) relative to control.

### **Tissue Microarray (TMA)**

Paraffin embedded TMA slides consisting of 204 tissue cores in total were purchased from U.S. Biomax (cat no. GL241, GL803, GL1001). Slides were deparaffinized in

xylene and decreasing percentages of ethanol according to the manufacturer's protocol. Antigen retrieval was performed at 95°C in citrate buffer (0.01M sodium citrate buffer, pH 6.0). Slides were washed in 1 times PBS and subjected to immunofluorescence using Spy1 antibody (Novus, NB 100-2521) followed by Alexa- 488 conjugated secondary antibody (Sigma). Nuclei were counterstained with TOTO-3 T-3600 (Molecular Probes). The fluorescent signal was detected and quantified by ScanArray Express (Perkin Elmer Inc.) The Spy1 signal intensity was normalized to nuclear stain signal.

### **Primary Cell Harvest & Neurosphere Assays**

Tissues were micro-dissected and primary cells were dissociated from the region surrounding the SVZ of P1-P4 mouse brains as described previously (Jacqueline, Kasia et al. 2006). Cells were seeded at less than  $5 \times 10^4$  cells per well in 6-well Ultra Low Cluster Plates (ULCP) (Corning, 3471) and cultured in serum free Dulbecco's Modified Eagle's Medium (DMEM)/ Ham's Nutrient Mixture F-12 media (Sigma) containing N2 supplement hEGF (20ng/ml; Gibco) and bFGF (10ng/ml; Sigma), 2mM L-glutamine at 37°C in 5% CO<sub>2</sub>. Formed spheres were subcultured every 5-10 days. Differentiation was conducted on primary spheres in media supplemented with 2% FBS as described previously (Kerosuo, Piltti et al. 2008). Primary, secondary and tertiary neurospheres were dissociated and 10000 cells were seeded in 100µl of media in 96 well anti-adhesive plates. 20µl of 5mg/ml MTT solution in PBS were added to each well and incubated for 4 hours. 100µl of extraction buffer was added for 2 hours to dissolve the formazan crystals and the absorbance at 590nm was assessed using Victor plate reader (Perkin Elmer). Clonal assays were conducted in neurosphere media in 96 well ULCP plates, cells were

plated by serial dilution and wells containing 1-10 cells/well were included in experiments and analysis.

### **Magnetic Bead Sorting**

Cells were incubated for 48 hours in stem cell media. Pellets were resuspended in PBS buffer pH 7.4 containing 0.1% BSA, (B1). 25 $\mu$ l of magnetic beads (Dynabeads M-450 Epoxy, Invitrogen) labeled with CD133 antibody according to Invitrogen protocol (Abcam, 27699) were used for 2.5x 10<sup>6</sup> cells/1ml B1. Suspension was incubated 20 minutes at 4°C with gentle rotation followed by 2 minute positive isolation using EasySepmagnet (Stem Cell Technologies, #18000). Bead- bound cells were washed 4 times using 1ml of B1.

### **Cell Pair Assay and Immunofluorescence**

Single cells were isolated with 0.05% Trypsin- EDTA and plated in a drop of media onto MaxGel™ ECM (Sigma, E0282) coated cover-slips. Cell division was monitored over 20 hours and then fixed in 3.7% paraformaldehyde (PFA) for 20 minutes at room temperature. Cells were washed, permeabilized and incubated with Numb antibody (Cell signaling, C29G11, 1:200). Alexa-488 conjugated secondary antibody (Invitrogen, 1:1000 dilution) was applied for 1/2 hour. Nuclei were stained with TOTO-3 T-3600 (Molecular Probes). CD133 antibody (Abcam, 27699) staining was performed directly in media without fixation and was followed by the immunofluorescence protocol. Five random fields of view were scored for Numb protein distribution in mitotic cell pairs, per treatment, per replicate. Analysis was performed using Leica CTR 6500 microscope (Leica Microsystems, Heidelberg, Germany) and AF software.



### **Statistical Analysis**

Student *t*-test was used and a *p*-value of 0.05 was considered significant. All data are reported as means  $\pm$  s.d. qRT-PCR statistics were performed as describe previously (Yuan, Reed et al. 2006). Briefly, Ct value of the housekeeping gene (*GAPDH*) was subtracted from the corresponding Ct value of a target gene producing dCt value further subjected to the Student *t*-test analysis. Statistical analyses and normality testing were performed using Statistica software.

## RESULTS

### **Spy1 Protein Levels are Elevated in Multiple Types of Glioma and Correlate with Increasing Tumour Grade**

Analysis of the protein levels of Spy1 in oligoastrocytoma (OAC; Fig. 1A), oligodendroglioma (ODG; Fig. 1B) and invasive glioblastoma multiforme (GBM; stage IV astrocytoma; Fig. 1C) tissue was conducted using tissues obtained from the Ontario Brain Tumour Tissue Bank. Each sample set analyzed consisted of tissue derived from the tumour center (I), peritumour (II-IV) and normal tissue (V). Average levels of Spy1 protein from tumour centre out to normal tissue were calculated over 3 sets of samples per patient (Fig. S1). Spy1 protein levels were significantly elevated in the tumour tissue over normal in 3 of 4 ODG and OAC sample sets and 1 of 4 GBM sample sets (Fig. S1). Notably, tumour samples from patients 976 and 977 (GBM; Fig. 1C) and 865 (OAC; Fig. 1A) were highly necrotic in patient records; Spy1 levels were not elevated in these samples. In all 32 sample sets combined, Spy1 protein levels were significantly elevated in 63% of tumour centre samples and 62% of peritumour samples in comparison to the pair matched control tissues.

To further correlate the levels of Spy1 protein with the grade of brain tumour we utilized tissue microarrays (TMAs) consisting of 188 different patient cores, including cores taken from non-cancerous (normal) brain samples. Representative H&E stained core images are presented in Fig.S2. IHC performed on TMAs revealed extensive Spy1 staining in tumour tissues over pair matched adjacent 'normal' brain tissues taken from the same patients (Fig. 1D, S3, S4). Spy1 protein levels were progressively elevated with increasing grade of astrocytoma, demonstrating statistical significance over benign tissue

as well as both pair match normal adjacent tissue and non-cancerous normal tissues (combined as 'normal') (Fig. 1E). While sample numbers were limited, we found that Spy1 levels correlated with increasing grade of OAC (Fig.S4A) and ODG (Fig.S4B). Overall, protein levels of Spy1 were significantly elevated, at least 2 fold, in 69% of the glioma tumour samples tested (Fig. 1A-E&S4A-B). Work performed by The Cancer Genome Atlas (TCGA) research network demonstrated a strong correlation between the established GBM classes and normal neural lineages (Verhaak, Hoadley et al. 2010). Notably, we found that in comparison to primary neural cells cultured in monolayer, *SPDYA* levels are significantly upregulated in neurospheres derived from clonal expansion of those cells and correlate with the expression of stemness markers such as *Nestin* and *Vimentin* (Fig. S4D).

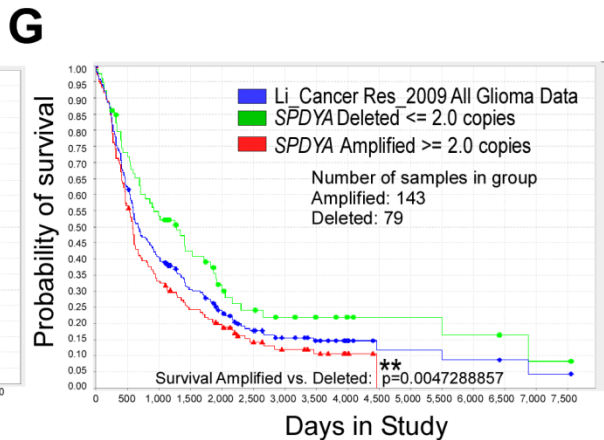
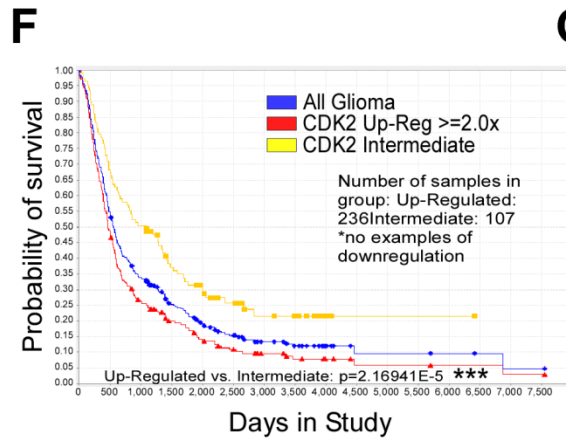
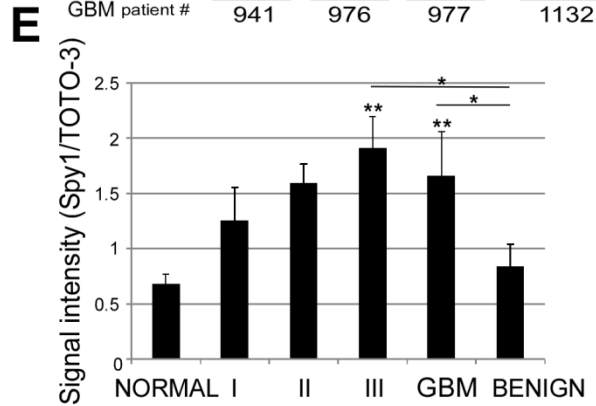
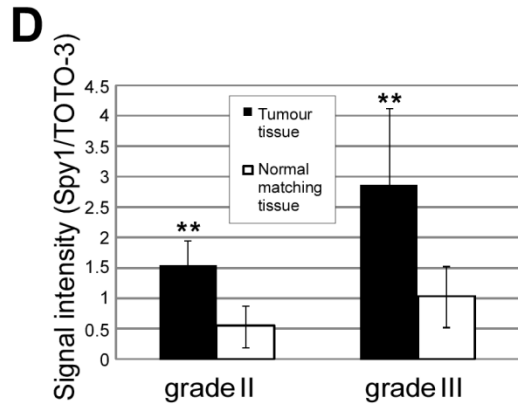
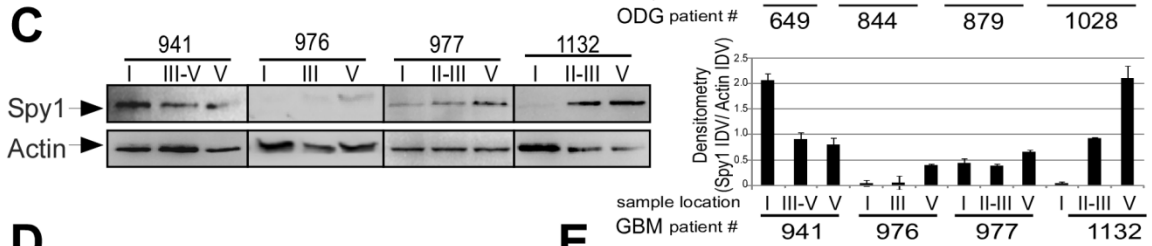
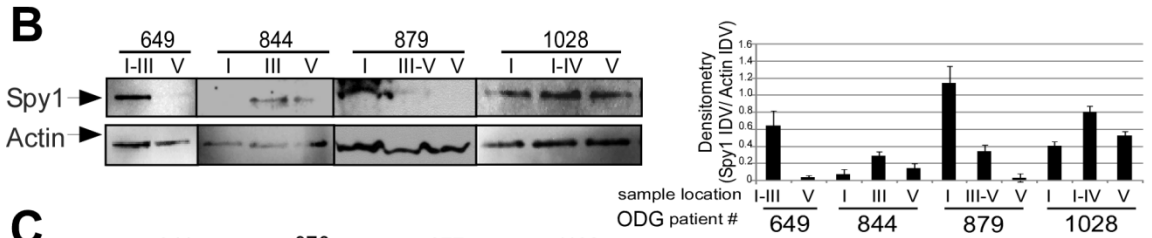
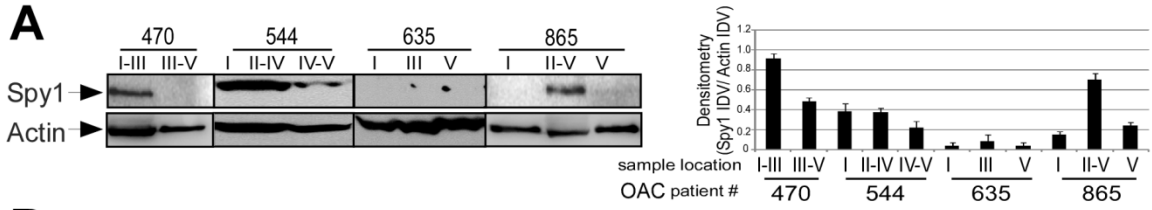


**Figure 1. Spy1 Protein is Overexpressed in High-Grade Glioma.**

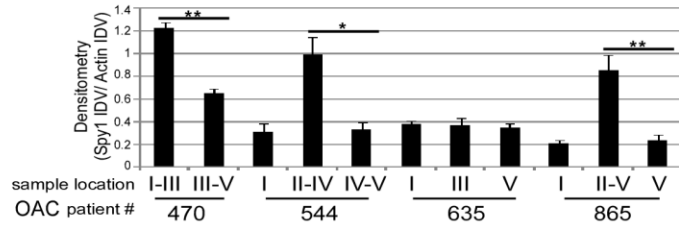
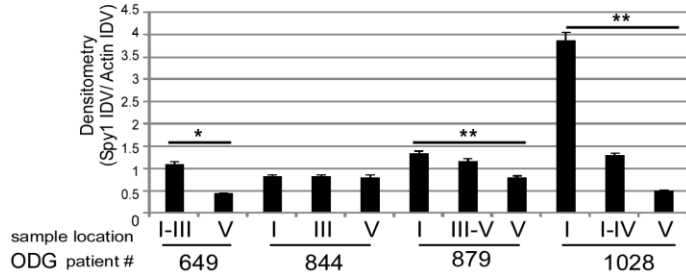
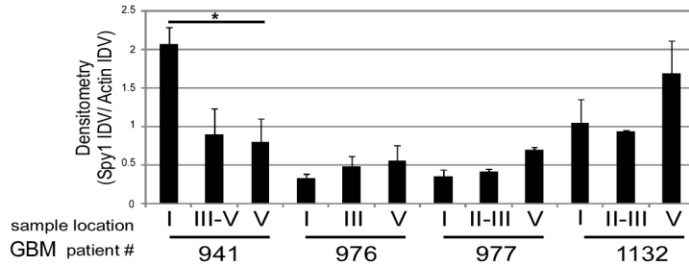
(A-C) Spy1 protein expression in human brain tumour tissues microdissected from OAC (A), ODG (B) and GBM (C) patients. Biopsies taken from the tumour center (I), peritumour (near tumour infiltrate - scant tumour cells; II-IV) or normal brain tissue (V). Patient identifier number is at the bottom of each graph panel. One representative blot of 3 is depicted. Values presented as the mean of Integrated Density Values (IDV) Spy1/Actin. Average values over multiple blots quantified in Fig.S1.

(D-E) TMAs containing normal brain and brain tumour tissue samples obtained from 188 different patients for Spy1 expression. The Spy1 signal intensity normalized to nuclear stain (TOTO-3) signal. Data are shown as mean  $\pm$ s.d; \* $p < 0.05$ , \*\* $p < 0.01$ .

(D) IHC of Spy1 positive cells in astrocytoma tissues of different grade (black bars) in comparison to normal adjacent brain tissue (white bars) over 2 separate arrays. Grade I-II astrocytoma (n=3), grade III astrocytoma (n=3) and normal controls (n=6). Data represented as mean  $\pm$ s.d. \*\* $p < 0.01$ .

(E) Spy1 protein levels analyzed in different grades of astrocytoma (I-III) (n=112), GBM (n=24) and benign brain tumours (n=8). See Fig.S2-S4. Data represented as mean  $\pm$ s.d. \* $p < 0.05$ , \*\* $p < 0.01$ .

(F-G) Patient survival data from Rembrandt NCI database correlated with CDK2 expression levels over all glioma samples (F) or *SPDYA* amplification/deletion from all glioma data (G). See Fig.S4C.

**A****B****C**

**Figure S1.** Spy1 protein levels are significantly elevated in patient brain tumour cores and peritumour compared to normal matched tissue. Spy1 protein expression in human brain tumour tissues microdissected from OAC (A), ODG (B) and GBM (C) patients. Biopsies taken from the tumour center (I), peritumour (near tumour infiltrate to scant tumour cells; II-IV) or normal brain tissue (V). Patient identifying number is located at the top of each panel. Data is presented as the mean of Integrated Density Values (IDV) Spy1/Actin. Average values over 3 representative blots for each patient are depicted. Errors  $\pm$ s.d. \* $p < 0.05$ , \*\* $p < 0.01$ .



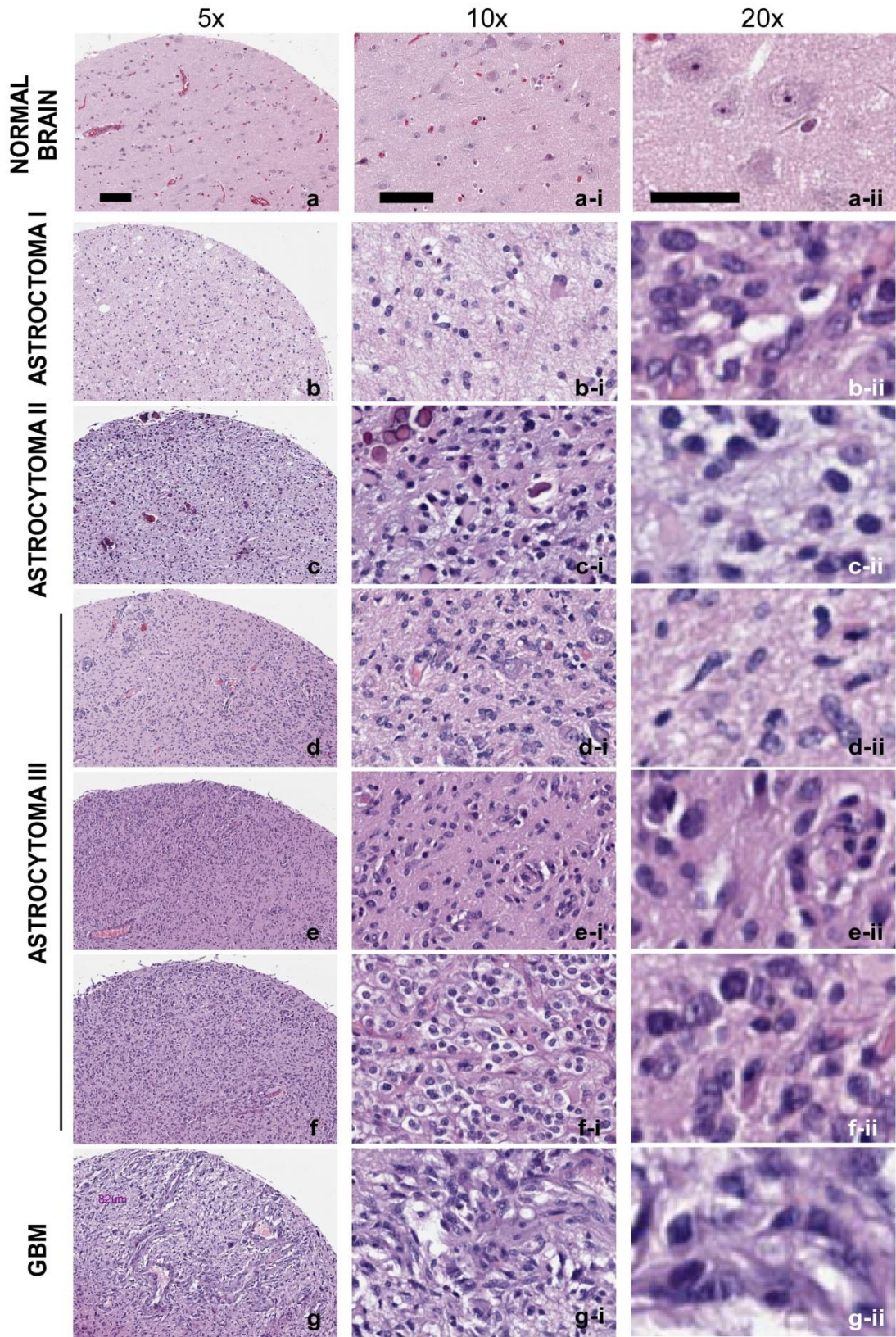




**Figure S2.** H&E stained sections from Human Normal and Brain Tumour TMA Cores. TMA core images at diverse magnifications were obtained from fully scanned TMA slides and are available at US. Biomax, Inc. website; <http://www.biomax.us/index.php>.(a) Normal brain tissue,(b) Astrocytoma grade I core, (c) Grade II of astrocytoma core, (d-f) three different cores representing grade III astrocytoma and (g) GBM cores. Columns represent 5x, 10x and 20x magnification as indicated. Scale bars: i & ii = 100 $\mu$ m, iii = 25  $\mu$ m.

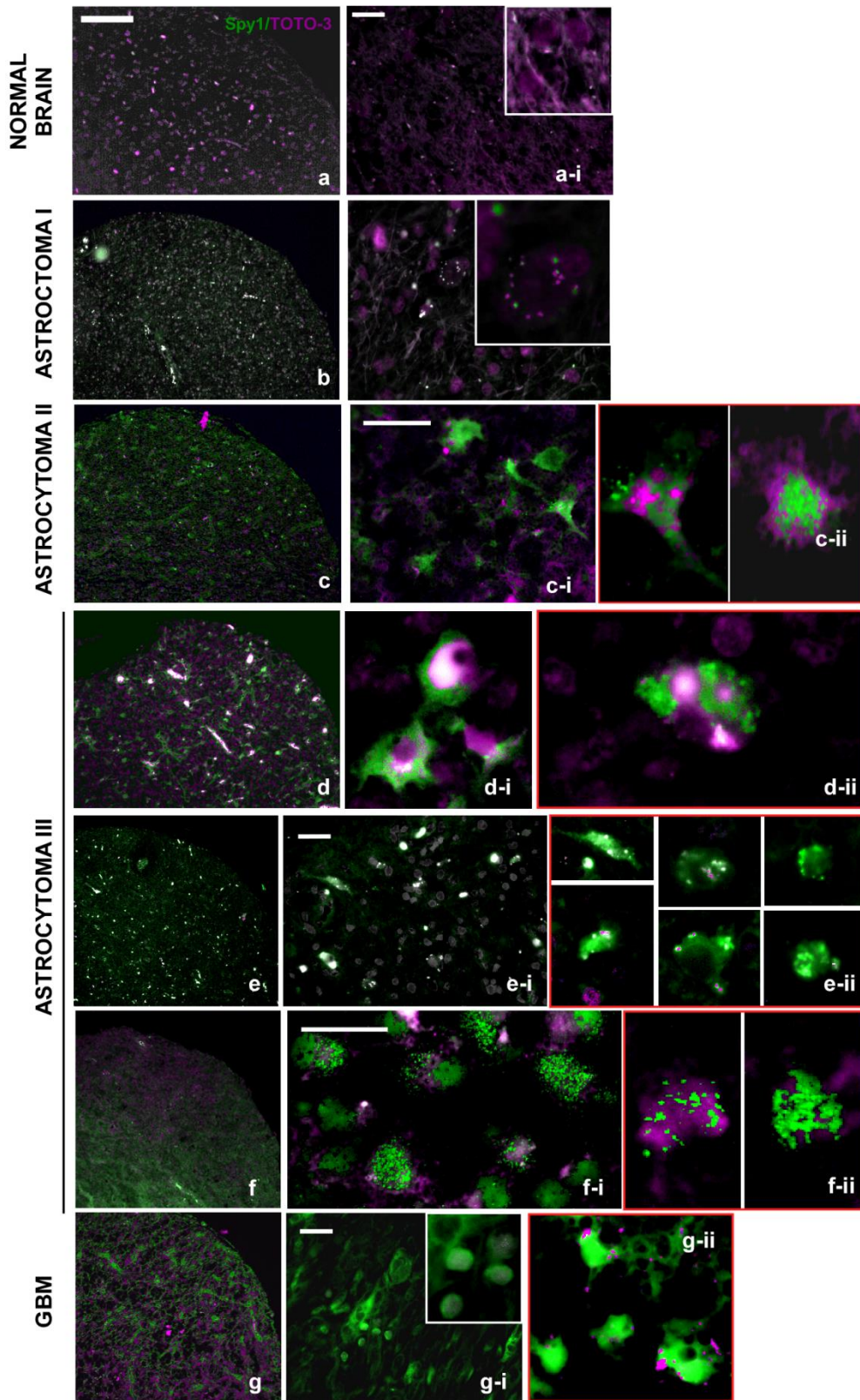


**Figure S3.** Immunofluorescent Detection of Spy1 Positive Cells in Human Normal and Brain Tumour TMA Cores.

Immunofluorescent image of TMA cores with Spy1 positive cells (green). Nuclei stained with TOTO-3(magenta). Rows represent:(a) Normal brain tissue, (b) Astrocytoma grade I, (c) Grade II astrocytoma, (d-f) Grade III astrocytoma, and (g) GBM. All cores in (i) are magnified in ii, or further magnified in iii. Scale bars= 25 $\mu$ m.

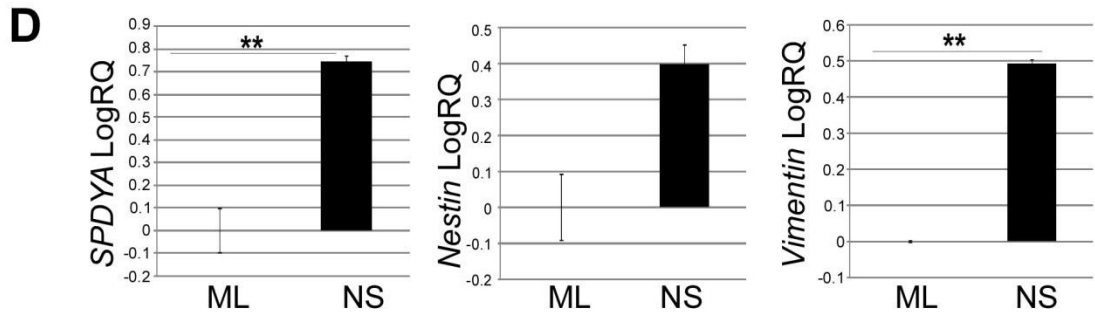
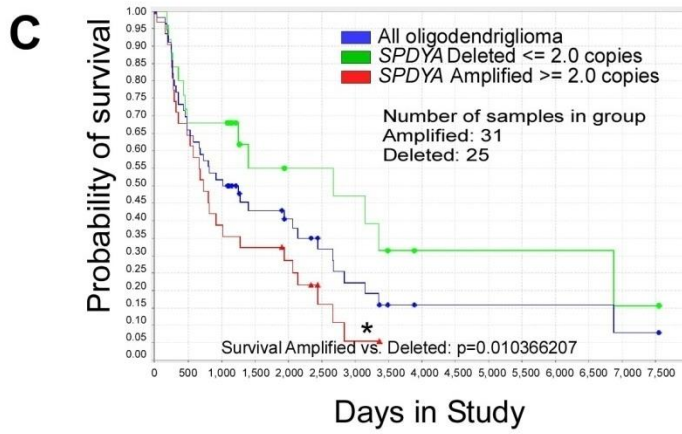
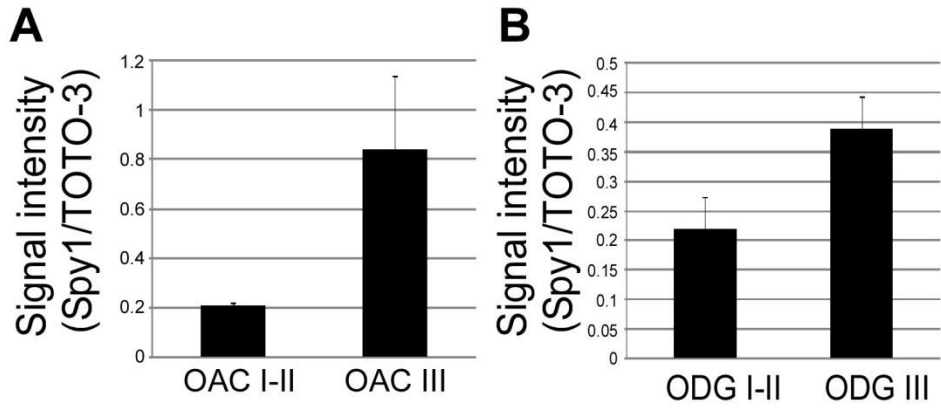


**Figure S4.** Spy1 is upregulated in malignant grades of OAC and ODG and its amplification correlates with reduced patient survival in ODG.

(A) Spy1 levels in lower grade (I-II) (n=3) vs. high grade (III) (n=6) of OAC.

(B) Spy1 levels in lower grade (I-II) (n=3) vs. high grade (III) (n=6) of ODG.

(C) Patient survival data from the Rembrandt NCI database correlated with Spy1 gene amplification/deletion from all ODG data. (D) Primary cell cultured as a monolayer (ML) or in neurosphere formation assay (NS) analysed by qRT-PCR for *SPDYA*, *Nestin* and *Vimentin* levels. Representative data shown as mean  $\pm$ s.d. n=3. \*\*p<0.01.

### **Amplification of the *SPDYA* Loci Correlates with Poor Patient Prognosis**

To determine if alterations at the genetic loci of Spy1 (*SPDYA*) could be implicated in patient prognosis, survival data from the Rembrandt NCI database was used to evaluate the effects of Spy1, and the Spy1 effector CDK2, on overall patient survival (NCI 2005). CDK2 was found to be overexpressed in 236 out of 343 cases of all glioma and overexpression very significantly correlated with reduced patient survival,  $p=0.00002$  (Fig. 1F). Importantly, there were no cases of downregulation of CDK2 in all 343 cases. Similarly in the dataset of Li *et al.* consisting of 257 patients (Li, Walling et al. 2009), there were 198 cases with upregulated CDK2, no cases of significant downregulation and upregulation very significantly correlated with decreased survival,  $p=0.0000007$  (data not shown). *SPDYA* was found to be amplified in 31 of 56 cases of ODG and amplification statistically correlated with reduced patient survival,  $p=0.01$  (Fig.S4C). *SPDYA* was amplified in 3 of 5 cases of mixed glioma and amplification correlated with reduced patient survival,  $p=0.06$  (data not shown). For total glioma cases, *SPDYA* was amplified in 143 out of 222 cases of all glioma and amplification significantly correlated with reduced patient survival,  $p=0.005$  (Fig. 1G). Notably, the Rembrandt database does not specify whether loci amplification is due to events such as focal amplification or whole arm gain. Nonetheless, from this data, amplification of *SPDYA* and overexpression of the Spy1 effector, CDK2, significantly correlate with reduced survival in glioma patients.

## **Knockdown of Spy1 Reduces Proliferation and Stemness Properties in Human Glioma**

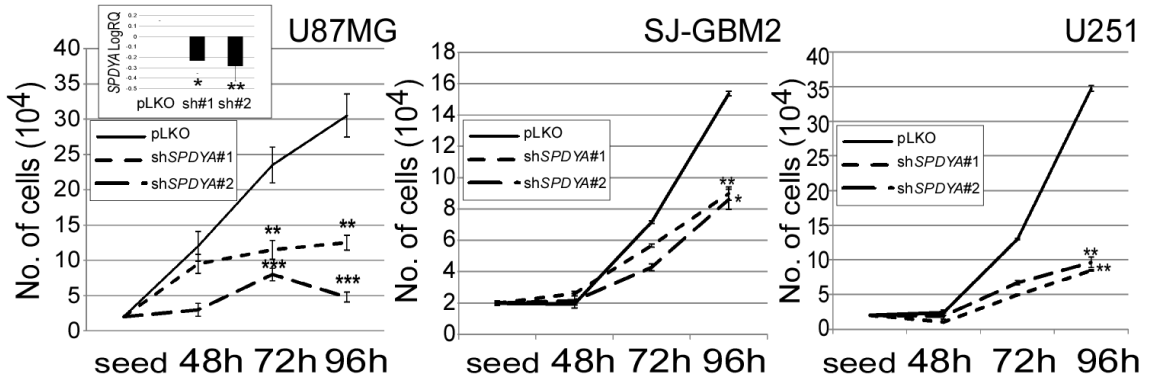
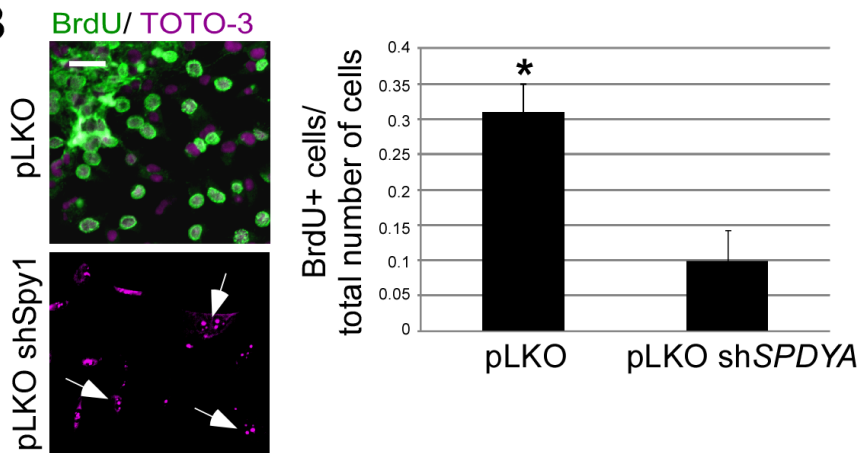
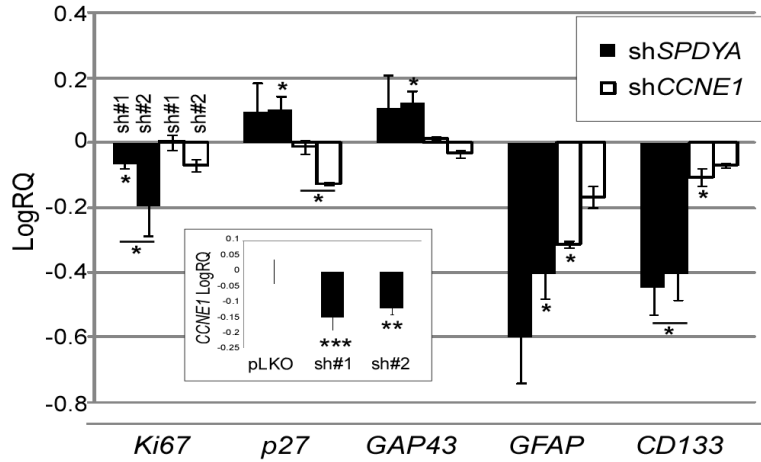
To address the importance of Spy1 protein in brain tumourigenesis *in vitro* we utilized the human U-87MG (U87), SJ-GBM2 and U251 glioma cell lines. The heterogeneous U87 and U251 cells contain a well characterized population of CD133+ cells established to be highly tumourigenic, possess stem-like properties and to be highly resistant to both radio- and chemo- therapy (Jeon, Jin et al. 2008; Verhaak, Hoadley et al. 2010). The SJ-GBM2 cells are established from pediatric glioma and constitute a model successfully used in evaluation of diverse chemotherapy strategies in childhood solid tumours (Middlemas, Stewart et al. 2000). Cells were infected with lentivirus carrying 2 different shRNA constructs against *SPDYA* (sh*SPDYA*) or a scrambled control (pLKO) and subsequently selected. Both of the *SPDYA*-shRNA constructs effectively reduced their targeted genes at least 3 fold (Fig. 2A inset). Proliferation kinetics show that *SPDYA* knockdown significantly reduces cell growth in all cell types tested (Fig. 2A). This result was confirmed by BrdU incorporation in the U87 line, where the sh*SPDYA* cells showed over a 60% reduction in DNA synthesis compared to control cells (Fig. 2B). Interestingly, sh*SPDYA* cells exhibited extensive chromatin condensation, characteristic of apoptotic nuclei (Fig. 2B; white arrows, left panel). Spy1 inhibits apoptosis (Gastwirt, Slavin et al. 2006), further studies are needed to determine whether *SPDYA* knockdown is indeed capable of triggering apoptotic events in these cells.

Marker analysis determined that Spy1 knockdown significantly reduced expression of the proliferation marker *Ki67* and enhanced expression of *p27* (Fig. 2C; black bars). Interestingly, *SPDYA* knockdown also correlated with increased levels of the

growth-associated protein 43 (*GAP43*), a marker of mature neurons, and decreased levels of markers known to identify both normal stem-like cells and BTICs, *CD133* and glial fibrillary acidic protein (*GFAP*). These data prompted the hypothesis that Spy1 levels may be important for both proliferation and directing the fate of at least subsets of cells within the heterogeneous tumour.

Spy1 binds and activates CDK2 in a unique manner, and Spy1-bound CDK2 has altered substrate specificity when compared to Cyclin E/A-bound CDK2 (Cheng, Gerry et al. 2005). Hence, to determine if the effects of Spy1 are due to a general reduction of CDK2 activity, or if Spy1 has unique roles in proliferation and stemness in human glioma, we compared *SPDYA* knockdown effects to the knockdown of the Cyclin E1 gene, *CCNE1*. Here we targeted *CCNE1* using two different shRNA constructs (Fig. 2C inset). Only *SPDYA* knockdown significantly altered expression of the proliferation marker *Ki67* (Fig. 2C). A reduction in *Ki67* with *SPDYA* knockdown was consistent with an increase in the cell cycle inhibitor *p27* and the neuronal marker *GAP43*. Both *SPDYA* and *CCNE1* knockdown did however reduce expression of both stemness markers *GFAP* and *CD133*, albeit the effect of Spy1 knockdown had a more robust effect. These data demonstrate that while depletion of either *SPDYA* or *CCNE1* demonstrate effects on cell fate markers GFAP and CD133, *SPDYA* knockdown had a more pronounced effect and also demonstrated effects on proliferation (*Ki67* and *p27*) and neuronal differentiation (*GAP43*).



**A****B****C**

**Figure 2.** Spy1 Levels are Essential for Proliferation and Stem-Like Properties of Human Glioma Cells.

(A: inset) qRT-PCR of U87 cells infected with scrambled control (pLKO) or two different shRNA against *SPDYA* (sh#1 and sh#2). Data shown as mean  $\pm$ s.d. n=3. \*p < 0.05, \*\*p < 0.01.

(A) Growth curves measured by trypan blue exclusion for U87 (left), SJ-GBM2 (middle) and U251 (right). Data represent mean cell number  $\pm$ s.d. n=3; \*p<0.05, \*\*p<0.01, \*\*\*p<0.001.

(B) Imaging (left panel) and quantification (right panel) of U87 cells positive for BrdU staining. Data shown as mean  $\pm$ s.d. At least 5 fields of view per infection. n=3; \*p<0.05. Scale bar, 10 $\mu$ m.

(C) qRT-PCR of U87 cells infected with scrambled control (pLKO) or two different shRNA against *SPDYA* (black bars) or *CCNE1* (hollow bars). Genes indicated on X-axis. Data shown as mean  $\pm$ s.d. n=3; \*p < 0.05.

(C; inset) qRT-PCR of *CCNE1* levels following infection of two different shRNA constructs (sh#1 and sh#2). Data shown as mean  $\pm$ s.d. n=3. \*\*p < 0.01, \*\*\*p < 0.001.

## **Spy1 Regulates Stemness Properties of the CD133+ Glioma Population**

To determine the potential role of Spy1 in the BTIC populations with neurosphere formation capacity, U87 cells were cultured and passaged in monolayer or as spheres to promote self-renewal *in vitro* (Lee, Kotliarova et al. 2006). *SPDYA* expression levels were upregulated when cells were cultured as spheres (Fig. 3A). This increase correlated with upregulation of the stemness markers *Nestin* and *CD133* and downregulation of *p27* and the oligodendrocyte marker *NG2* (Fig. 3A). CD133<sup>-</sup> cells are capable of initiating tumours *in vivo*, however sorting for a CD133<sup>+</sup> population in human glioma has been shown to enrich sphere formation, initiate glioma in a mouse xenograft model and to correlate with decreased prognosis for glioma patients (Bao, Wu et al. 2006; Zeppernick, Ahmadi et al. 2008). *SPDYA* expression is significantly higher in the CD133<sup>+</sup> population, and this correlates positively with expression of the stem/progenitor markers *Nestin* and *Vimentin* (Fig. 3B&C). This population also expressed higher amounts of the proliferation marker *Ki67* along with the oncogenes *c-Myc* and *MYCN* and reduced expression of *p27* (Fig. 3C). Additionally, the CD133<sup>+</sup> population was characterized by lower expression of oligodendrocyte markers *OLIG2* and *NG2* which, along with the upregulated levels of *GFAP*, suggests an astrocyte progenitor lineage and supports NSC nature of these cells. Downregulation of *BMI1* suggested that the sorted population represents a higher stem-like hierarchy, as BMI1 was recently shown to mark progenitor populations at the intermediate stages of differentiation within human glioma (Venugopal, Li et al. 2012).

We then measured the effects of depleting Spy1 on stemness characteristics of the CD133<sup>+</sup> population in multiple cell lines. In U87 cells sorted for CD133 (Fig. 1D, top panel), knockdown of *SPDYA* (Fig. 1D, lower right panel) resulted in a marked reduction

of *CD133* levels that occurred along with a decline in BTIC/proliferation markers *GFAP*, *Ki67*, *c-Myc* and upregulation of *p27* levels (Fig. 3D; bottom left panel). These results were similar in other glioma cell lines known to contain a CD133+ population (Fig. S5A & S5B). Notably, the *c-Myc*, *Ki67* and *p27* effects were not significant in the U251 cells (Fig. S5B). Although both shRNA constructs consistently reduced *CCNE1* expression levels at least 14 fold in the sorted population (Fig. S5C), there were no significant effects on the expression of the BTIC marker *CD133* (Fig. 3E). Furthermore, when comparing the effects of *SPDYA* knockdown to that of *CCNE1*, depletion of *Spy1* significantly reduced stemness markers *Nestin* and *GFAP* and upregulated progenitor markers *BMII* and *GAP43* markers over that of *CCNE1* knockdown (Fig. 3F). This data supports marked differences in the requirement for specific CDK partners in select BTIC populations.

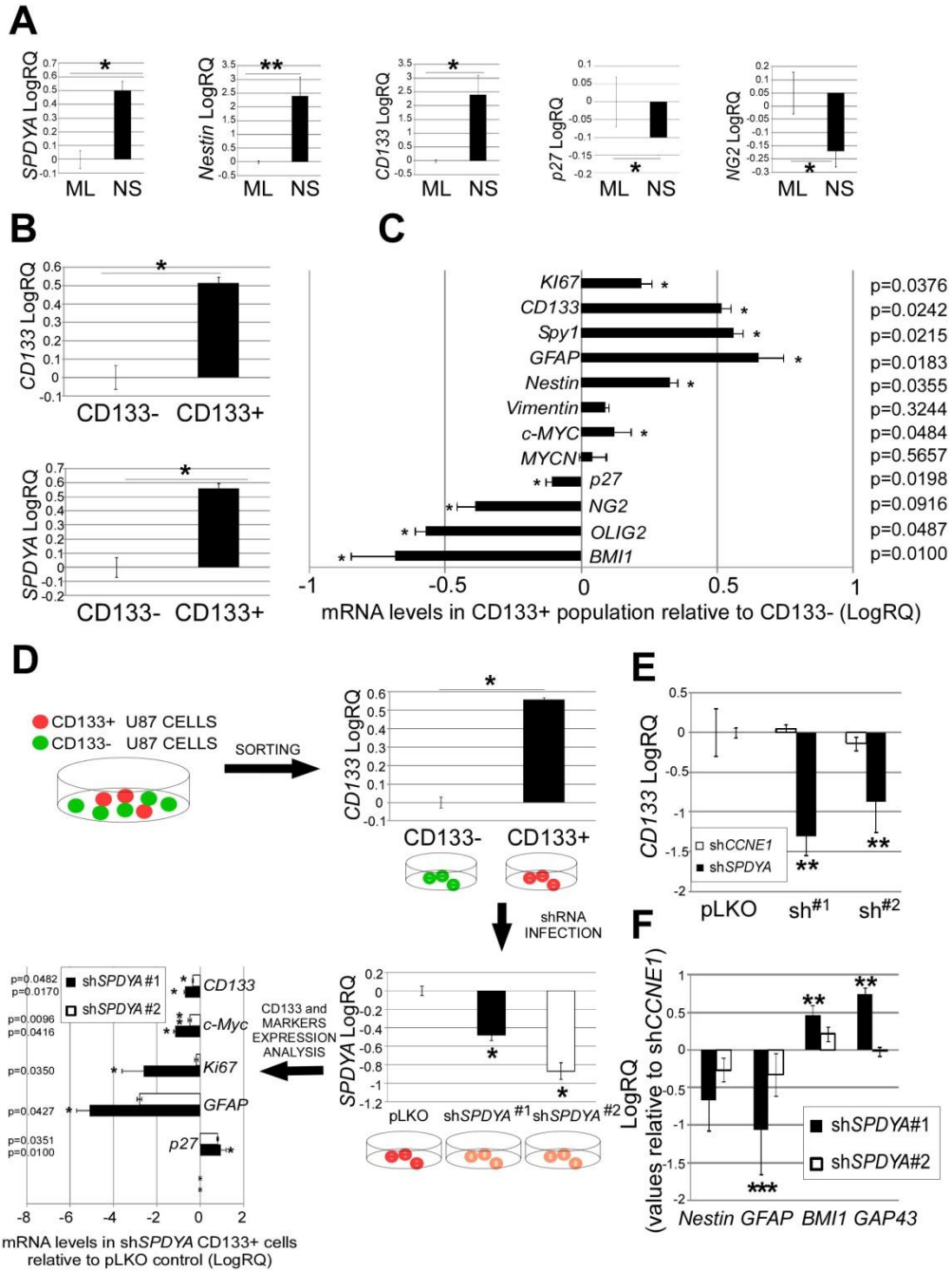


**Figure 3.** *Spy1* Expression Plays a Critical Role in the Stemness Properties of the CD133+ BTIC Population.

(A) qRT-PCR of U87 cells cultured as monolayer (ML) or in a neurosphere formation assay (NS) at passage 5. Data shown as mean  $\pm$ s.d. n=3. \* $p < 0.05$ , \*\* $p < 0.01$ .

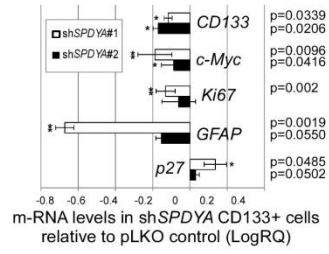
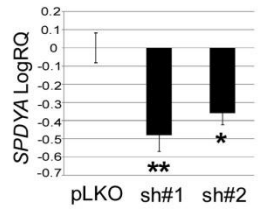
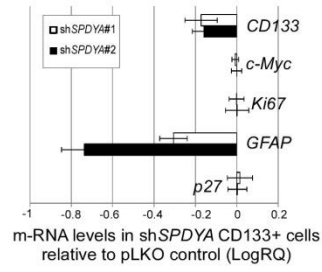
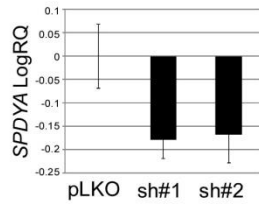
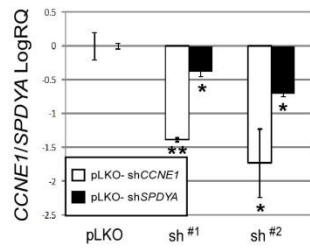
(B) U87 cells sorted and CD133+ and CD133- populations analyzed by qRT-PCR for *CD133* (upper panel) and *SPDYA* (lower panel) levels. Data shown as mean  $\pm$ s.d. n=3.\* $p < 0.05$ .

(C) CD133+ and CD133- populations analyzed by qRT-PCR for several genes. The CD133+ population is compared to the CD133- population. Data shown represent mean  $\pm$ s.d. n=3. \* $p < 0.05$  and  $p$ - values presented.

(D) U87 cells sorted for CD133 (confirmed by qRT, top right graph). The CD133+ population was infected with either shRNA scrambled control (pLKO) or one of two sh*SPDYA* constructs (sh*SPDYA*<sup>#1</sup> (hollow bars) or sh*SPDYA*<sup>#2</sup> (solid bars)). Knockdown confirmed by qRT-PCR (lower right graph). Effects on gene expression reported as relative expression of sh*SPDYA* over pLKO-scrambled control (Lower left graph). Data shown represent mean  $\pm$ s.d. n=3. \* $p < 0.05$ , \*\* $p < 0.01$  and  $p$ - values presented. See Fig.S5A & B.

(E) qRT-PCR for *CD133* in cells infected with sh*SPDYA* or sh*CCNE1* as comparison to control (pLKO). Representative data shown as mean  $\pm$ s.d. n=3. \*\* $p < 0.01$ . See Fig.S5C.

(F) qRT-PCR of different markers (X-axis) in a CD133+ population treated with two sh*SPDYA* constructs (sh*SPDYA*<sup>#1</sup> (solid bars) or sh*SPDYA*<sup>#2</sup> (hollow bars)). Data shown as relative to levels with knockdown for sh*CCNE1*. Representative data shown as mean  $\pm$ s.d. n=3. \*\* $p < 0.01$ , \*\*\* $p < 0.001$

**A****B****C**

**Figure S5.** Spy1 Expression Plays a Critical Role in the Stemness Properties of the CD133+ BTIC Population in diverse glioma cell lines.

(A) qRT-PCR analysis of CD133+ SJ-GBM2 cells infected with a scrambled control vector (pLKO) and two different constructs (sh#1, sh#2) against *SPDYA* (sh*SPDYA*). Representative data shown as mean  $\pm$ s.d. n=3. \*p<0.05, \*\*p<0.01.

(B) qRT-PCR analysis of CD133+ U251 cells infected with a scrambled control vector (pLKO) and two different constructs (sh#1, sh#2) against *SPDYA* (sh*SPDYA*). Representative data shown as mean  $\pm$ s.d. n=2.

(C) qRT-PCR analysis of *SPDYA* and *CCNE1* levels in CD133+ U87 cells. Representative data shown as mean  $\pm$ s.d. n=3. \*p<0.05, \*\*p<0.01.



## Downregulation of Spy1 is Critical for Specific Differentiation Decisions

Given that *SPDYA* knockdown reduced stem/progenitor markers and increased neuronal differentiation markers, we questioned whether Spy1 was endogenously regulated during differentiation. Primary neural cells obtained from the neurogenic regions of early post-natal mouse brains grown as neurospheres (Fig. 4A) or monolayer (Fig. 4B) were subjected to differentiation using 2% FBS. In both cases Spy1 expression decreased with differentiation morphology and correlated with a decrease in stemness markers *GFAP* and *Nestin* (Fig. 4A& B) and an increase in the neuronal differentiation marker *GAP43* (Fig. 4B). To determine whether Spy1 levels are similarly reduced along a neuronal differentiation lineage in human neural progenitor cells, PC12 pheochromocytoma cells were induced to differentiate over several days using nerve growth factor (NGF). Cells were scored as differentiated when the neurite length exceeded twice the size of the cell body (Fig. 4C; upper panel). Spy1 protein levels are undetectable by day 6 when 80-90% of control cells are differentiated (Fig. 4C; lower left panel). Notably, Spy1 expression was inversely correlated with that of p27, where p27 levels reached maximal levels by day 4-5 post-differentiation. QRT-PCR of *SPDYA* demonstrates that expression followed a similar trend, being significantly decreased by day 4 of differentiation (Fig. 4C; lower right panel). These changes occur with a decrease in CDK2 kinase activity (Fig. 4D).

To determine whether decreasing levels of Spy1 protein are essential for differentiation to occur, *SPDYA*, or an empty vector control, were overexpressed in both the PC12 cell line (Fig. 5A) and primary neural cells (Fig. 5B). PC12 stable cell lines were induced to differentiate and observed over an 8 day time course (Fig. 5A). By day 8,

95% of the control cells underwent differentiation, while only 50% of the Spy1 overexpressing counterparts were differentiated. Similarly, in primary neurospheres, 60% of control spheres successfully differentiated by 72 hours, while only ~20% of Spy1 overexpressing neurospheres were visibly differentiating (Fig. 5B). Spy1 overexpressing cells, induced to differentiate, had reduced expression of the neuronal differentiation marker *GAP43* and enhanced expression of the progenitor marker *GFAP* (Fig. 5B; right panel). While levels of *Nestin* were increased, they were not significant (Fig. 5B; right upper panel). Effects on mature astrocytes require further investigation pending the expansion of available markers. Depletion of *SPDYA* in primary neural cells using shRNA demonstrated a significant increase in functional differentiation; these effects were rescued using a human *SPDYA* overexpression plasmid resistant to knockdown with *SPDYA* shRNA (Fig. S6A). These results support that elevated levels of Spy1 favor expansion of stem/progenitor cells possessing glial characteristics and prevent functional differentiation toward a neuronal lineage.

To further determine whether Spy1 levels are critical for normal stem/progenitor characteristics; primary neural cells manipulated for *SPDYA* or control were assessed for self-renewal capacity and neurosphere formation. Spy1 overexpressing cells significantly increased the overall number, clonality and viability of neurospheres as compared to controls (Fig. 5C-E). An opposite effect was observed with *SPDYA* knockdown (Fig. S6B). Cells overexpressing Spy1 had notable elevation in stemness markers such as *Nestin*, *Vimentin* and *CD133* (Fig. 5F). These data demonstrate that the cyclin-like protein Spy1 is an important regulator in the expansion and growth of NSCs. Although this data does not reveal a cell of origin for glioma, we provide an additional mechanistic link regulating the common growth characteristics between NSC and BTIC populations.

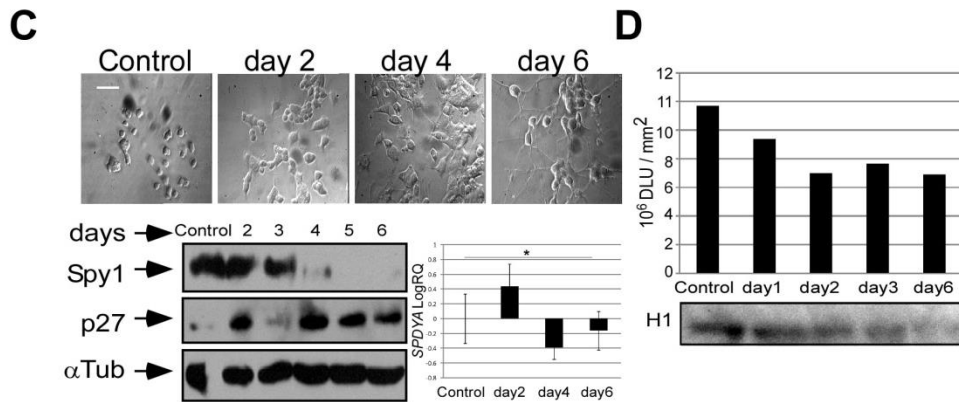
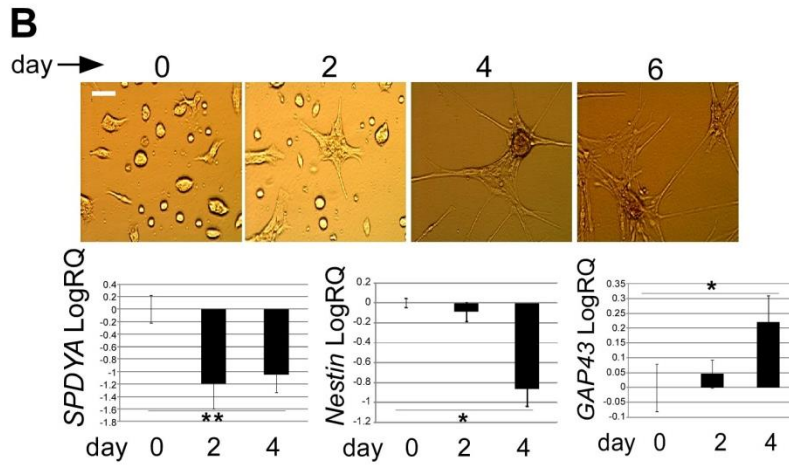
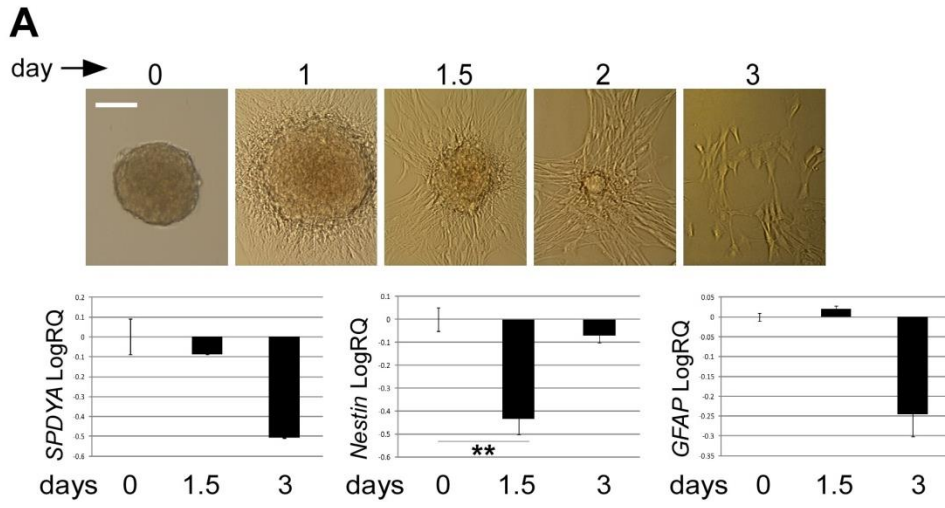


**Figure 4.** Spy1 Protein Levels are Tightly Regulated During Neural Progenitor Fate Decisions.

(A) Differentiation of mouse primary neural cells grown as neurospheres. Morphology assessed by phase contrast microscopy (upper panel). Scale bar, 25 $\mu$ m. *SPDYA*, *Nestin* and *GFAP* levels analyzed at indicated time points by qRT-PCR (lower panels). Representative data shown as mean  $\pm$ s.d. n=3. \*\*p<0.01.

(B) Differentiation of mouse primary neural cells recorded by phase contrast microscopy (upper panels; Scale bar, 10 $\mu$ m). qRT-PCR of *SPDYA*, *GAP43* and *Nestin* tested along the differentiation time course (lower panel). Non-treated cells were used as a control. Results presented as mean  $\pm$ s.d. n=4; \*p < 0.05.

(C) NGF-induced differentiation of PC12 cells recorded by phase contrast microscopy (upper panel). Spy1 expression analyzed by SDS-PAGE (lower left panel).  $\alpha$ -Tubulin used as a loading control. Scale bar, 10 $\mu$ m. qRT-PCR of *SPDYA* levels at each time point of differentiation (lower right panel). Non-treated cells were used as a control. Results presented as mean  $\pm$ s.d. n=3; \*p < 0.05.

(D) CDK2 activity measured by histone 1 (H1) kinase assay and quantified as Density Light Units (DLU) /mm<sup>2</sup> along PC12 differentiation time course (top panel). Lower panel indicates kinase activity detected by phosphorimaging. One representative experiment of two.

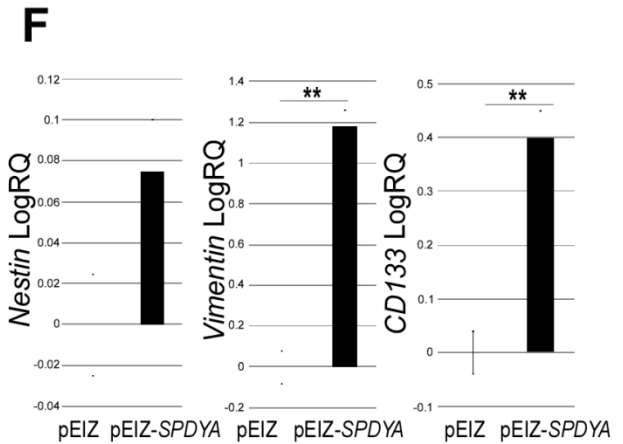
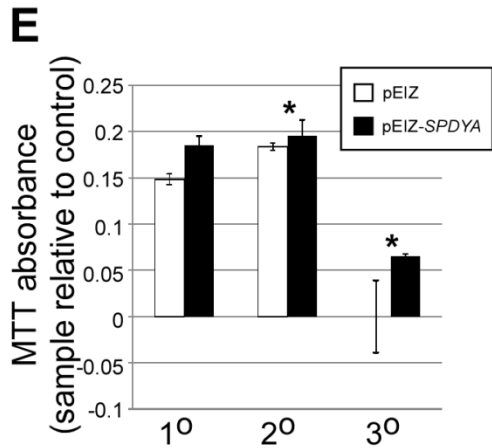
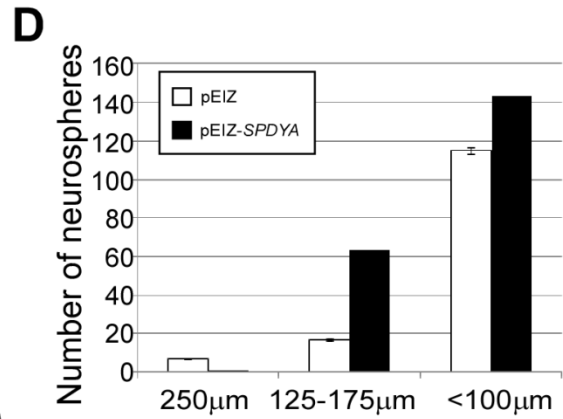
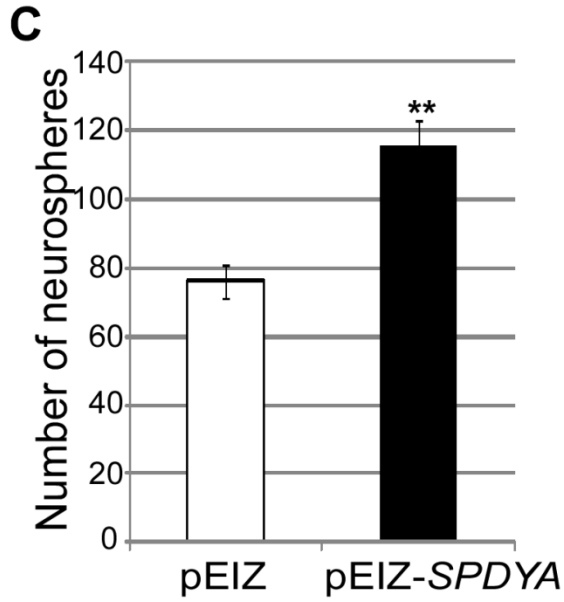
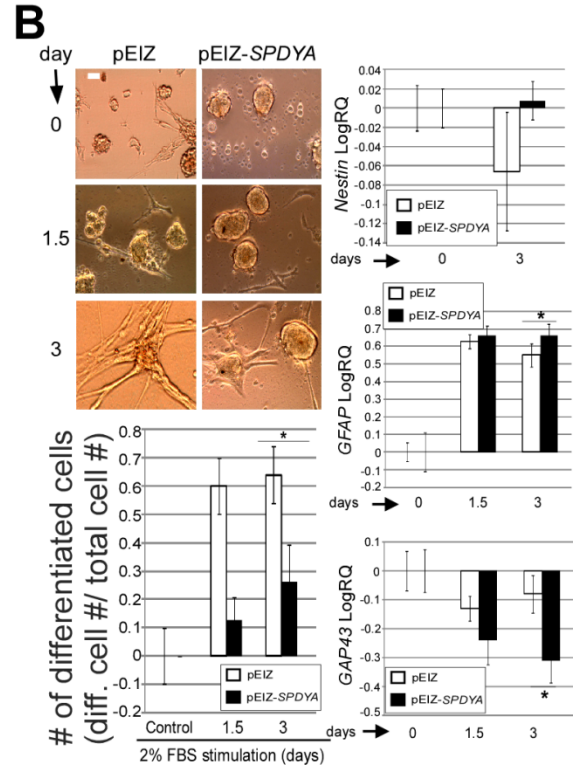
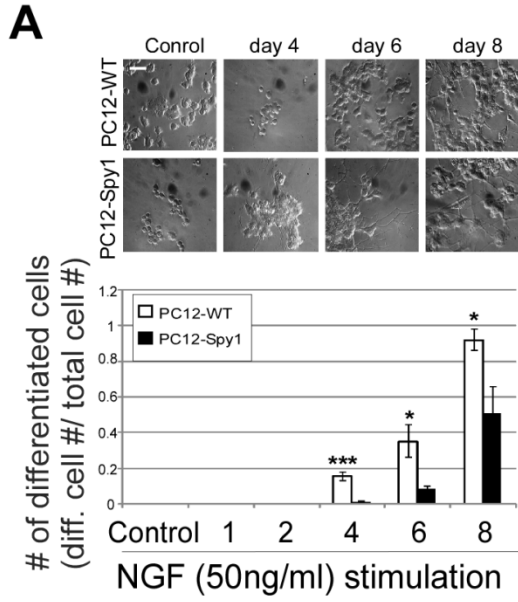


**Figure 5.** Spy1 Overexpression Abrogates Neuronal Differentiation and Promotes Neurosphere Clonal Growth.

(A) Differentiation of PC12 cells stably infected with flag-tagged *SPDYA* (PC12-*SPDYA*) versus empty vector (PC12-WT). Morphology by light microscopy (upper panel). Scale bar, 25 $\mu$ m. Differentiation scored by axon length. Ratio of differentiated cells to total cell number presented. Control (hollow), *SPDYA* overexpressing (black bars). Values are mean  $\pm$  s.d. n=3; \*p < 0.05, \*\*\*p < 0.001.

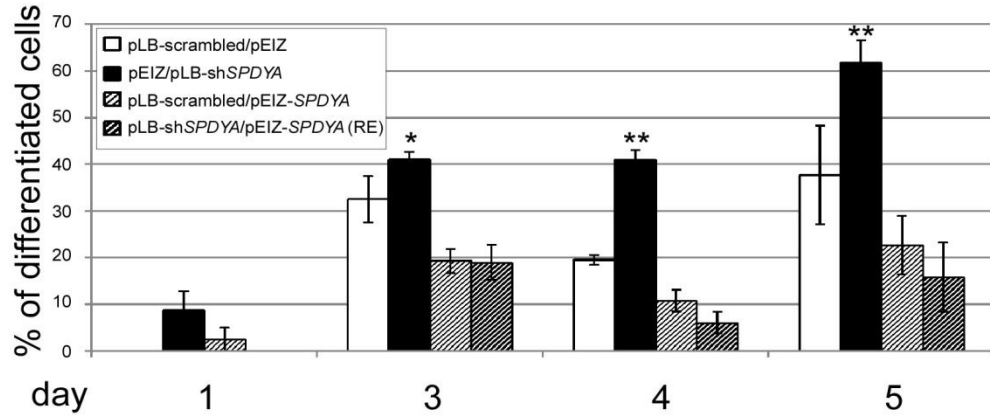
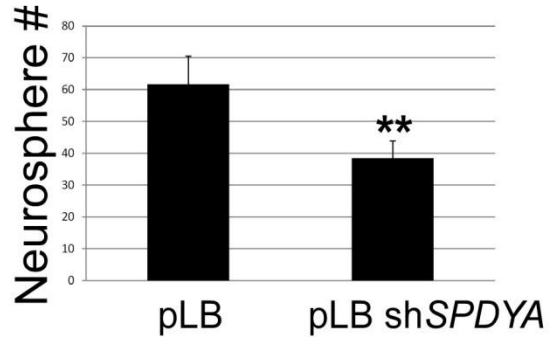
(B) Primary neurospheres infected with pEIZ-*SPDYA* versus control (pEIZ) over the indicated time points. Morphology was monitored by light microscopy (upper left panel). Scale bar, 25 $\mu$ m. Differentiation was scored by neurite length and presented as the ratio of differentiated spheres to total spheres (lower left panel). Control (hollow), *SPDYA* overexpressing (black bars). Values are mean  $\pm$  s.d. n=3; \*p < 0.05. qRT-PCR of markers in control (pEIZ) and Spy1 overexpressing (pEIZ-*SPDYA*) primary cells (right panel top to bottom). Representative data are shown as mean  $\pm$  s.d; n=3; \*p < 0.05. See Fig.S6A&B.

(C) Clonal assay performed on primary neural cells overexpressing Spy1 (pEIZ-*SPDYA*) vs. control (pEIZ). Total neurosphere numbers indicated as mean  $\pm$  s.d. n=3; \*\*p < 0.01.

(D) Neurospheres scored according to diameter after they were maintained in culture for 14-20 days. mean  $\pm$  s.d. n=2.

(E) Longevity of pEIZ or pEIZ-*SPDYA* primary, secondary and tertiary neurospheres (NS) in culture assessed by MTT assay. Neurospheres were passaged as single cells every 6-9 days. Absorbance at 590nm corrected for background absorbance. Representative data shown as mean  $\pm$  s.d. n=3; \*p < 0.05.

(F) qRT-PCR of stemness markers in pEIZ or pEIZ-*SPDYA* primary cells cultured as neurospheres (NS). Data shown is mean  $\pm$ s.d. n=3; \*\*p < 0.01.

**A****B**



**Figure S6.** The *SPDYA* knockdown accelerates differentiation and decreases neurosphere forming capacity in primary neural cell populations.

(A) The target specificity of the shRNA construct used was confirmed in rescue assays utilizing shRNA against mouse *SPDYA* (pLB-sh*SPDYA*) and human *Spy1* overexpressing vector (pEIZ-*SPDYA*). Primary neural cells treated with control vectors (pLB-scrambled or pEIZ), control vector and *SPDYA* shRNA (pEIZ/ pLB-sh*Spy1*), control vector and *SPDYA* overexpressing plasmid (pLB/ pEIZ-*SPDYA*) and the rescue treatment (RE) consisting of pLB-sh*SPDYA* and pEIZ-*SPDYA*, subjected to differentiation time course. Differentiated cells were scored according to neurite length, and the ratio of differentiated cells to total cell number represented as percentage was scored at the indicated time points. Data shown is mean  $\pm$ s.d. n=3; \*p<0.05, \*\*p<0.01.

(B) Clonal assay performed on Balb/c primary neural cells infected with shRNA against *SPDYA* (pLB-*SPDYA*) vs. scrambled control (pLB). Representative data are shown as mean  $\pm$ s.d. n=3; \*\*p < 0.01.

## Symmetric Division of CD133+ U87 Glioma Cells Relies Uniquely on Spy1

To assess Spy1 effects on the self-renewal characteristics of BTICs in human glioma, cell lines with manipulated levels of either *SPDYA* or *CCNE1* (Fig. S5C) were cultured at low densities (<10 cells/well) in media supporting self-renewal. Sphere formation was measured over 28 days after plating and spheres of 25  $\mu$ m or more in diameter were scored (Fig. 6A&B). *SPDYA* knockdown caused significant reduction in both the number and diameter of resulting spheres; characteristics previously correlated with tumorigenic capacity and percent of CD133+/Nestin+ cells in glioma (Wang, Wang et al. 2008; Yoon, Kim et al. 2012). Sphere formation over an excess of 10 passages in CD133+ U87 cells revealed that *SPDYA* knockdown caused a 5 fold decrease in number and longevity of spheres compared to control (Fig. S7A; left panel and S7B). The reciprocal effect was also noted in cells over-expressing Spy1 (pEIZ- *SPDYA*; Fig. S7A; right panel). EGF and FGF are essential growth factors that support stem cell self-renewal (Morshead, Reynolds et al. 1994; Li, Wang et al. 2009). Sorted cells were cultured in media without EGF and FGF for 48 hours. Interestingly, Spy1 overexpression resulted in significantly increased levels of *CD133* in the absence of EGF/FGF (Fig. S7C), suggesting that cell cycle regulation by Spy1 may lie downstream of associated growth factor signaling.

How BTICs use symmetric vs. asymmetric division to regulate expansion and support tumour growth are very important points that are not fully understood. Utilizing computer modeling Boman *et al.* have established that increasing symmetric division is the only mechanism to adequately explain the expansion of the cancer stem cell population (Boman, Wicha et al. 2007). *Drosophila* and mammalian systems have shown

that symmetry of division is influenced by the segregation of the protein Numb (Knoblich, Sauer et al. 1994; Lu, Rothenberg et al. 1998). Numb is able to promote neural differentiation, at least in part, through antagonizing Notch and Hedgehog pathways; thus localization of Numb serves as an indicator of cellular fate determination (Di Marcotullio, Ferretti et al. 2006; Couturier, Vodovar et al. 2012). While the functional role is unknown, asymmetric distribution of CD133 also co-localizes with Numb in differentiating glioma stem cells (Wang, Wang et al. 2008). Utilizing the cell pair assay to monitor protein expression in single cells through division we found that Spy1 knockdown resulted in marked asymmetric distribution of both Numb and CD133 protein (Fig. 6C (left panel)&S7D&E). Analysis over multiple infections of multiple glioma cell lines with 2 separate knockdown constructs for *CCNE1* and *SPDYA* showed significant asymmetric localization of Numb protein in the *SPDYA* -knockdown cells, but not in the *CCNE1* knockdown (Fig. 6C; right panel). Western blot analysis of Numb protein expression levels in CD133+ cells upon *SPDYA* or *CCNE1* knockdown show that *SPDYA* downregulation, but not downregulation of *CCNE1*, causes a significant and repeatable accumulation of Numb protein levels (Fig. 6D). Interestingly, even within heterogeneous populations of human glioma *SPDYA* levels were found to inversely correlate with Numb and p21 levels (Fig. S7F). These data support the hypothesis that levels of the atypical cyclin-like protein Spy1 promote NSC self-renewal and expansion of stem/progenitor populations by regulating the balance of symmetric vs. asymmetric division.

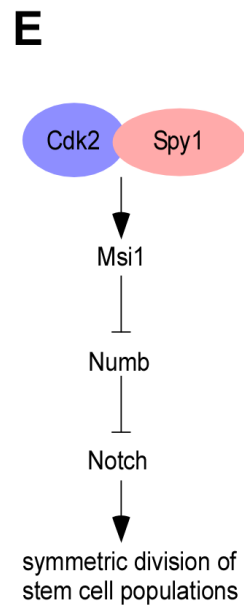
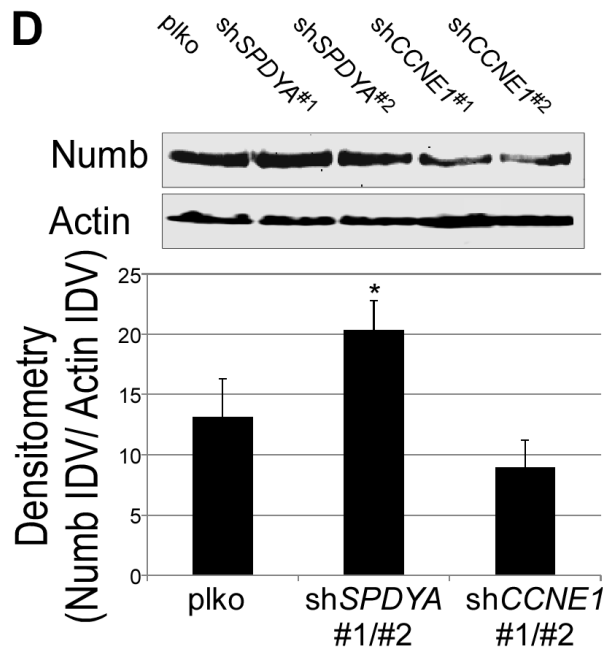
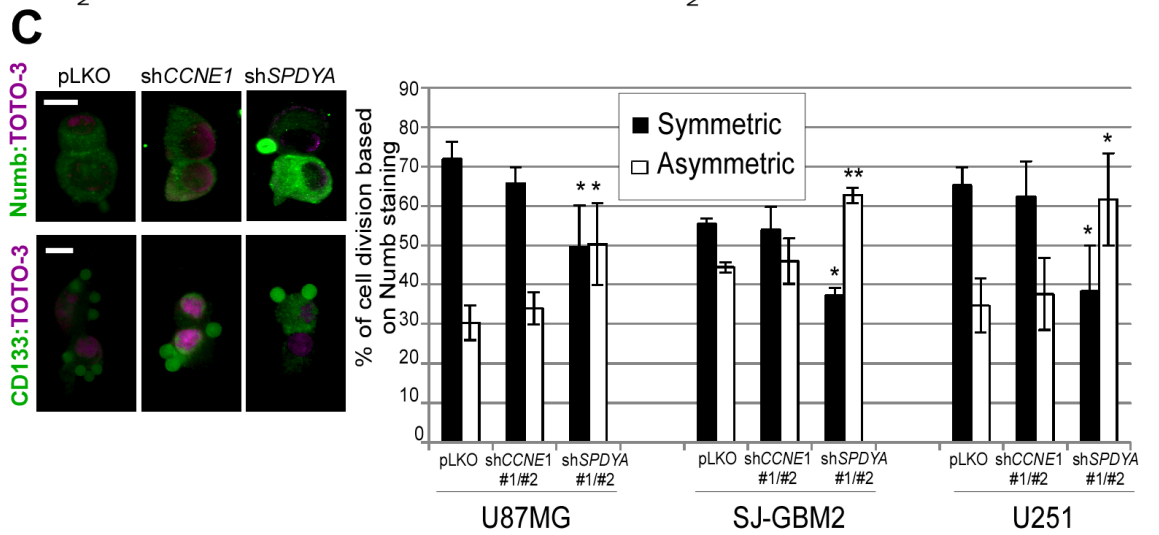
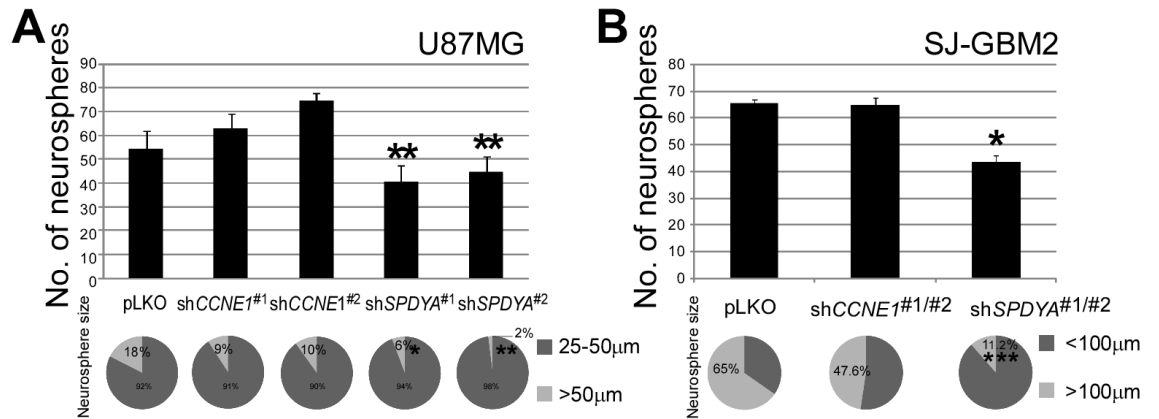


**Figure 6.** Spyl is Critical for Symmetric Division and Self-Renewal of CD133+ Cells.

(A) Clonal assay performed on pLKO-Control, sh*SPDYA*<sup>#1/#2</sup> and sh*CCNE1*<sup>#1/#2</sup> U87 CD133+ cells. Emerging neurospheres of over 25µm scored per well. Min. of 30 wells per replicate (upper panel). Neurosphere size presented as a pie chart. Data shown as mean ±s.d. n=3; \*\*p < 0.01. See Fig. S7A-C.

(B) As described for (A) using the CD133+ population in the SJ-GBM2 cells. Data shown as mean ±s.d. n=3; \*\*p < 0.01. Results obtained from both shRNA constructs were pooled.

(C) Cell pair assay conducted using the CD133+ population of U87, SJ-GBM2 and U251 cells treated with pLKO-scrambled control (pLKO), sh*SPDYA*<sup>#1/#2</sup> and sh*CCNE1*<sup>#1/#2</sup>. Representative U87 cells stained for Numb (left upper panel) and CD133 (left lower panel). Quantification of each cell type scored for Numb distribution (right panel). Data shown as mean ±s.d. n=3; \*p < 0.05, \*\*p < 0.01. Scale bars: 10 µm. See Fig.S7D-E.

(D) Levels of Numb protein in U87 cells treated with sh*SPDYA* or sh*CCNE1*. One representative blot of 3 (upper panel). Values are presented as the mean of Integrated Density Values (IDV) Numb/Actin. Data shown as mean ±s.d. n=3; \*\*p < 0.01. See Fig.S7F.

(E) Cartoon of putative mechanism for Spyl-mediated effects on division characteristics.

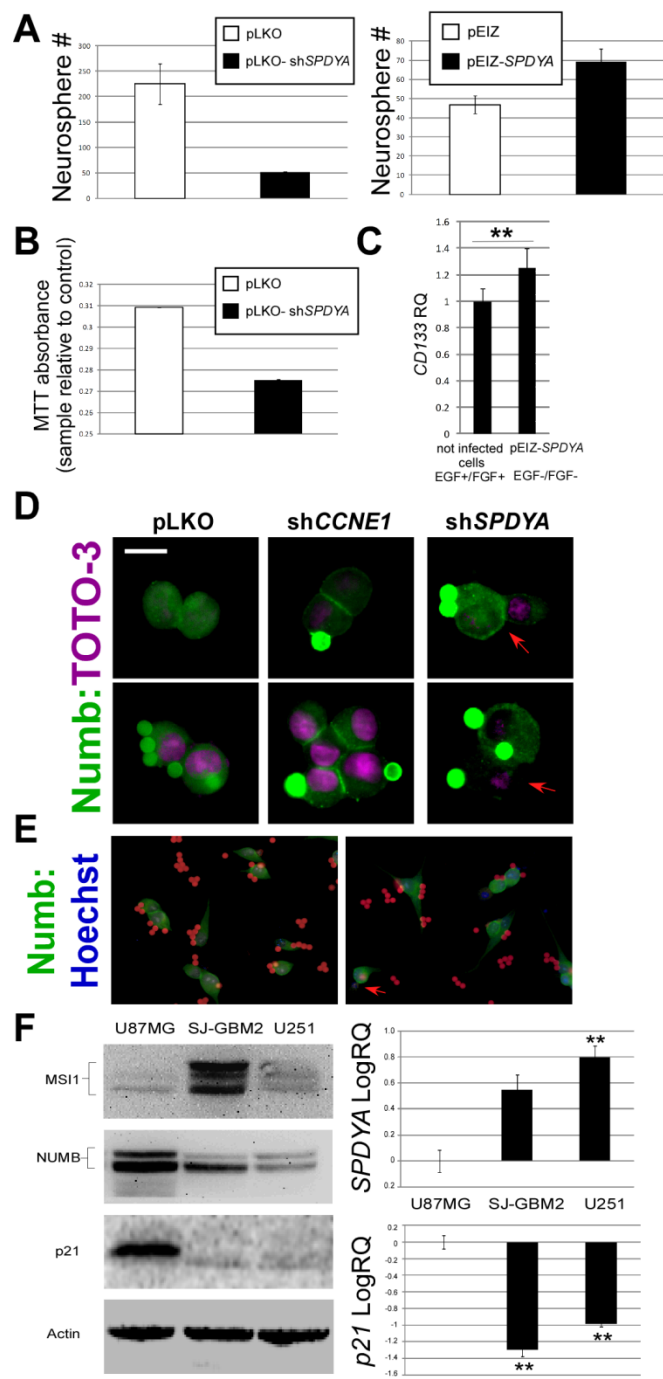


**Figure S7.** Spy1 Sustains Viability of Glioma Tumourspheres in Long Term Culture and Supports CD133 Expression Upon Growth Factor Withdrawal.

(A-B) Knockdown (left panel) and overexpression (right panel) of *SPDYA* in CD133+ U87 neurosphere long-term cultures.

(A) Number of neurospheres formed. Neurospheres were passaged at least 10 times and total number of spheres generated per well were scored per  $10^3$  cells plated initially. Data shown is mean  $\pm$ s.d.

(B) MTT assay in *SPDYA* knockdown CD133+ U87 cells. Spheres were cultured and passaged over a time period of 90 days prior to analysis. The obtained absorbance at 590nm was corrected for background absorbance. Data shown is mean  $\pm$ s.d.

(C) Spy1 effects on *CD133* expression upon withdrawal of growth factors. CD133+ U87 cells were infected with pEIZ-Cnt and pEIZ-*SPDYA*. qRT-PCR analysis of *CD133* expression in pEIZ-*SPDYA* and non-infected cells upon growth factor withdrawal. pEIZ-*SPDYA* levels were corrected for pEIZ. Data shown is mean  $\pm$ s.d. n=3, \*\*p<0.01, \*\*\*p<0.001.

(D) Additional images of cell pair assay conducted using the CD133+ U87 cells treated with pLKO-Control, sh*SPDYA*<sup>#1/#2</sup> and sh*CCNE1*<sup>#1/#2</sup>. Representative immunofluorescent micrograph analysis of U87 cells stained for Numb. Scale bar: 10 $\mu$ m.

(E) Low magnification images of cell pair assay using CD133+ U87 cells treated with sh*SPDYA* and sh*CCNE1*. Scale bar: 25 $\mu$ m.

(F) Endogenous levels of MSI1, Numb and p21 from cell lines listed above panels were measured by western blot (left panels). Right panels depict qRT-PCR reactions from cDNA prepared from each of the specified cell lines. *SPDYA* levels (upper right) and *p21*

levels (lower right) are depicted for each. Data is corrected for *GAPDH* and then graphically depicted as normalized to the lowest value (U87). Error bars reflect mean  $\pm$ s.d. n=3, \*\*p<0.01.



## DISCUSSION

The dynamics of neurogenesis rely on the balance of stem/progenitor self-renewal with commitment to specific lineages. Extensive literature indicates that anti-proliferative genes preventing the activation of G1/S CDKs act as important timers to permit neurogenesis (Durand, Fero et al. 1998; Hindley and Philpott 2012). Similarly, while not as extensively investigated, proliferative genes and signals resulting in an activation of the G1/S CDKs support expansion of stem/proliferative populations and retard successful neurogenesis (Dobashi, Kudoh et al. 1995; Lange and Calegari 2010). Which cyclin-CDKs regulate specific neurogenic events, and how their activation is controlled remains to be elucidated. As multicellular organisms have evolved to possess regenerative systems capable of sustaining long life, so have the families of proteins regulating cell cycle progression. The Spy1/RINGO family of cyclin-like proteins is such an example. Expressed in all vertebrates and some invertebrates, these proteins have demonstrated roles in spinal cord regeneration and to possess stem-like qualities in the developing mammary gland (Golipour, Myers et al. 2008; Huang, Liu et al. 2009). In this work we demonstrate that one member of the Spy1/RINGO family, Spy1A1, is expressed at high levels in clonally derived neurospheres and levels decline during differentiation. Elevated levels of Spy1 prevent functional differentiation and enhance the number and longevity of neural stem/progenitor cells able to grow in neurosphere culture. While the link between NSCs and BTICs remains to be determined, BTICs are found to express several normal NSC markers and possess growth characteristics mimicking that of normal NSCs (Chen, McKay et al. 2012). Hence, regardless of the BTIC origin, resolving the regulatory

properties driving normal NSCs may shed light on novel ways to target these aggressive populations therapeutically.

Another defining property of NSCs and BTICs alike, is the ability to divide both symmetrically and asymmetrically. A shift in division characteristics to favor symmetric division is thought to contribute to exponential increase in the numbers of cancer stem cells in a variety of different types of tumours (Gonczy 2008). One mechanism regulating the critical switch between modes of division depends on the cellular distribution of the protein Numb (Song and Lu 2012). Functionally Numb inhibits the Notch pathway to permit asymmetric division and subsequent differentiation (Song and Lu 2012). Our study demonstrates that Spy1 is important for maintaining symmetric mode of division and self-renewal, implicating a mechanistic role for this cyclin-like protein in retaining the hallmark properties of BTICs. A recent study published by Arumugam *et al.* pointed at the Spy1 (RINGO)/CDK signaling pathway as a highly conserved activator of Musashi-1 (Msi1) during cell cycle re-entry in oocyte maturation (Arumugam, MacNicol et al. 2012). Activated mammalian Msi1 stimulates Notch signaling through the translational repression of Numb (Toda, Iizuka et al. 2001). Hence, Msi1 may rely on Spy1-directed CDKs to mediate the self-renewal of normal NSCs as well as clonal expansion, malignancy and proliferation of glioblastoma cells (Sakakibara, Nakamura et al. 2002; Muto, Imai et al. 2012) (Fig. 6E). Our data reveals that downregulation of *SPDYA*, but not *CCNE1*, leads to increased levels of Numb protein followed by altered expression of select Notch transcriptional targets. Spy1 activates both CDK1 and CDK2, and CDK1 is an essential regulator of the switch between symmetric/asymmetric division in *Drosophila* neuroblasts (Tio, Udolph et al. 2001); hence Spy1-CDK1 could have unique functions in regulating effects on neural symmetry in vertebrates. The altered regulation

of Numb, and consequently Notch, may also alter overall self-renewal parameters. A study by Nosedá *et al.* showed that Notch can act as a transcriptional repressor of p21 which further prevents nuclear localization of Cyclin D/CDK4 (Nosedá, Chang *et al.* 2004). In mammals p21 maintains quiescence of adult NSC populations (Kippin, Martens *et al.* 2005). Hence, Spy1 appears to coordinate signals directing both self-renewal as well as the balance of symmetric/asymmetric division. Both of these activities are not simply due to CDK2 activation, as the effects of manipulating Spy1 do not mirror the effects seen with Cyclin E1. We show that while both Spy1- and Cyclin E1- activated CDKs play a role in proliferation of cancer stem cells, Spy1 uniquely demonstrates an effect on the stemness characteristics of the CD133+ population.

It is known that Spy1 activates CDKs in a Cyclin Activating Kinase (CAK) independent manner and demonstrates less stringent substrate specificity than cyclin-bound CDKs (Cheng, Gerry *et al.* 2005). In addition, atypical of cyclins, Spy1 can both activate CDKs as well as directly bind and promote the degradation of the CDK inhibitor p27 (Porter, Kong-Beltran *et al.* 2003). Functional differentiation requires a decrease in the kinase activity of CDK2 as well as an accumulation in p27 protein levels (Dobashi, Kudoh *et al.* 1995; Sasaki, Tamura *et al.* 2000). This work therefore supports the specific requirement for this unique class of proteins over the established CDK2 partners Cyclins E and A during neural differentiation and in promoting stemness properties in neural cells. The importance of these unique 'cyclin-like' proteins has been overlooked in the cancer therapeutics arena for over a decade (Porter, Dellinger *et al.* 2002). Although CDK inhibitors are being tested clinically for a number of different types of cancer, the studies in brain malignancies remain preliminary (Fischer and Lane 2000; Jane, Premkumar *et al.* 2006). In other types of cancer, despite the pre-clinical success of this approach, the data

on actual therapeutic outcome has been quite disappointing (Stone, Sutherland et al. 2012). Therefore, this work adds to the accumulating evidence that will aid in improving the effectiveness of CDK inhibitors in their use as chemotherapeutic agents for specific subsets of cancer.

Directing therapy to the appropriate patient population is also a pressing area of importance. *Spy1* levels were most significantly elevated in high grade of glioma, known to be more anaplastic with features resembling immature astrocytes and/or oligodendrocytes. This correlates with the elevated levels of glial progenitor markers seen in our cell systems overexpressing *Spy1*, such as the BTIC marker *CD133*. A significant amount of data supports the use of *CD133* as a stem cell surface antigen to identify a subpopulation of brain tumour initiating stem cells (Singh, Hawkins et al. 2004). While *CD133*- BTIC populations are able to generate heterogeneous tumours *in vivo* (Korur, Huber et al. 2009), tumours containing a *CD133*+ BTIC population correlate positively with higher grades of glioma, poorer patient prognosis, as well as multi-drug resistance (Dean, Fojo et al. 2005; Zeppernick, Ahmadi et al. 2008; Yan, Ma et al. 2011). Resolving the lineage commitment, stage of differentiation and genetic/genomic signatures of BTIC populations for the different forms and stages of glioma is an essential next step in correlating prognostic markers with effective treatments for brain cancers. Importantly, knockdown of *SPDYA* levels in a heterogeneous population of GBM cells decreased the proliferative index, as well as expression levels of *CD133* and *GFAP*. Abrogation of normal differentiation events can contribute to the initiation of tumourigenesis and understanding such events has proven to constitute a valuable strategy in the treatment of acute promyelocytic leukemia (Nakamura, Ramaswamy et al. 2000). Hence, it is feasible that a similar strategy would be a valuable approach for a cancer of neural origin.

## REFERENCES

- Al Sorkhy, M., Ferraiuolo, R.M., Jalili, E., Malysa, A., Fratiloiu, A.R., Sloane, B.F., and Porter, L.A. (2012). The cyclin-like protein Spy1/RINGO promotes mammary transformation and is elevated in human breast cancer. *BMC Cancer* 12, 45.
- Arumugam, K., MacNicol, M.C., Wang, Y., Cragle, C.E., Tackett, A.J., Hardy, L.L., and MacNicol, A.M. (2012). Ringo/cyclin-dependent kinase and mitogen-activated protein kinase signaling pathways regulate the activity of the cell fate determinant Musashi to promote cell cycle re-entry in *Xenopus* oocytes. *J Biol Chem* 287, 10639-10649.
- Bao, S., Wu, Q., Sathornsumetee, S., Hao, Y., Li, Z., Hjelmeland, A.B., Shi, Q., McLendon, R.E., Bigner, D.D., and Rich, J.N. (2006). Stem cell-like glioma cells promote tumor angiogenesis through vascular endothelial growth factor. *Cancer Res* 66, 7843-7848.
- Boman, B.M., Wicha, M.S., Fields, J.Z., and Runquist, O.A. (2007). Symmetric division of cancer stem cells--a key mechanism in tumor growth that should be targeted in future therapeutic approaches. *Clin Pharmacol Ther* 81, 893-898.
- Chen, J., McKay, R.M., and Parada, L.F. (2012). Malignant glioma: lessons from genomics, mouse models, and stem cells. *Cell* 149, 36-47.
- Cheng, A., Gerry, S., Kaldis, P., and Solomon, M.J. (2005a). Biochemical characterization of Cdk2-Speedy/Ringo A2 *BMC Biochem* 6, 19.
- Cheng, A., Xiong, W., Ferrell, J.E., Jr., and Solomon, M.J. (2005b). Identification and comparative analysis of multiple mammalian Speedy/Ringo proteins. *Cell Cycle* 4, 155-165.
- Couturier, L., Vodovar, N., and Schweisguth, F. (2012). Endocytosis by Numb breaks Notch symmetry at cytokinesis. *Nat Cell Biol* 14, 131-139.
- Dean, M., Fojo, T., and Bates, S. (2005). Tumour stem cells and drug resistance. *Nat Rev Cancer* 5, 275-284.
- Di Marcotullio, L., Ferretti, E., Greco, A., De Smaele, E., Po, A., Sico, M.A., Alimandi, M., Giannini, G., Maroder, M., Screpanti, I., *et al.* (2006). Numb is a suppressor of Hedgehog signalling and targets Gli1 for Itch-dependent ubiquitination. *Nat Cell Biol* 8, 1415-1423.
- Dobashi, Y., Kudoh, T., Matsumine, A., Toyoshima, K., and Akiyama, T. (1995). Constitutive overexpression of CDK2 inhibits neuronal differentiation of rat pheochromocytoma PC12 cells. *J Biol Chem* 270, 23031-23037.

- Dobashi, Y., Shoji, M., Kitagawa, M., Noguchi, T., and Kameya, T. (2000). Simultaneous suppression of cdc2 and cdk2 activities induces neuronal differentiation of PC12 cells. *J Biol Chem* 275, 12572-12580.
- Durand, B., Fero, M.L., Roberts, J.M., and Raff, M.C. (1998). p27Kip1 alters the response of cells to mitogen and is part of a cell-intrinsic timer that arrests the cell cycle and initiates differentiation. *Curr Biol* 8, 431-440.
- Fiano, V., Ghimentì, C., and Schiffer, D. (2003). Expression of cyclins, cyclin-dependent kinases and cyclin-dependent kinase inhibitors in oligodendrogliomas in humans. *Neurosci Lett* 347, 111-115.
- Fischer, P.M., and Lane, D.P. (2000). Inhibitors of cyclin-dependent kinases as anti-cancer therapeutics. *Curr Med Chem* 7, 1213-1245.
- Gastwirt, R.F., Slavin, D.A., McAndrew, C.W., and Donoghue, D.J. (2006). Spy1 expression prevents normal cellular responses to DNA damage: inhibition of apoptosis and checkpoint activation. *J Biol Chem* 281, 35425-35435.
- Golipour, A., Myers, D., Seagroves, T., Murphy, D., Evan, G.I., Donoghue, D.J., Moorehead, R.A., and Porter, L.A. (2008). The Spy1/RINGO family represents a novel mechanism regulating mammary growth and tumorigenesis. *Cancer Res* 68, 3591-3600.
- Gonczy, P. (2008). Mechanisms of asymmetric cell division: flies and worms pave the way. *Nat Rev Mol Cell Biol* 9, 355-366.
- Hemmati, H.D., Nakano, I., Lazareff, J.A., Masterman-Smith, M., Geschwind, D.H., Bronner-Fraser, M., and Kornblum, H.I. (2003). Cancerous stem cells can arise from pediatric brain tumors. *Proc Natl Acad Sci U S A* 100, 15178-15183.
- Hidaka, T., Hama, S., Shrestha, P., Saito, T., Kajiwara, Y., Yamasaki, F., Sugiyama, K., and Kurisu, K. (2009). The combination of low cytoplasmic and high nuclear expression of p27 predicts a better prognosis in high-grade astrocytoma. *Anticancer Res* 29, 597-603.
- Hindley, C., and Philpott, A. (2012). Co-ordination of cell cycle and differentiation in the developing nervous system. *Biochem J* 444, 375-382.
- Huang, Y., Liu, Y., Chen, Y., Yu, X., Yang, J., Lu, M., Lu, Q., Ke, Q., Shen, A., and Yan, M. (2009). Peripheral nerve lesion induces an up-regulation of Spy1 in rat spinal cord. *Cell Mol Neurobiol* 29, 403-411.
- Imai, T., Tokunaga, A., Yoshida, T., Hashimoto, M., Mikoshiba, K., Weinmaster, G., Nakafuku, M., and Okano, H. (2001). The neural RNA-binding protein Musashi1

- translationally regulates mammalian numb gene expression by interacting with its mRNA. *Mol Cell Biol* 21, 3888-3900.
- Jablonska, B., Aguirre, A., Vandenbosch, R., Belachew, S., Berthet, C., Kaldis, P., and Gallo, V. (2007). Cdk2 is critical for proliferation and self-renewal of neural progenitor cells in the adult subventricular zone. *J Cell Biol* 179, 1231-1245.
- Jacqueline, G.A., Kasia, T., Laura, P.K.K., Laurie, D.C., and Shelley, S. (2006). Neural Stem Cell Culture: Neurosphere generation, microscopical analysis and cryopreservation.
- Jane, E.P., Premkumar, D.R., and Pollack, I.F. (2006). Coadministration of sorafenib with rottlerin potently inhibits cell proliferation and migration in human malignant glioma cells. *J Pharmacol Exp Ther* 319, 1070-1080.
- Jin, F., Gao, C., Zhao, L., Zhang, H., Wang, H.T., Shao, T., Zhang, S.L., Wei, Y.J., Jiang, X.B., Zhou, Y.P., *et al.* (2011). Using CD133 positive U251 glioblastoma stem cells to establish nude mice model of transplanted tumor. *Brain Res* 1368, 82-90.
- Kelly, S.E., Di Benedetto, A., Greco, A., Howard, C.M., Sollars, V.E., Primerano, D.A., Valluri, J.V., and Claudio, P.P. (2010). Rapid selection and proliferation of CD133+ cells from cancer cell lines: chemotherapeutic implications. *PLoS ONE* 5, e10035.
- Kerosuo, L., Piltti, K., Fox, H., Angers-Loustau, A., Hayry, V., Eilers, M., Sariola, H., and Wartiovaara, K. (2008). Myc increases self-renewal in neural progenitor cells through Miz-1. *J Cell Sci* 121, 3941-3950.
- Kippin, T.E., Martens, D.J., and van der Kooy, D. (2005). p21 loss compromises the relative quiescence of forebrain stem cell proliferation leading to exhaustion of their proliferation capacity. *Genes Dev* 19, 756-767.
- Knoblich, J.A., Jan, L.Y., and Jan, Y.N. (1995). Asymmetric segregation of Numb and Prospero during cell division. *Nature* 377, 624-627.
- Korur, S., Huber, R.M., Sivasankaran, B., Petrich, M., Morin, P., Jr., Hemmings, B.A., Merlo, A., and Lino, M.M. (2009). GSK3beta regulates differentiation and growth arrest in glioblastoma. *PLoS One* 4, e7443.
- Kranenburg, O., Scharnhorst, V., Van der Eb, A.J., and Zantema, A. (1995). Inhibition of cyclin-dependent kinase activity triggers neuronal differentiation of mouse neuroblastoma cells. *J Cell Biol* 131, 227-234.
- Lange, C., and Calegari, F. (2010). Cdks and cyclins link G1 length and differentiation of embryonic, neural and hematopoietic stem cells. *Cell Cycle* 9, 1893-1900.

- Lathia, J.D., Hitomi, M., Gallagher, J., Gadani, S.P., Adkins, J., Vasanji, A., Liu, L., Eyler, C.E., Heddleston, J.M., Wu, Q., *et al.* (2011). Distribution of CD133 reveals glioma stem cells self-renew through symmetric and asymmetric cell divisions. *Cell Death Dis* 2, e200.
- Lee, J., Kotliarova, S., Kotliarov, Y., Li, A., Su, Q., Donin, N.M., Pastorino, S., Purow, B.W., Christopher, N., Zhang, W., *et al.* (2006). Tumor stem cells derived from glioblastomas cultured in bFGF and EGF more closely mirror the phenotype and genotype of primary tumors than do serum-cultured cell lines. *Cancer Cell* 9, 391-403.
- Lenormand, J.L., Dellinger, R.W., Knudsen, K.E., Subramani, S., and Donoghue, D.J. (1999a). Speedy: a novel cell cycle regulator of the G2/M transition *Embo J* 18, 1869-1877.
- Lenormand, J.L., Dellinger, R.W., Knudsen, K.E., Subramani, S., and Donoghue, D.J. (1999b). Speedy: a novel cell cycle regulator of the G2/M transition. *Embo J* 18, 1869-1877.
- Li, A., Walling, J., Ahn, S., Kotliarov, Y., Su, Q., Quezado, M., Oberholtzer, J.C., Park, J., Zenklusen, J.C., and Fine, H.A. (2009a). Unsupervised analysis of transcriptomic profiles reveals six glioma subtypes. *Cancer Res* 69, 2091-2099.
- Li, X., Tang, X., Jablonska, B., Aguirre, A., Gallo, V., and Luskin, M.B. (2009b). p27(KIP1) regulates neurogenesis in the rostral migratory stream and olfactory bulb of the postnatal mouse. *J Neurosci* 29, 2902-2914.
- Li, Z., Wang, H., Eyler, C.E., Hjelmeland, A.B., and Rich, J.N. (2009c). Turning cancer stem cells inside out: an exploration of glioma stem cell signaling pathways. *J Biol Chem* 284, 16705-16709.
- Lu, B., Rothenberg, M., Jan, L.Y., and Jan, Y.N. (1998). Partner of Numb colocalizes with Numb during mitosis and directs Numb asymmetric localization in *Drosophila* neural and muscle progenitors. *Cell* 95, 225-235.
- McAndrew, C.W., Gastwirt, R.F., Meyer, A.N., Porter, L.A., and Donoghue, D.J. (2007). Spyl1 enhances phosphorylation and degradation of the cell cycle inhibitor p27. *Cell Cycle* 6, 1937-1945.
- Middlemas, D.S., Stewart, C.F., Kirstein, M.N., Poquette, C., Friedman, H.S., Houghton, P.J., and Brent, T.P. (2000). Biochemical correlates of temozolomide sensitivity in pediatric solid tumor xenograft models. *Clin Cancer Res* 6, 998-1007.
- Muto, J., Imai, T., Ogawa, D., Nishimoto, Y., Okada, Y., Mabuchi, Y., Kawase, T., Iwanami, A., Mischel, P.S., Saya, H., *et al.* (2012). RNA-binding protein Musashi1 modulates glioma cell growth through the post-transcriptional



- regulation of Notch and PI3 kinase/Akt signaling pathways. *PLoS ONE* 7, e33431.
- Narita, Y., Nagane, M., Mishima, K., Huang, H.J., Furnari, F.B., and Cavenee, W.K. (2002). Mutant epidermal growth factor receptor signaling down-regulates p27 through activation of the phosphatidylinositol 3-kinase/Akt pathway in glioblastomas. *Cancer Res* 62, 6764-6769.
- NCI (2005). <http://rembrandtncinihgov>, Accessed 2011 May 2018.
- Nosedá, M., Chang, L., McLean, G., Grim, J.E., Clurman, B.E., Smith, L.L., and Karsan, A. (2004). Notch activation induces endothelial cell cycle arrest and participates in contact inhibition: role of p21Cip1 repression. *Mol Cell Biol* 24, 8813-8822.
- Porter, L.A., Dellinger, R.W., Tynan, J.A., Barnes, E.A., Kong, M., Lenormand, J.L., and Donoghue, D.J. (2002). Human Speedy: a novel cell cycle regulator that enhances proliferation through activation of Cdk2. *J Cell Biol* 157, 357-366.
- Porter, L.A., Kong-Beltran, M., and Donoghue, D.J. (2003). Spy1 interacts with p27Kip1 to allow G1/S progression. *Mol Biol Cell* 14, 3664-3674.
- Reynolds, B.A., and Weiss, S. (1992). Generation of neurons and astrocytes from isolated cells of the adult mammalian central nervous system. *Science* 255, 1707-1710.
- Sakakibara, S., Nakamura, Y., Yoshida, T., Shibata, S., Koike, M., Takano, H., Ueda, S., Uchiyama, Y., Noda, T., and Okano, H. (2002). RNA-binding protein Musashi family: roles for CNS stem cells and a subpopulation of ependymal cells revealed by targeted disruption and antisense ablation. *Proc Natl Acad Sci U S A* 99, 15194-15199.
- Sasaki, K., Tamura, S., Tachibana, H., Sugita, M., Gao, Y., Furuyama, J., Kakishita, E., Sakai, T., Tamaoki, T., and Hashimoto-Tamaoki, T. (2000). Expression and role of p27(kip1) in neuronal differentiation of embryonal carcinoma cells. *Brain Res Mol Brain Res* 77, 209-221.
- Sell, S. (2005). Leukemia: stem cells, maturation arrest, and differentiation therapy. *Stem Cell Rev* 1, 197-205.
- Singh, S.K., Hawkins, C., Clarke, I.D., Squire, J.A., Bayani, J., Hide, T., Henkelman, R.M., Cusimano, M.D., and Dirks, P.B. (2004). Identification of human brain tumour initiating cells. *Nature* 432, 396-401.
- Song, Y., and Lu, B. (2012). Interaction of Notch signaling modulator Numb with alpha-Adaptin regulates endocytosis of Notch pathway components and cell fate determination of neural stem cells. *J Biol Chem* 287, 17716-17728.

- Stone, A., Sutherland, R.L., and Musgrove, E.A. (2012). Inhibitors of cell cycle kinases: recent advances and future prospects as cancer therapeutics. *Crit Rev Oncog* 17, 175-198.
- Tio, M., Udolph, G., Yang, X., and Chia, W. (2001). cdc2 links the Drosophila cell cycle and asymmetric division machineries. *Nature* 409, 1063-1067.
- Venugopal, C., Li, N., Wang, X., Manoranjan, B., Hawkins, C., Gunnarsson, T., Hollenberg, R., Klurfan, P., Murty, N., Kwiecien, J., *et al.* (2012). Bmi1 marks intermediate precursors during differentiation of human brain tumor initiating cells. *Stem Cell Res* 8, 141-153.
- Verhaak, R.G., Hoadley, K.A., Purdom, E., Wang, V., Qi, Y., Wilkerson, M.D., Miller, C.R., Ding, L., Golub, T., Mesirov, J.P., *et al.* (2010). Integrated genomic analysis identifies clinically relevant subtypes of glioblastoma characterized by abnormalities in PDGFRA, IDH1, EGFR, and NF1. *Cancer Cell* 17, 98-110.
- Wang, J., Wang, H., Li, Z., Wu, Q., Lathia, J.D., McLendon, R.E., Hjelmeland, A.B., and Rich, J.N. (2008). c-Myc is required for maintenance of glioma cancer stem cells. *PLoS ONE* 3, e3769.
- Yan, C., Lu, J., Zhang, G., Gan, T., Zeng, Q., Shao, Z., Duerksen-Hughes, P.J., and Yang, J. (2011a). Benzo[a]pyrene induces complex H2AX phosphorylation patterns by multiple kinases including ATM, ATR, and DNA-PK. *Toxicol In Vitro* 25, 91-99.
- Yan, X., Ma, L., Yi, D., Yoon, J.G., Diercks, A., Foltz, G., Price, N.D., Hood, L.E., and Tian, Q. (2011b). A CD133-related gene expression signature identifies an aggressive glioblastoma subtype with excessive mutations. *Proc Natl Acad Sci U S A* 108, 1591-1596.
- Yoon, C.H., Kim, M.J., Kim, R.K., Lim, E.J., Choi, K.S., An, S., Hwang, S.G., Kang, S.G., Suh, Y., Park, M.J., *et al.* (2012). c-Jun N-terminal kinase has a pivotal role in the maintenance of self-renewal and tumorigenicity in glioma stem-like cells. *Oncogene* 31, 4655-4666.
- Yuan, J.S., Reed, A., Chen, F., and Stewart, C.N., Jr. (2006). Statistical analysis of real-time PCR data. *BMC Bioinformatics* 7, 85.
- Zeppernick, F., Ahmadi, R., Campos, B., Dictus, C., Helmke, B.M., Becker, N., Lichter, P., Unterberg, A., Radlwimmer, B., and Herold-Mende, C.C. (2008). Stem cell marker CD133 affects clinical outcome in glioma patients. *Clin Cancer Res* 14, 123-129.
- Zhang, L., Shen, A., Ke, Q., Zhao, W., Yan, M., and Cheng, C. (2012). Spyl is frequently overexpressed in malignant gliomas and critically regulates the proliferation of glioma cells. *J Mol Neurosci* 47, 485-494.

## CHAPTER 3

### THE ROLE OF SPY1 IN ADULT NEUROGENESIS

## INTRODUCTION

The dynamics of neurogenesis rely on different factors including the size of the stem/ progenitor cell population and the commitment of cells to specific lineages followed by neuronal growth and differentiation. Differences in the mechanisms of cell cycle regulation between embryonic and adult stages are responsible for the diverse developmental potential of neural progenitors. Active neurogenesis is associated with fluctuations in the cell cycle status throughout central nervous system (CNS) development (Ma, Qi et al. 2009). The specifics of how the cell cycle drives CNS developmental mechanisms, particularly with regard to stem/progenitor cell turnover and regulation of the neurogenic niche density, remain to be established. Embryonic stem cells (ESCs) use their self-renewing pluripotent potential at early stages of development; thereby expanding in number to establish a population of multilineage progenitors. ESCs demonstrate unique dynamics of the cell cycle. Their rapid division rate is attributed to an extremely short cell cycle due to a significant reduction in G1 phase (Takahashi, Nowakowski et al. 1995). Shortening of G1 in ESCs may also conserve their pluripotency and prevent differentiation (Orford and Scadden 2008; Singh and Dalton 2009; Lange and Calegari 2010). In contrast, adult stem cells need to carefully control growth to ensure that they are capable of expanding and differentiating throughout the life of an organism reviewed in (Mimeault and Batra 2006; Mimeault, Hauke et al. 2007). Adult stem cells predominantly accomplish this by residing in a quiescent state maintained by a network of cell cycle inhibitors. This ultimately reflects the stem cell commitment to preserve genomic integrity and prevent proliferative exhaustion.

Early postnatal development of the CNS is characterized by an important window of apoptotic events and synaptogenesis to form networks between mature neurons. These events are necessary for proper development and are potentially linked to events such as learning (Gordon 1995; Han, Wu et al. 2009). In the mature mammalian brain, proliferation and neurogenesis are limited to the populations of slowly proliferating adult stem cells. The primary neurogenic regions in the adult brain are restricted to the forebrain subventricular zone (SVZ) of the lateral ventricles (Doetsch, Caille et al. 1999) and subgranular zone within the dentate gyrus of the hippocampus (Palmer, Ray et al. 1995). A rare population of adult neural stem cells (NSC)s has also been found in the migratory circuit between the SVZ and olfactory bulb (Gritti, Bonfanti et al. 2002). A significant amount of research is accumulating to characterize factors regulating stem and progenitor cell proliferation as well as fate determination within these regions of the brain (Falk, Wurdak et al. 2008; Schmidt, Bicker et al. 2009). Cell cycle regulation plays a key role as the control system, not only during neurogenesis in the developing brain, but also in sustaining proliferative potential in the adult brain.

Spy1 (Speedy, Spdya, RINGO), encoded by *SPDYA* gene, belongs to a family of unconventional cell cycle regulators that can stimulate cyclin dependent kinase 2 (CDK2) independent of classically defined post-translational modifications required to activate Cyclin-CDK complexes (Karaiskou, Perez et al. 2001; Cheng, Xiong et al. 2005). Spy1 can also bind directly to the CDK-inhibitor p27, promoting further activation of CDK2 and subsequent degradation of p27 (Porter, Kong-Beltran et al. 2003; McAndrew, Gastwirt et al. 2007) and Spy1 overexpression reduces the length of G1 phase and promotes cell proliferation (Porter, Dellinger et al. 2002). Importantly, Spy1-mediated effects have been implicated in a variety of different human cancers as well as in normal

development (Golipour, Myers et al. 2008; Ke, Ji et al. 2009; Zhang, Shen et al. 2012). Recently, Spy1 has been suggested to participate in the neuroregenerative processes of the spinal cord (Huang, Nagane et al. 1997; Cao, Yang et al. 2013). Several lines of evidence support a role for the Spy1-effectors CDK2 and p27 in regulating the balance between self-renewal and differentiation among adult stem cells in the postnatal brain (Ghiani and Gallo 2001; Doetsch, Verdugo et al. 2002; Lukaszewicz, Savatier et al. 2005; Jablonska, Aguirre et al. 2007; Li, Collado et al. 2012). Collectively, these published data suggest a role for Spy1 in neural progenitors during adult neurogenesis.

This study investigates the spatio-temporal expression of Spy1 in the mammalian CNS. We demonstrate for the first time that Spy1 protein is found at sites of adult neurogenesis and that Spy1 expression correlates with NSC and progenitor populations of the SVZ. Moreover, Spy1 levels peak during late stages of murine embryogenesis and decline in the early postnatal brain, suggesting that Spy1 expression is tightly regulated at the different stages of mammalian CNS development. The outcome of this study will shed light on cell cycle regulation in populations of self-renewing neural progenitors. This advance in knowledge is indispensable for creating new strategies for regenerative medicine and brain cancer therapy.

## **EXPERIMENTAL PROCEDURES**

### **Animals**

Balb/c mice (Jackson Labs) were bred on site for the purposes of this study. Mice were maintained and cared for following the Canadian Council for Animal Care guidelines under the University of Windsor AUPP# 10-08.

### **Immunohistochemistry**

Rat brain cryosections (obtained from Dr. Zhang, University of Windsor), mouse brain cryosections or formalin-fixed and paraffin-embedded brain tissue sections were incubated 15 minutes in 4% paraformaldehyde at 4°C on microscope slides and then washed 3 times with PBS. They were permeabilized in 0.2% TritonX-100 in PBS for 1 hour at room temperature followed by 3 washes with PBS-TritonX-100. Sections were blocked in normal goat serum for 1 hour at 37°C. Antibodies were added for 2 hours at 37°C, followed by a 10 minute wash in PBS-TritonX-100 containing 1% of blocking Normal Goat Serum. Secondary antibodies were applied for 1 hour at 37°C, washed 2 times for 10 minutes each in PBS-TritonX-100, 1 time in Hank's Balanced Salt Solution (HBSS) and incubated with Hoechst 33342 (Sigma) (0.35 mg/ml) for 30 minutes. Counterstained sections were washed with HBSS 3 times for 5 minutes. Tissues were mounted with Vectashield mounting medium and imaged using a IX8I Olympus confocal microscope, using Fluoview 1.7 software. The proper antibodies were used at the following concentrations: human Spy1 – 1:1000-1:10000 (Novus), GAP43 G9264 (Sigma) 1:1000 GFAP G4546 (Sigma) 1-1000, Nestin G-20 (Santa Cruz) 1:1000.

### **Protein isolation from brain tissues**

Flash frozen brain samples were thawed quickly and cut into 0.03-0.13 g pieces. Tissue pieces were weighed and 250  $\mu$ l of NP40 Extraction Buffer (50 mM Tris-HCl pH 7.5, 1% NP40, 1 mM EGTA pH 8.0, 0.2% SDS, 150 mM NaCl, 0.25% sodium deoxycholate, 1.5% antifoam A) with protease inhibitors (leupeptin 2  $\mu$ g/mL, aprotinin 5  $\mu$ g/mL, sodium fluoride 50 mM, pepstatin A 1  $\mu$ g/mL and PMSF 100  $\mu$ g/mL) was used per 0.1 g of tissue. Tissues and extraction buffer were homogenized on ice (3 times, 10 seconds). Samples were then centrifuged at 13,000 rpm for 15 minutes at 4°C. Supernatant was collected and stored at -20°C until use.

### **Western blotting**

Protein concentrations were assessed by Bradford assay, samples were prepared with 4x sample buffer (10% glycerol, 62.5 mM Tris-HCl pH 6.8, 2% SDS, 0.01 mg/mL bromophenol blue, 2%  $\beta$ -mercaptoethanol), and boiled for 5 minutes at 95-105°C. Samples were loaded onto 10% polyacrylamide gels and run at 110 volts for 3- 4.5 hours. Proteins were then transferred to PVDF membranes through semi-wet transfer at 30 volts for 2.5 hours. Membranes were blotted in 3% milk for durations ranging from 2 hours to overnight. Primary antibodies were incubated overnight at 4°C except for Actin mouse which was incubated for 2 hours at room temperature. Membranes were washed with Tris-Buffered Saline Tween-20 (TBST) 3 times for 5-10 minutes, followed by a 1 hour incubation in secondary antibody at room temperature. Membranes were washed with TBST 3 times for 15 minutes and were visualized using FluorChem HD2 imaging system (Alpha Innotech). The proper antibodies were used at the following concentrations: Actin



MAB150 1R (Chemicon- Millipore; 1:1000),  $\alpha$ -Tubulin TU-02 (Sigma; 1:1000), human Spy1 (Novus; – 1:1000-1:10000), p27<sup>Kip1</sup> NA35 (Calbiochem; 1:100).

### **qRT-PCR**

Total RNA was extracted using the RNAeasy Plus Mini Kit (Qiagen) and reverse transcribed using 200U Superscript II (Invitrogen), 0.5  $\mu$ g OligodT's and 0.5  $\mu$ g random nanomers (Sigma) according to the manufacturer instructions. Real time PCR was carried out using SYBR green detection (Applied Biosystems) with 250-400 nM of each primer (Table 1; Suppl. Mat.) and was performed using an ABI Prism 7300 thermocycler. Data were analyzed using ABI 7300 software and represent  $\log_{10}$  relative quantification (RQ) relative to control. Primers were designed using Primer Express software (Applied Biosystems).

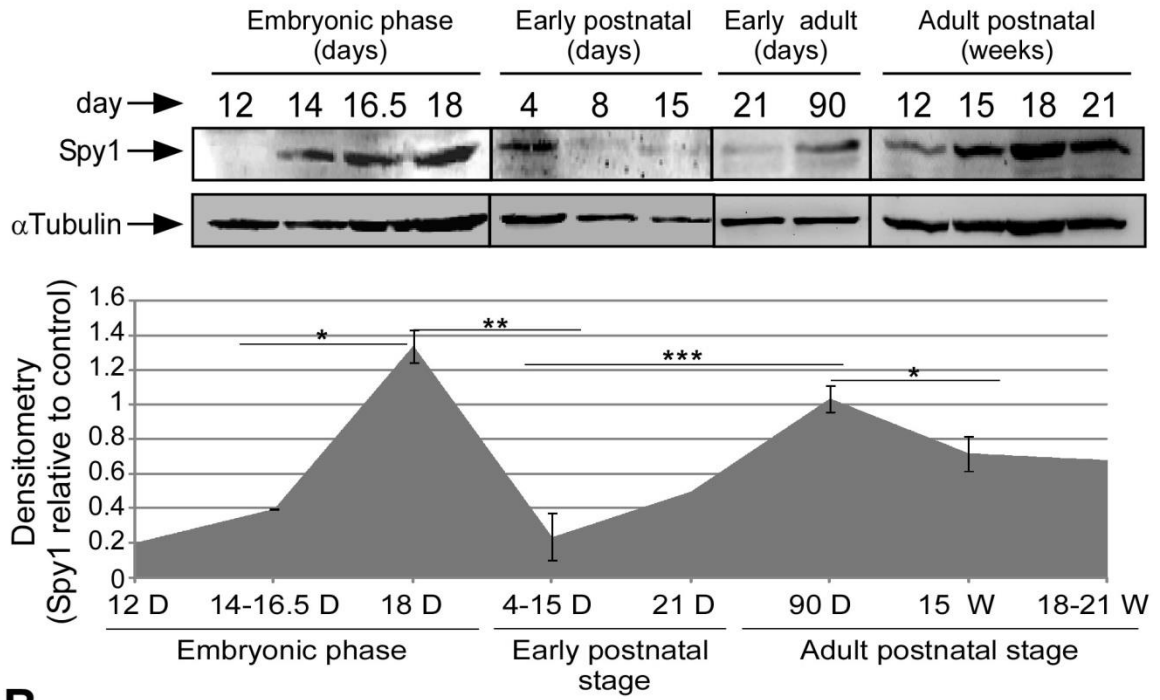
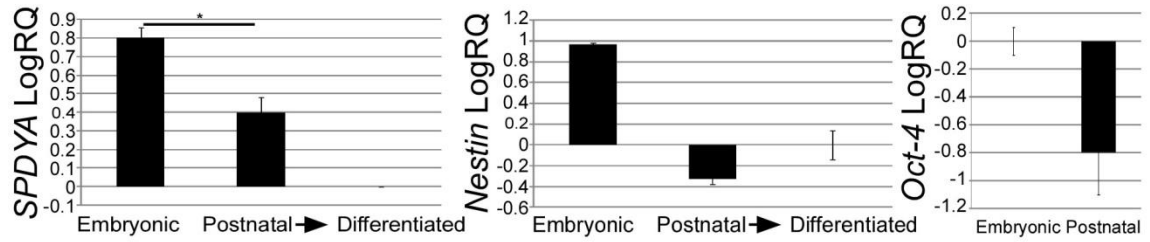
### **Statistical analyses**

Student's *t*-test was used to perform statistical analyses. A p-value of 0.05 was considered significant. All data are reported as means  $\pm$  s.d. Real time PCR analyses were performed as described previously (Yuan, Reed et al. 2006). Briefly, the Ct value of the housekeeping gene (*GAPDH*) was subtracted from the corresponding Ct value of a target gene to produce a dCt value which was further subjected to the Student's *t*-test analysis. Statistical analyses and normality testing were performed using Statistica software.

## RESULTS

### **Spy1 protein levels are tightly regulated during neural progenitor lineage commitment**

To determine how Spy1 protein levels are regulated through neural development, endogenous protein levels in the murine brain were measured at embryonic days (E) 12-18 and postnatal days 4 through to 21 weeks. At the postnatal stages Spy1 levels were measured in the tissues microdissected from the hippocampus and olfactory bulb that were pooled for the protein analysis. A dramatic accumulation of Spy1 protein was observed during late embryonic stages, E 14-18, and then again in late postnatal stages, beginning to rise at day 15 and continuing to accumulate through to approximately day 90. Spy1 levels were reduced at time points correlating with decreased neurogenesis such as early postnatal stages (day 4-15) and in the aging brain (> day 90) (Fig. 1A). Cells were then isolated from E14 brains or from the neurogenic regions of postnatal brains (days 2-7) and expression levels were measured by q-RT-PCR. In correlation with the NSC marker *Nestin* and the pluripotency marker *Oct-4*, *SPDYA* expression substantially declined with age and during differentiation (Fig. 1B).

**A****B**

**Figure 1.** *Spy1* is tightly regulated in neurogenic regions of the developing brain.

(A) Balb/c mice were sacrificed at the indicated time points (D=days; W=weeks). Neurogenic sites (hippocampus and olfactory bulb) were microdissected and subjected to western blot analysis (upper panel). Samples were pooled over at least 3 mice per data point, bands were quantified by densitometry analysis and values are expressed as the Integrated Density Values (IDV) of *Spy1*/  $\alpha$ -Tubulin (lower panel). Results are presented as mean  $\pm$ s.d. n=3; \*p < 0.05, \*\*p < 0.001, \*\*\*p < 0.0001 between selected groups.

(B) Primary cell cultures established from embryonic (E14) and postnatal (PN2-7) mouse brains plated in serum free media supplemented with 20ng/ml EGF and 10ng/ml bFGF or differentiated for 5 days upon addition of 2% FBS. Analyzed using qRT-PCR for *SPDYA* (left graph), *Nestin* (middle graph) and *Oct-4* (right graph). Error bars represent triplicate of each sample; n=3. Results are presented as mean  $\pm$ s.d. n=3; \*p < 0.05.

## **Spy1 protein localizes to the neurogenic regions of the mammalian brain**

Spy1 protein levels were high in neurogenic regions of the adult brain including the hippocampus and olfactory bulbs (Fig. 2A). While a lower band of Spy1 was also found in the cerebellum, it is noted that p27 levels were significantly reduced only in the neurogenic regions; this provides the possibility that Spy1 is functionally active in the neurogenic tissues. Quantification of Spy1 expression over multiple postnatal brains demonstrated that Spy1 protein levels were significantly upregulated in the olfactory bulbs containing neural progenitors in comparison to a non-neurogenic region (cortex) (Fig.2B). Interestingly, q-RT-PCR analysis of *SPDYA* in the olfactory bulbs at different developmental stages demonstrated higher levels of *SPDYA* mRNA at the sites of ongoing neurogenesis at both early and late postnatal stages when compared to the cortex (Fig. 2C). Spy1 was found to be localized specifically in the dentate gyrus along the subgranular zone, a region associated with high levels of neurogenesis (Goldman and Chen 2011) (Fig. 2D; left panels). Moreover, Spy1 positive cells were observed in the choroid plexus, subependymal zone around the lateral ventricles and SVZ (Fig. 2D; right panels). Immunolabeling with the NSC marker Nestin revealed its colocalization with Spy1 protein, supporting the progenitor nature of detected cells. Stem-like properties of neural progenitors can be addressed in a neurosphere formation assay where specific culture conditions support the self-renewing potential and clonal growth of true stem cells (Pastrana, Silva-Vargas et al. 2011). The microenvironment within the neurosphere facilitates heterogeneity where the populations capable of clonal growth that express stem cell markers like Nestin coexist among more committed progenitors (Suslov, Kukekov et al. 2002). Culturing cells as neurospheres revealed that Spy1 is consistently expressed in

Nestin positive cells (Fig. 2E). Neurospheres were treated with 2% FBS and stained for the differentiation markers Growth-Associated Protein (GAP43) and Glial Fibrillary Acidic Protein (GFAP) to test their ability to functionally differentiate (Fig. 2E; right panels). Spy1 and Nestin levels were undetectable following differentiation (data not shown).

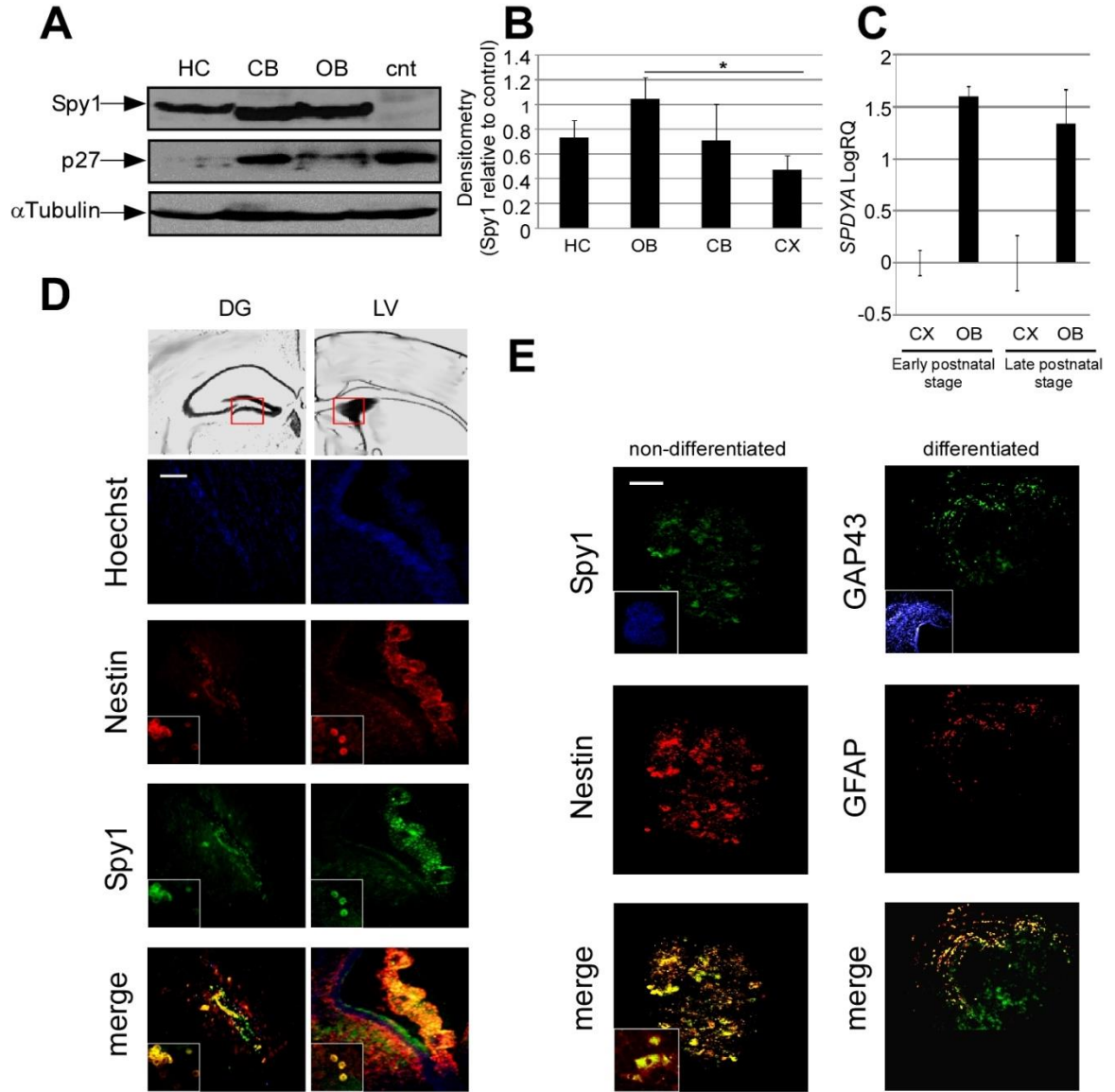


**Figure 2.** Spy1 protein localizes to the neurogenic regions of the mammalian brain.

(A) Neurogenic sites: HC, and OB or non-neurogenic sites: CX or CB microdissected from Wistar albino rat brains and analyzed by SDS-PAGE (left panel). Liver was used as a control and  $\alpha$ -Tubulin as a loading control.

(B) HC, OB, CB and CX were microdissected from 8 mouse brains at different developmental stages and analyzed by SDS-PAGE. Densitometry is presented as the Integrated Density Values (IDV) of Spy1/  $\alpha$ -Tubulin control. Results are presented as mean  $\pm$ s.d. n=8; \*p < 0.05.

(C) *SPDYA* expression levels in OB and CX of mouse brains at early (2-7 days) and late postnatal (81- 90 days) analyzed using qRT- PCR. Values are mean  $\pm$ s.d. for triplicate samples from a representative experiment.

(D) IHC on rat coronal cryosections of the DG (left column) or LVs (right column). Colocalization of Spy1 (green) and neural stem cell marker Nestin (red) is marked in yellow (merge). Hoechst 33342 was used to counterstain nuclei. Scale bar, 50  $\mu$ m.

(E) Primary cells extracted from neurogenic sites of a mouse brain were passaged using neurosphere assays. Undifferentiated neurospheres (left column) were probed with Spy1 (green) and Nestin (red). Coexpression visualized in yellow (merge). Differentiated neurospheres (right column) were subjected to phenotype analysis using neuronal (GAP43) and glial (GFAP) markers; cells magnified in insets. Hoechst 33342 was used as a nuclear control. Scale bar, 50 $\mu$ m. Abbreviations: hippocampus (HC), olfactory bulb (OB), cortex (CX), cerebellum (CB), dentate gyrus (DG), lateral ventricles (LVs).



## **Spy1 is expressed in cells within the rostral migratory stream and SGZ of the hippocampus**

Murine brain sections were stained for Spy1 and analyzed using bright field microscopy. Spy1 positive cells were found along the rostral migratory stream (Fig. 3A i-iii) and in the region of the olfactory bulb (Fig. 3A iv-vi). Cells found in the former presented morphology typical for migratory neural stem cells. Analysis of the dentate gyrus also revealed Spy1 positive cells along the subgranular zone (Fig. 3A vii-viii). Interestingly, the most intensive Spy1 specific labeling was found in the region of the subependymal zone on the lateral and anterior wall of the lateral ventricles (Fig. 3B i-v). The three-dimensional model for the organization within the SVZ proposed by Doetsch *et al.* addresses the specific cell morphology and topographical relationship between the cells (Fig. 3B vi). Using the morphology criteria proposed by this model, the cells that stained positively for Spy1 resemble B-type cells. Immunohistochemical analysis of specific markers is required to further determine the SVZ phenotype of the Spy1 positive cells.

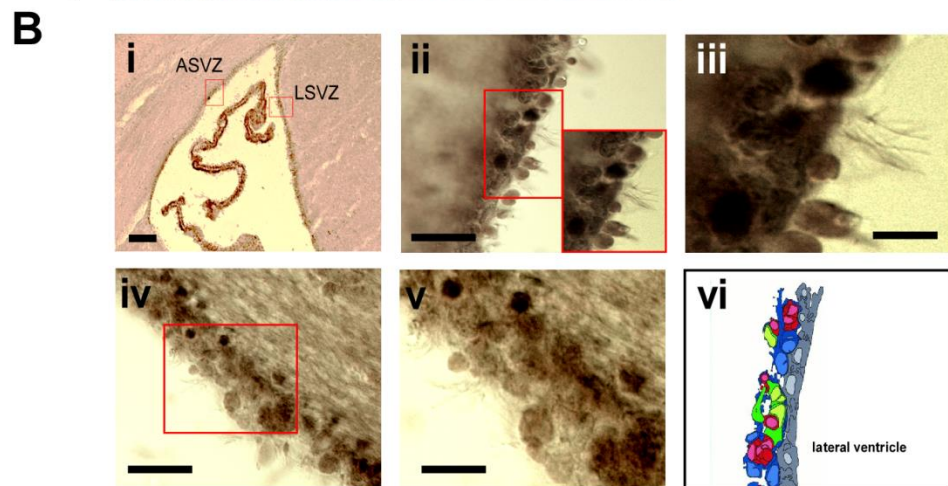
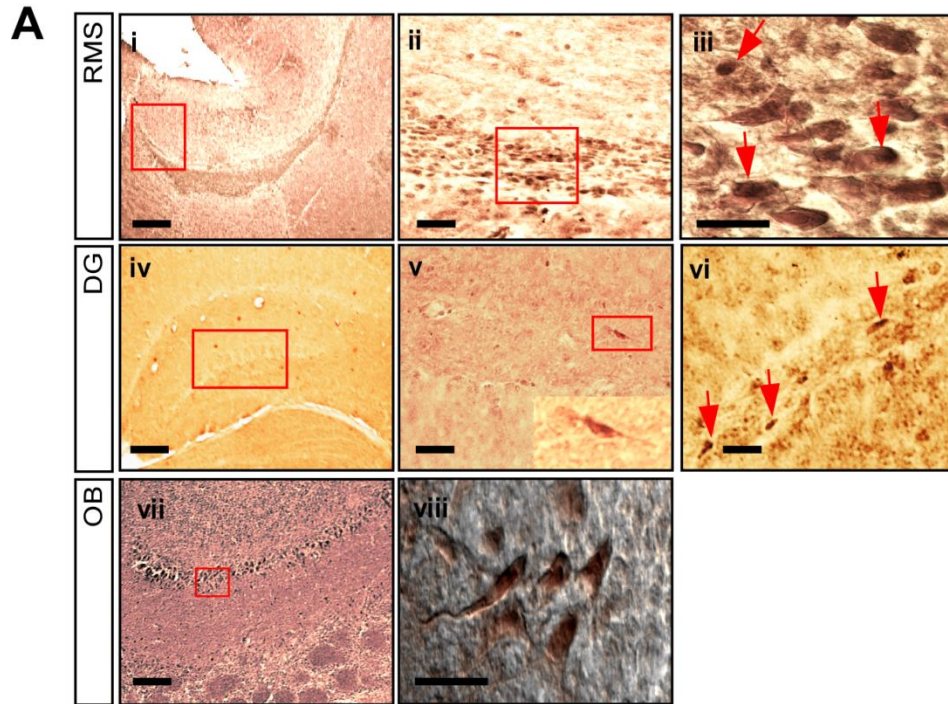


**Figure 3.** *Spy1* positive populations of neural cells are found in the RMS, SGZ and SVZ of the LVs.

Coronal and sagittal sections from mice between 3-10 weeks of age were analyzed by DAB IHC for *Spy1* expression.

(A) (i-iii) RMS *Spy1* immunostaining. (i) Low magnification view. (ii) Magnification from boxed region in (i) (Boxed in region is further magnified in iii). (iv) DG of hippocampus. Box is further magnified in images v and vi. (vii) OB; (viii magnified box from vii). *Spy1* positive cells (indicated with an arrow on some panels) present morphology typical for migratory neural stem cells. Scale bars: (i),(iv) and (vii), 100 $\mu$ m; (ii),(v) and (vi) 25 $\mu$ m; (iii) and (viii), 10 $\mu$ m.

(B) (i) *Spy1* specific staining found in the ASVZ and in the LSVZ of the LVs. Boxed in region of ASVZ is magnified in (ii) which has a further boxed in region magnified in the inset. The inset of (ii) is further magnified in (iii). (iv-v) View of the LSVZ. (v) A magnified view of the boxed in region in (iv). (vi) Contiguous electron micrographs of the SVZ were assembled onto a computer and in depth analysis conducted to determine the characteristics and positioning of the A cells (red), B cells (blue), C cells (green), ependymal (ciliated cells; grey). Used with permission: Doetsch F. *et al.* J. Neurosci. 1997;17:5046-5061. Scale bars: (i),100 $\mu$ m; (ii) and (iv), 25 $\mu$ m; (iii) and (v), 10 $\mu$ m. Abbreviations: rostral migratory stream (RMS), subgranular zone (SGZ), subventricular zone (SVZ), lateral ventricles (LVs), dentate gyrus (DG), olfactory bulb (OB), anterior subventricular zone (ASVZ), lateral subventricular zone (LSVZ).

## **Spy1 positive cells in the SVZ express markers of B-type cell subpopulation**

Data from Doetsch *et al.* originally identified the subtypes of cells residing in the germinal layer of SVZ and the markers to adequately define these cells continue to evolve (Fig. 3B vi) (Doetsch, Garcia-Verdugo *et al.* 1997; Kriegstein and Alvarez-Buylla 2009; Ihrie, Shah *et al.* 2011). In general, astrocyte-like cells, referred to as B-cells, stain positively for GFAP and Nestin and give rise to the transient amplifying C-cells that only stain at low levels for Nestin. C-cells in turn differentiate into migrating neuroblasts (A-cells) staining with neural specific markers. Although multiciliated ependymal cells were previously reported to acquire stem-like characteristics upon injury (Mothe and Tator 2005), it has been established that they neither divide *in vivo* nor form neurospheres *in vitro* (Doetsch, Caille *et al.* 1999; Mirzadeh, Merkle *et al.* 2008). Moreover, in contrary to the conventional model describing the ependymal cells as directly contacting the ventricle, the B-type cells were reported to constitute 31% of the population lining the LVs (Mirzadeh, Merkle *et al.* 2008). To further investigate the identity of the SVZ Spy1 positive cells, immunofluorescent analysis was performed using stemness and glial markers (Fig. 4A). The obtained data showed that Spy1 expressing cells observed along the anterior wall of the LV not only contact the ventricle, but also co-stain with SSEA-1/CD15/Lewis X (LeX) (Fig. 4A ai-ci). LeX was previously found to enrich for tumour initiating cells (TIC) along with the CD133 marker in 85% of established TIC cell lines (Son, Woolard *et al.* 2009). Immunolabeling with the NSC marker Nestin (Fig. 4B d-di) as well as with GFAP (Fig.4B; e-ei), along the lateral wall of the LVs, revealed that both markers colocalized with Spy1; this supports the glial and progenitor nature of the detected cells (Doetsch, Garcia-Verdugo *et al.* 1997).

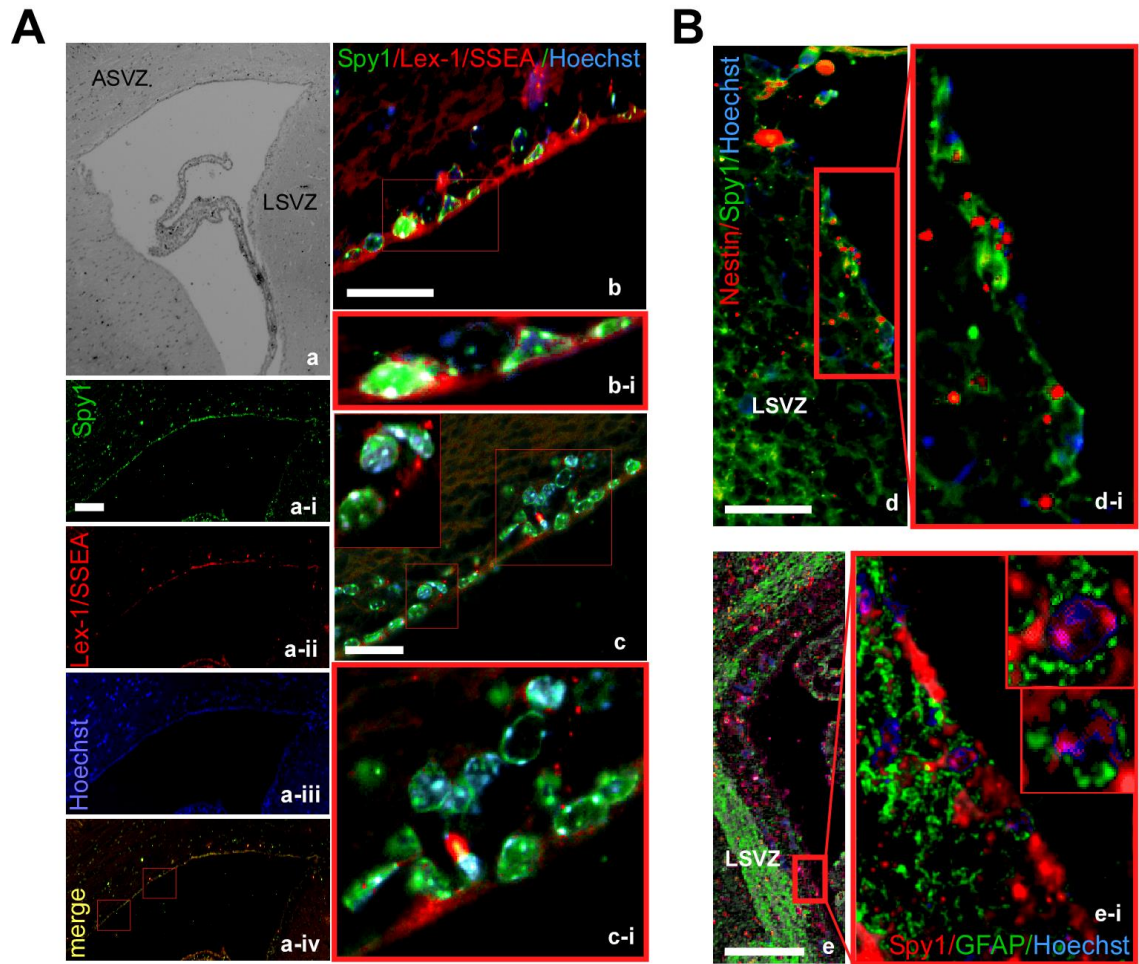


**Figure 4.** Spy1 colocalizes with glial and stemness markers in the SVZ.

(A) Immunofluorescent analysis of the localization of Spy1, SSEA-1/LeX, Nestin and GFAP positive cells within the ASVZ. Sections stained with Spy1 (a-i), SSEA-1/LeX (a-ii), Hoechst 33342 (a-iii) and merge of both (a-iv). Scale bar, 100 $\mu$ m. SVZ staining with Spy1 and SSEA-1/LeX is further presented in higher magnification in (b) and (c) and the insets are further magnified in (b-i) and (c-i), respectively. Scale bars: 25 $\mu$ m.

(B) Colocalization of Spy1 with Nestin (d; further magnified in d-i) and GFAP (e; further magnified in e-i) in the LSVZ. Scale bars: (d), 25 $\mu$ m and (e), 100 $\mu$ m. Abbreviations: subventricular zone (SVZ), anterior subventricular zone (ASVZ), lateral subventricular zone (LSVZ), glial acidic fibrillary protein (GFAP).

## **DISCUSSION**

E10-12 represents a period of development coincident with onset of the astroglial marker expression within the ventricular zone and predominant expansion of glial progenitors throughout most regions of the brain (Hartfuss, Galli et al. 2001; Kriegstein and Gotz 2003). The findings presented here demonstrate that Spy1 protein begins accumulating at these early stages and becomes dramatically elevated between E14-E18, a period of development shown previously to correlate with extensive accumulation of proliferating newly born precursors in the SVZ (Mathis, Schroter et al. 2010). Furthermore, differential gene expression analysis has demonstrated that E18 represents an important day in CNS development, whereby there is a robust activation of genes involved in cell division and proliferation (Han, Wu et al. 2009). The formation of mature brain architecture at the early postnatal stages is unequivocal of extensive formation of neuronal networks and apoptosis. Spy1 inhibits apoptotic events in response to DNA damage and interestingly, Spy1 levels were found to be dramatically reduced at early postnatal stages (Barnes, Porter et al. 2003; Gastwirt, Slavin et al. 2006). Hence, this inverse correlation may suggest a role for Spy1 in maintaining pro-neurogenic populations of cells and may further suggest that Spy1 is subsequently downregulated to allow for p53 driven differentiation or apoptosis. Interestingly, these results demonstrate that Spy1 protein levels undergo progressive upregulation with the onset of early juvenile stages and peak at the later adult time points. Notably, the Spy1 effector CDK2 has been demonstrated to be essential for adult, but not for early postnatal neurogenesis (Jablonska, Aguirre et al. 2007). Further exploration into the specific requirement for Spy1 over the established CDK2 partners, Cyclins E and A, as well as the essentiality of Spy1 for p27

regulation in the developing brain and during neural differentiation is warranted. Importantly, *Spy1* expression in the hippocampus correlated with a significant decrease of p27 protein levels (Fig. 2A) suggesting that *Spy1*/CDK2-mediated p27 degradation may occur at this neurogenic niche. The immunohistochemistry analysis revealed *Spy1* positive cells not only in the SGZ (Fig. 3A iv-vi), but also in the progenitor cells along the rostral migratory stream (RMS) between the SVZ and the olfactory bulbs (Fig. 3A i-iii). The progenitor cells with neurogenic potential are born in the SVZ and migrate out to join the RMS en route to the olfactory bulb where they terminally differentiate (Lois and Alvarez-Buylla 1994). The alkaline phosphatase tracing of the GFAP positive cells revealed that the activated B-type astrocytes constitute the main migratory component that gives rise to neurons of the olfactory bulb. Importantly, the RMS cells staining positively for *Spy1* exhibited the migratory morphology reported before by Doetsch *et al.* (Doetsch, Caille *et al.* 1999). The data suggest that *Spy1* may be a component of the cell cycle machinery driving the astrocyte progenitor cells migrating out of the SVZ. According to the model proposed by Doetsch *et al.*, among the defined subsets of neural progenitors that reside in the neurogenic niche of the SVZ, the B-type astrocytes were reported to serve as adult NSCs due to their ability to form multipotent spheres *in vitro* and to regenerate the SVZ network upon ablation of both migrating neuroblasts (A-cells) and C-cells (Doetsch, Caille *et al.* 1999). B-type astrocyte populations were enriched in Nestin and GFAP expression (Doetsch, Garcia-Verdugo *et al.* 1997) and *Spy1* colocalized with both markers (Fig. 2D-E & Fig. 4B). Moreover, *Spy1* overexpression was demonstrated to upregulate the levels of *Nestin* and *GFAP* (Chapter 2; Fig. 5B & F) and to confer the self-renewing potential to primary neural cells (Chapter 2; Fig. 5). Given the heterogeneous nature of the NSC population (Alvarez-Buylla, Kohwi *et al.* 2008; Lee *et al.*,



Gianino et al. 2012), these results suggest that *Spy1* expression may be found in the neural stem cells characterized as SSEA-1/LeX non-ependymal cells as well as in at least one B-cell population. Further analysis is required to determine the specific SVZ cell type containing the highest levels of *Spy1* and the functional significance of this on the cellular composition of the SVZ. Moreover, the populations type B adult NSCs are characterized by BrdU label retention which is indicative of infrequent cell division and cellular quiescence (Doetsch, Caille et al. 1999). Utilizing BrdU labeling time course *in vivo* in coordination with *Spy1* expression analysis can be helpful in resolving the particular cell type within the SVZ that is *Spy1* positive. We speculate that controlled regulation of *Spy1*'s expression within the quiescent cell population potentially confers senescence resistance to those cells whereas *Spy1* upregulation is observed in activated glia during regenerative processes (Huang, Liu et al. 2009).

Utilizing an *in vitro* primary neural system, it was observed that *SPDYA* levels were upregulated in embryonic progenitors and declined in the postnatal and terminally differentiated cells (Fig. 1B), suggesting that *Spy1*-mediated cell cycle control may differ depending on the stage of development. Importantly, in ESCs the early portion of G1 phase is actively omitted due to the continuous and phase-independent overexpression of Cyclin E1. Therefore, ESCs attribute their unusual cell cycle structure to continuous activation of CDK2 (Savatier, Huang et al. 1994; Orford and Scadden 2008). The observed overexpression of *SPDYA* in embryonic cell culture in comparison to the lineage committed cells suggests that *Spy1* can participate in the cell cycle machinery that is specific to ESCs and can contribute to the retention of continuous CDK2 activity.

In conclusion, this study demonstrated that *Spy1* is tightly regulated during the development of the mammalian CNS and is expressed at the sites of adult neurogenesis.

The stem cell and astrocyte marker localization as well as expression analysis suggests that *Spy1* is expressed within the B-type cells of the SVZ; cells previously proved to constitute a pool of adult multipotent stem cells. Further study is required however to firmly conclude that the unconventional fashion in which *Spy1* drives the cell cycle is a part of the molecular mechanism behind adult neurogenesis and constitutes a potential link to brain tumorigenesis.

## REFERENCES

- Alvarez-Buylla, A., M. Kohwi, et al. (2008). "The heterogeneity of adult neural stem cells and the emerging complexity of their niche." *Cold Spring Harb Symp Quant Biol* **73**: 357-65.
- Barnes, E. A., L. A. Porter, et al. (2003). "Human Spy1 promotes survival of mammalian cells following DNA damage." *Cancer Res* **63**(13): 3701-7.
- Cao, J., J. Yang, et al. (2013). "Temporal-spatial expressions of spy1 in rat sciatic nerve after crush." *Cell Mol Neurobiol* **33**(2): 213-21.
- Cheng, A., W. Xiong, et al. (2005). "Identification and comparative analysis of multiple mammalian Speedy/Ringo proteins." *Cell Cycle* **4**(1): 155-65.
- Doetsch, F., I. Caille, et al. (1999). "Subventricular zone astrocytes are neural stem cells in the adult mammalian brain." *Cell* **97**(6): 703-16.
- Doetsch, F., J. M. Garcia-Verdugo, et al. (1997). "Cellular composition and three-dimensional organization of the subventricular germinal zone in the adult mammalian brain." *J Neurosci* **17**(13): 5046-61.
- Doetsch, F., J. M. Verdugo, et al. (2002). "Lack of the cell-cycle inhibitor p27Kip1 results in selective increase of transit-amplifying cells for adult neurogenesis." *J Neurosci* **22**(6): 2255-64.
- Falk, S., H. Wurdak, et al. (2008). "Brain area-specific effect of TGF-beta signaling on Wnt-dependent neural stem cell expansion." *Cell Stem Cell* **2**(5): 472-83.
- Gastwirt, R. F., D. A. Slavin, et al. (2006). "Spy1 expression prevents normal cellular responses to DNA damage: Inhibition of apoptosis and checkpoint activation " *J Biol Chem*.
- Ghiani, C. and V. Gallo (2001). "Inhibition of cyclin E-cyclin-dependent kinase 2 complex formation and activity is associated with cell cycle arrest and withdrawal in oligodendrocyte progenitor cells." *J Neurosci* **21**(4): 1274-82.
- Goldman, S. A. and Z. Chen (2011). "Perivascular instruction of cell genesis and fate in the adult brain." *Nat Neurosci* **14**(11): 1382-9.
- Golipour, A., D. Myers, et al. (2008). "The Spy1/RINGO family represents a novel mechanism regulating mammary growth and tumorigenesis." *Cancer Res* **68**(10): 3591-600.

- Gordon, N. (1995). "Apoptosis (programmed cell death) and other reasons for elimination of neurons and axons." *Brain Dev* **17**(1): 73-7.
- Gritti, A., L. Bonfanti, et al. (2002). "Multipotent neural stem cells reside into the rostral extension and olfactory bulb of adult rodents." *J Neurosci* **22**(2): 437-45.
- Han, X., X. Wu, et al. (2009). "Transcriptome of embryonic and neonatal mouse cortex by high-throughput RNA sequencing." *Proc Natl Acad Sci U S A* **106**(31): 12741-6.
- Hartfuss, E., R. Galli, et al. (2001). "Characterization of CNS precursor subtypes and radial glia." *Dev Biol* **229**(1): 15-30.
- Huang, H. S., M. Nagane, et al. (1997). "The enhanced tumourigenic activity of a mutant epidermal growth factor receptor common in human cancers is mediated by threshold levels of constitutive tyrosine phosphorylation and unattenuated signaling." *J Biol Chem* **272**(5): 2927-35.
- Ihrie, R. A., J. K. Shah, et al. (2011). "Persistent sonic hedgehog signaling in adult brain determines neural stem cell positional identity." *Neuron* **71**(2): 250-62.
- Jablonska, B., A. Aguirre, et al. (2007). "Cdk2 is critical for proliferation and self-renewal of neural progenitor cells in the adult subventricular zone." *J Cell Biol* **179**(6): 1231-45.
- Karaiskou, A., L. H. Perez, et al. (2001). "Differential regulation of Cdc2 and Cdk2 by RINGO and cyclins." *J Biol Chem* **276**(38): 36028-34.
- Ke, Q., J. Ji, et al. (2009). "Expression and prognostic role of Spy1 as a novel cell cycle protein in hepatocellular carcinoma." *Exp Mol Pathol* **87**(3): 167-72.
- Kriegstein, A. and A. Alvarez-Buylla (2009). "The glial nature of embryonic and adult neural stem cells." *Annu Rev Neurosci* **32**: 149-84.
- Kriegstein, A. R. and M. Gotz (2003). "Radial glia diversity: a matter of cell fate." *Glia* **43**(1): 37-43.
- Lange, C. and F. Calegari (2010). "Cdks and cyclins link G1 length and differentiation of embryonic, neural and hematopoietic stem cells." *Cell Cycle* **9**(10): 1893-900.
- Lee da, Y., S. M. Gianino, et al. (2012). "Innate neural stem cell heterogeneity determines the patterning of glioma formation in children." *Cancer Cell* **22**(1): 131-8.

- Li, H., M. Collado, et al. (2012). "p27(Kip1) directly represses Sox2 during embryonic stem cell differentiation." *Cell Stem Cell* **11**(6): 845-52.
- Lois, C. and A. Alvarez-Buylla (1994). "Long-distance neuronal migration in the adult mammalian brain." *Science* **264**(5162): 1145-8.
- Lukaszewicz, A., P. Savatier, et al. (2005). "G1 phase regulation, area-specific cell cycle control, and cytoarchitectonics in the primate cortex." *Neuron* **47**(3): 353-64.
- Ma, Y., X. Qi, et al. (2009). "Identification of candidate genes for human pituitary development by EST analysis." *BMC Genomics* **10**: 109.
- Mathis, C., A. Schroter, et al. (2010). "Nogo-a regulates neural precursor migration in the embryonic mouse cortex." *Cereb Cortex* **20**(10): 2380-90.
- McAndrew, C. W., R. F. Gastwirt, et al. (2007). "Spy1 enhances phosphorylation and degradation of the cell cycle inhibitor p27." *Cell Cycle* **6**(15): 1937-45.
- Mimeault, M. and S. K. Batra (2006). "Concise review: recent advances on the significance of stem cells in tissue regeneration and cancer therapies." *Stem Cells* **24**(11): 2319-45.
- Mimeault, M., R. Hauke, et al. (2007). "Stem cells: a revolution in therapeutics-recent advances in stem cell biology and their therapeutic applications in regenerative medicine and cancer therapies." *Clin Pharmacol Ther* **82**(3): 252-64.
- Mirzadeh, Z., F. T. Merkle, et al. (2008). "Neural stem cells confer unique pinwheel architecture to the ventricular surface in neurogenic regions of the adult brain." *Cell Stem Cell* **3**(3): 265-78.
- Mothe, A. J. and C. H. Tator (2005). "Proliferation, migration, and differentiation of endogenous ependymal region stem/progenitor cells following minimal spinal cord injury in the adult rat." *Neuroscience* **131**(1): 177-87.
- Orford, K. W. and D. T. Scadden (2008). "Deconstructing stem cell self-renewal: genetic insights into cell-cycle regulation." *Nat Rev Genet* **9**(2): 115-28.
- Palmer, T. D., J. Ray, et al. (1995). "FGF-2-responsive neuronal progenitors reside in proliferative and quiescent regions of the adult rodent brain." *Mol Cell Neurosci* **6**(5): 474-86.
- Pastrana, E., V. Silva-Vargas, et al. (2011). "Eyes wide open: a critical review of sphere-formation as an assay for stem cells." *Cell Stem Cell* **8**(5): 486-98.

- Porter, L. A., R. W. Dellinger, et al. (2002). "Human Speedy: a novel cell cycle regulator that enhances proliferation through activation of Cdk2." *J Cell Biol* **157**(3): 357-66.
- Porter, L. A., M. Kong-Beltran, et al. (2003). "Spy1 interacts with p27Kip1 to allow G1/S progression." *Mol Biol Cell* **14**(9): 3664-74.
- Savatier, P., S. Huang, et al. (1994). "Contrasting patterns of retinoblastoma protein expression in mouse embryonic stem cells and embryonic fibroblasts." *Oncogene* **9**(3): 809-18.
- Schmidt, M. H., F. Bicker, et al. (2009). "Epidermal growth factor-like domain 7 (EGFL7) modulates Notch signalling and affects neural stem cell renewal." *Nat Cell Biol* **11**(7): 873-80.
- Singh, A. M. and S. Dalton (2009). "The cell cycle and Myc intersect with mechanisms that regulate pluripotency and reprogramming." *Cell Stem Cell* **5**(2): 141-9.
- Son, M. J., K. Woolard, et al. (2009). "SSEA-1 is an enrichment marker for tumour-initiating cells in human glioblastoma." *Cell Stem Cell* **4**(5): 440-52.
- Suslov, O. N., V. G. Kukekov, et al. (2002). "Neural stem cell heterogeneity demonstrated by molecular phenotyping of clonal neurospheres." *Proc Natl Acad Sci U S A* **99**(22): 14506-11.
- Takahashi, T., R. S. Nowakowski, et al. (1995). "The cell cycle of the pseudostratified ventricular epithelium of the embryonic murine cerebral wall." *J Neurosci* **15**(9): 6046-57.
- Yuan, J. S., A. Reed, et al. (2006). "Statistical analysis of real-time PCR data." *BMC Bioinformatics* **7**: 85.
- Zhang, L., A. Shen, et al. (2012). "Spy1 is frequently overexpressed in malignant gliomas and critically regulates the proliferation of glioma cells." *J Mol Neurosci* **47**(3): 485-94.

CHAPTER 4  
THE ROLE OF SPY1  
IN THE DIFFERENTIATION AND SELF-RENEWAL OF NEUROBLASTOMA

## INTRODUCTION

Neuroblastoma is the most common pediatric extra cranial malignancy with 98% of patients diagnosed by the age of 10 (Brodeur, Look et al. 2001; Maris, Hogarty et al. 2007). The disease has an unpredictable clinical course and poor prognosis, with only 30% long-term survival (Brodeur, Look et al. 2001; Maris, Hogarty et al. 2007). Due to its origin in the migratory neural crest, neuroblastoma occurs in the peripheral nervous system arising in sympathetic ganglia and adrenal medulla (Anderson 1997; Brodeur 2003; Dyer 2004). The neural crest is a population of stem cells that derives from the neural tube during embryogenesis. Therefore, the transient embryonic structure of the tumours is reflected in the enormous genetic and phenotypic heterogeneity of neuroblastoma. Although an inherited genetic predisposition was shown in a small subset of patients, spontaneous genetic changes are the most frequently observed. This commonly includes activation of oncogenes like MYCN and H-Ras, gain or loss of alleles, and alternations in cell ploidy (Schwab, Alitalo et al. 1983; Kaneko, Kanda et al. 1987; Tanaka, Slamon et al. 1988; Ireland 1989). Neuroblastoma tumours display diverse immature cell types such as neuroblasts and glial precursors and an array of heterogeneous cell types at different stages of differentiation. Accumulating *in vitro* and *in vivo* evidence suggests that alteration in cell cycle control may affect the stage of tumour differentiation and ultimately contribute to neuroblastoma pathogenesis (Mei, Wang et al.). Indeed those tumours with a poorly differentiated phenotype correlate negatively with clinical outcomes (Mei, Wang et al.; Zha, Ding et al.). In addition, self-renewing tumour initiating cells (TICs) were reported to correlate with refractory or relapse state following the initial good response to therapy observed in patients



(Vangipuram, Wang et al. 2010). The neuroblastoma stem-like TICs were identified among the heterogeneous population in cultured human cell lines (Ciccarone, Spengler et al. 1989; Ross, Biedler et al. 2003; Ross and Spengler 2007). Interestingly, several groups demonstrated the three principle populations of neuroblastoma cells: the highly proliferative yet weakly tumorigenic N-cells, the crest derived non-neuronal S precursors and the I-type malignant and multipotent neural crest stem cells of TIC potential (Ross, Spengler et al. 1995). The latter express CD133 and c-kit stem cell marker proteins, are capable of self-renewal and form rapidly growing tumours (Ross and Spengler 2007; Takenobu, Shimozato et al. 2011

; Cournoyer, Nyalendo et al. 2012). Importantly, the pentaspan protein CD133 was shown to regulate cellular proliferation and differentiation in neuroblastoma (Takenobu, Shimozato et al. 2011). Proliferation and differentiation are under control of the cell cycle, however what regulates the balance of these decisions in the populations of cells found in neuroblastoma remains to be determined.

Spy1 (Spdya; Speedy; Spy1A; RINGO), encoded by *SPDYA* gene, is a novel cell cycle regulator that controls CDK2 activity and G1-S phase transition in a fashion unique from that established for the classical cyclin proteins. The Spy1-CDK2 complex doesn't require CDK activating kinase (CAK) -mediated phosphorylation on CDK2 and it is less sensitive to inhibitory phosphorylation by regulators such as p21<sup>Cip1</sup> and p27<sup>Kip1</sup> (Cheng, Xiong et al. 2005; Dinarina, Perez et al. 2005); (Porter, Kong-Beltran et al. 2003; McAndrew, Gastwirt et al. 2007). Thus, Spy1 is able to override several known cell cycle checkpoints, including DNA damage checkpoints (Barnes, Porter et al. 2003; Gastwirt, McAndrew et al. 2007). Both CDK2 and p27<sup>Kip1</sup> are known to play an important role in neuroblastoma progression and patient prognosis (Matsuo and Thiele 1998; Matsuo, Seth

et al. 2001; Molenaar, Ebus et al. 2009). Notably, p27<sup>Kip</sup> was demonstrated to accumulate in neuroblastoma cells treated with retinoids and to necessitate neuronal differentiation (Cuende, Moreno et al. 2008), whereas increased CDK2 activity correlated with a differentiation blockage (Kranenburg, Scharnhorst et al. 1995).

This study investigated the role of Spy1 in proliferation, self-renewal and differentiation of human neuroblastoma cells. We found that Spy1 overexpression in the N-type neuroblastoma SH-SY5Y cells resulted in significantly upregulated proliferation and resistance to the 13-*cis*-Retinoic Acid (RA)-induced differentiation. Interestingly, Spy1 overexpressing cells demonstrated increased self-renewal in a neurosphere formation assay and upregulation of markers indicative of the multipotency. The forced upregulation of Spy1 levels conferred increased prolonged clonality and survival to serially subcultured spheres. The obtained data provides insight into the potential role of a novel cell cycle mechanism in driving tumourigenicity of neural crest stem cells. Importantly, this mechanism has strong implications in regulating resistance in at least subsets of neuroblastoma. Elucidating the mechanism by which Spy1 regulates these effects is of high importance for moving these results forward for clinical benefit.

## **EXPERIMENTAL PROCEDURES**

### **Generation of stable cell lines**

Utilizing BBS/CaCl<sub>2</sub> delivery method (pH 7.05) PT67 packaging cells were transiently transfected with the DNA construct of choice. Following an 8 hour incubation (37°C and 3% CO<sub>2</sub>) media was changed, and cells were allowed to recover at 37°C and 5% CO<sub>2</sub>. 24 hours later cell media containing the virus was harvested, centrifuged for 5 minutes at 2,000 g and filter sterilized using a 0.45 µm filter. Using the PT67 cell system the virus was amplified overnight, filter sterilized and stored at -80°C. SH-SY5Y cells were infected with P2 virus at ~70-80% confluency upon overnight incubation in 1:2 volume/volume virus to cell media ratio containing polybrene (25 µg/ml). Media was changed the next day and 24 hours later infected cells were selected in media containing 600 µg of G418. Individual colonies as well as mixed populations of cells were maintained and the incorporation of *SPDYA* cDNA was checked using genomic DNA and primers spanning the exon-exon junctions. Following adequate selection cells were maintained in media containing 200 µg/mL of G418.

### **Differentiation assays**

SH-SY5Y cells were grown on 60 mm or 100 mm plates to 60% confluency. 13-*cis*-Retinoic Acid (2 µM) was added to SH-SY5Y growth media in order to induce neurite outgrowth. Cover-slips and cell pellets were harvested each day, and control samples (kept in growth media) were harvested on day 1. Cells were pelleted by centrifugation at 13,000 rpm for 15 minutes at 4°C, supernatant was removed, and pellets were stored at -20°C until use. Cell pellets were lysed in 0.1% NP40 Lysis Buffer (0.1% NP40, 20 mM

Tris pH 7.5, 5 mM EDTA pH 8.0, 100 mM sodium chloride) for 1 hour, with mixing every 10 minutes. Samples were centrifuged again at 13,000rpm for 15 minutes at 4°C to remove cell debris, and stored at -20°C until use. Imaging was done on the AxioSkope2 Plus microscope (Zeiss) (Dr M. Crawford lab – U of Windsor) using Northern Eclipse computer software.

### **BrdU assay and fluorescent detection**

SH-SY5Y cells were grown on cover slips in 60 mm culture dishes. Over a differentiation time course BrdU (Cat# 550891; BD Sciences) was added to the differentiation media to achieve a final concentration of 10 µM and allowed to incubate for 30 minutes prior to cover slips harvesting. The cell culture density never exceeded  $2 \times 10^6$  cells/ml. The cells were fixed with 70% ethanol for 30 minutes at room temperature followed by incubation with 0.07N NaOH for 2 minutes and neutralization in PBS, pH 8.5. Primary antibody against BrdU (Cat# 347580, BD Sciences) was applied for 30 minutes in humidified chamber. The cells were then washed 3 times with PBS and incubated with secondary antibody conjugated to Alexa- 488 fluorophore (A11059, Invitrogen) for 30 minutes at room temperature. The cell nuclei was labeled with Propidium Iodide (0.04 µg/ml) for 1 minute. The cover slips were finally washed with water and mounted on microscope slides with Vectashield mounting medium. The imaging was done on Eclipse E800 microscope (Nikon, Japan)

### **Proliferation kinetics**

Cells were maintained at the density  $0.5 \times 10^4$  cells/ml in 6 well plates. The medium and growth factors were changed daily for SH-SY5Y cell line. Proliferation kinetics was determined by cell counting at indicated time points using hemocytometer.

### **MTT assay**

The primary, secondary and tertiary neurospheres generated by SH-SY5Y-*SPDYA* and SH-SY5Y-control cells were dissociated and  $10^4$  cells were seeded in 100  $\mu$ l of media in 96 well anti adhesive plates. 20  $\mu$ l of 5 mg/ml MTT solution in PBS were added to each well and incubated for 4 hours. 100  $\mu$ l of extraction buffer were added for 2 hours to dissolve the formazan crystals and the absorbance at 590 nm was assessed using Victor plate reader (Perkin Elmer)

### **Neurosphere formation assay**

For the purpose of the neurosphere formation assay SH-SY5Y cells were seeded at  $5 \times 10^4$  cells per well into 6-well Ultra Low Cluster Plates (Corning Life Sciences, cat. no.3471). The serum free culture medium DMEM/F12 (Sigma) was supplemented with 60  $\mu$ M putrescin, 20 nM progesterone, 5  $\mu$ g/ml insulin, 100  $\mu$ g/ml transferrin, 30 nM sodium selenite and 6  $\mu$ g/ml glucose. Growth factors: human Epidermal Growth Factor (Gibco) and basic Fibroblast Growth Factor (Sigma) were added every 48-72 hours in final concentration of 20 ng/ml and 10 ng/ml in media, respectively. Differentiation of primary neurospheres was obtained as described previously (Kerosuo, Piltti et al. 2008). Neurospheres were transferred on Poly-D-Lysine coated cover-slips placed in 6 well plates and allowed to attach over night in a drop of culture medium. To induce differentiation wells were filled with culture medium supplemented with 2% FBS. After 7-14 days the cover-slips were examined for neural differentiation and subjected to immunocytochemistry. To study secondary neurosphere formation SH-SY5Y cells were seeded into 24 or 96-well plate at  $10^2$  cells per well. After 6-7 days the number and size

of the neurospheres formed was recorded. The neurosphere diameter was assessed optically with an object micrometer.

### **Western blotting**

Protein samples were prepared with 4 times sample buffer (10% glycerol, 62.5 mM Tris-HCl pH 6.8, 2% SDS, 0.01 mg/mL bromophenol blue, 2%  $\beta$ -mercaptoethanol), and boiled for 5 minutes at 95-105 °C. Samples were loaded onto 10% polyacrylamide gels and run at 110 volts for 4.5 hours. Proteins were then transferred to PVDF membranes through semi-wet transfer at 30 volts for 2.5 hours. Membranes were blotted in 3% milk 2 hours to overnight. Primary antibodies were incubated overnight at 4°C, except for Actin mouse, which was incubated 1 hour at room temperature. Antibody concentrations used are as follows: Actin MAB150 1R, (Chemicon- Millipore; 1:1000),  $\alpha$ -Tubulin TU-02 (Sigma; 1:1000), CDK2 mouse D-12 (Sigma 1:1000), CDK2 rabbit M2 (Sigma; 1:500), human Spy1 (Novus; 1:1000-1:10000), p27<sup>Kip1</sup> NA35 (Calbiochem 1:100), GAP43 G9264 (Sigma 1:1000), GFAP G4546 (Sigma 1:1000), Nestin G-20 (Santa Cruz 1:1000). Membranes were washed with TBST 3 times for 5-10 minutes, followed by a 1 hour incubation in secondary antibody (mouse, rabbit or goat – 1:10000) at room temperature. Membranes were then washed with TBST 3 times for 15 minutes and were visualized using FluorChemHD2 imaging system (Alpha Innotech).

### **Immunoprecipitation and CDK2 kinase assay**

Bradford assays were performed to ensure equal protein loading, and 100-250  $\mu$ g of protein was immunoprecipitated from SH-SY5Y cell lysates. Protein was incubated with 5  $\mu$ L of CDK2-mouse antibody overnight at 4°C. The following day, 5  $\mu$ L of protein A

sepharose beads were added to the samples and incubated for 1 hour at 4°C. Samples were then washed three times with NP-40 lysis buffer at 4°C and aspirated to a final volume of 25µl. CDK2 kinase assays were performed in kinase buffer (50 mM Tris-Hcl pH 7.5, 10 mM MgCl<sub>2</sub>, 1 mM DTT, 20 mM EGTA) and 0.5 µCi/µL [ $\gamma$ -<sup>32</sup>P]ATP- ~3,000 Ci/mmol obtained from Perkin Elmer. 4 µg of Histone H1 was added to each 25 µl immunoprecipitated sample (described above) incubated with 25 µL of 2 times kinase buffer. Samples were incubated at 30°C for 30 minutes, followed by the addition of 25 µL of 4 times sample buffer. Samples were boiled for 5 minutes at 95-105°C and loaded onto 10% polyacrylamide gels. SDS-PAGE and transfer were performed as described above. Membranes were exposed using a Cyclone PlusPhosphoimager (Perkin Elmer – U of Windsor), and analyzed using OptiQuant software.

### **qRT-PCR**

Total RNA was extracted from cells or tissues utilizing RNAeasyPlus Mini Kit (Qiagen) and reverse transcribed using 200U Superscript II (Invitrogen), 0.5 µg OligodT's and 0.5 µg random nanomers (Sigma) according to the manufacturer instructions. For each experiment the samples were reverse transcribed at the same time and cDNA was stored at -20°C. Real time PCR with SYBR green (Applied Biosystems) fluorescent detection and 400 nM of each primer was performed using ABI Prism 7300 thermocycler. *GAPDH* was used as the endogenous control. Data was analyzed using ABI 7300 software and represented as log<sub>10</sub> relative quantification (RQ) relative to control.

## RESULTS

### **Endogenous levels of Spy1 are downregulated during RA-induced differentiation in neuroblastoma**

To determine how Spy1 is expressed through differentiation in neural progenitor cells human neuroblastoma SH-SY5Y cells were induced to differentiate over several days using RA. Cells were scored as differentiated when the neurite length exceeded twice the size of the cell body. In SH-SY5Y cells, Spy1 protein levels were abruptly depleted upon addition of RA, with levels being significantly depleted between 16-48 hours post-differentiation (Fig. 1A). This occurs concurrent with an upregulation of the differentiation marker GAP43 and a downregulation of the stemness marker Nestin (Fig. 1A; lower panel). QRT-PCR analysis upon RA stimulation revealed that *SPDYA* expression levels were significantly downregulated by 48 hours after the addition of RA (Fig. 1B). Kinase assays showed that *in vitro* CDK2 kinase activity declines in parallel with Spy1 expression levels (Fig. 1C).



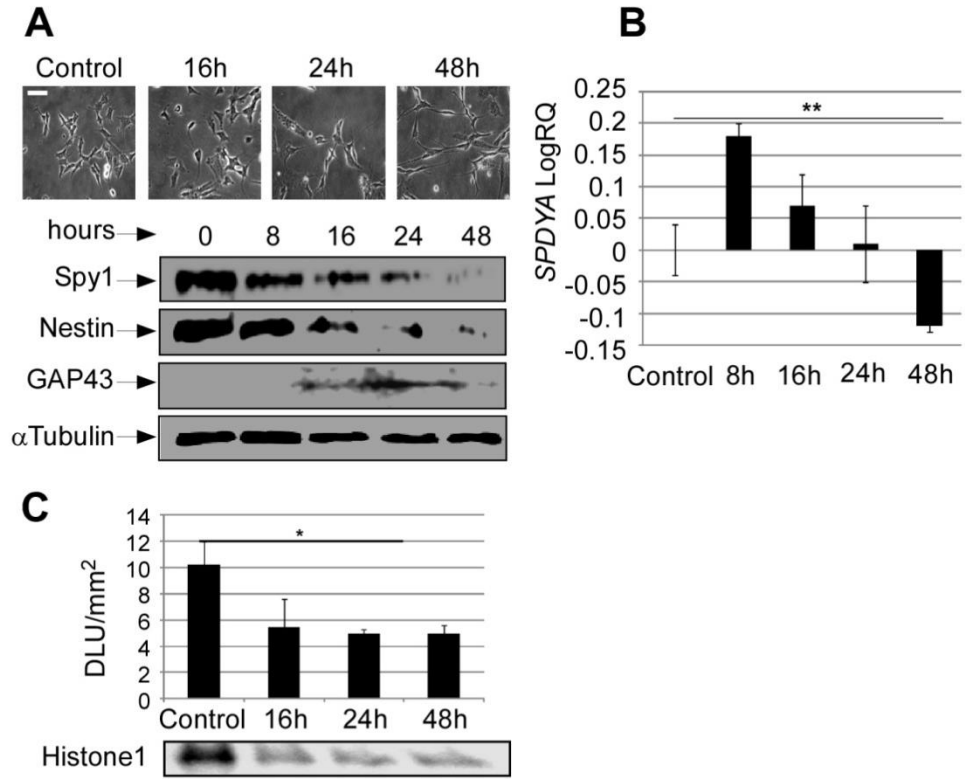


**Figure 1.** Spyl protein levels are tightly regulated during neuroblastoma progenitor fate decisions.

(A) SH-SY5Y cells differentiated in 13-*cis* Retinoic Acid (RA) (2 $\mu$ M) and assayed at the indicated times. Differentiation was recorded by phase contrast inverted microscopy (upper panel) and cell lysates were analysed by SDS-PAGE (lower panel). Neuronal differentiation was confirmed by detection of GAP43 expression.  $\alpha$ -Tubulin was used as a loading control. Scale bar, 50  $\mu$ m.

(B) *SPDYA* expression was assessed over a differentiation time course in SH-SY5Y cells by qRT-PCR. Non-treated cells were used as a control. Results are presented as mean  $\pm$ s.d. for triplicate samples from a representative experiment. n=4, \*\*p < 0.01 (Student's *t*-test).

(C) CDK2 activity was analyzed at the indicated time points post RA treatment in SH-SY5Y cells. Untreated cells were used as a control. Phosphorimaging analysis is demonstrated as Density Light Units (DLU) /mm<sup>2</sup> (upper panel). Lower panel depicts a representative phosphorimage. Results are presented as mean  $\pm$ s.d of a representative experiment. n=2, \*p < 0.05 (Student's *t*-test).

## **Stable overexpression of Spy1 causes delayed neural differentiation**

To determine whether decreasing levels of Spy1 protein are essential for the observed differentiation in neuroblastoma, Spy1 or an empty vector control were stably overexpressed in SH-SY5Y cells. SH-SY5Y-WT and SH-SY5Y-Spy1 cell lines were induced to differentiate and observed over a 72 hour time course. By 72 hours post-differentiation over 75% of control cells successfully differentiated while no signs of differentiation in the Spy1 overexpressing cells are visible (Fig. 2A; right panel), suggesting that Spy1 induces complete resistance to RA stimulated differentiation. To determine whether effects could be due to the known proliferative effects of Spy1, cell numbers, BrdU incorporation and PCNA staining was conducted (Fig. 2B & 2C). At 96 hours post-differentiation SH-SY5Y-Spy1 cells continued to proliferate, while SH-SY5Y-WT cells had significantly reduced proliferation indicative of terminal differentiation (Fig. 2B). This was also demonstrated by incorporation of BrdU (Fig. 2C; left panel) and PCNA (Fig. 2C; right panel). In each assay Spy1 overexpressing cells continued to synthesize DNA and cycle at 72 hours post-differentiation while over 50% of control cells enter quiescence by 48 hours post-differentiation. Interestingly, qRT-PCR of cells overexpressing Spy1 in the presence of differentiation stimuli revealed significantly higher levels of the neural stem cell (NSC) marker *Nestin* (Fig. 2D) and significantly lower expression of the neuronal differentiation marker, growth associated protein 43 (*GAP43*) (Fig. 2E), than control counterparts.

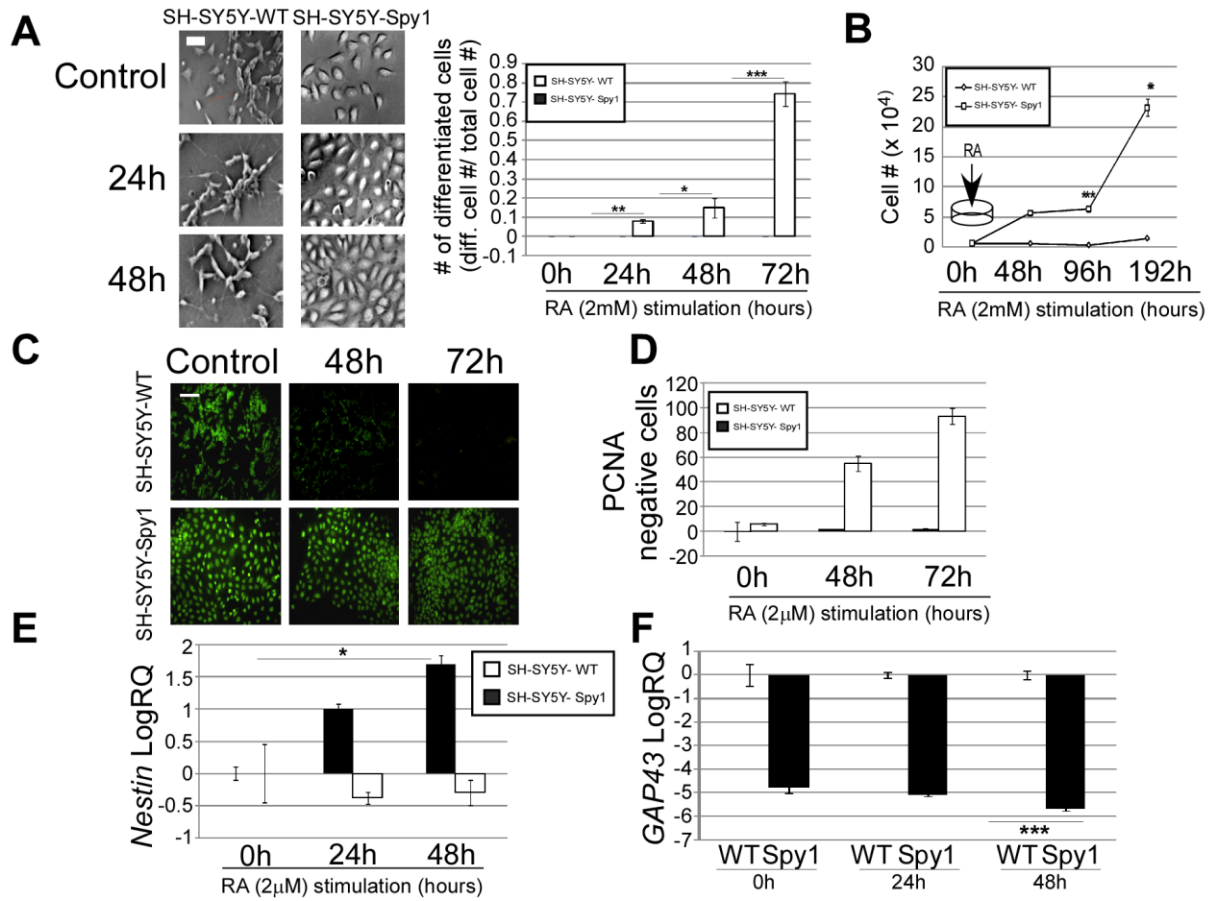


**Figure 2.** Spy1 overexpression abrogates neuronal differentiation of neuroblastoma.

SH-SY5Y cell line was generated stably expressing flag-tagged Spy1 (SH-SY5Y-Spy1) and empty vector (SH-SY5Y-WT).

(A) Cells were differentiated using 2 $\mu$ M 13-cis-Retinoic Acid (RA). Morphology over a time course was documented using inverted phase contrast microscopy (left panel). Differentiation was scored according to axon length, and the ratio of differentiated cells to total cell number was calculated (right panel). Control bars (hollow), Spy1 overexpressing (black bars). Values are mean  $\pm$  s.d. n=3; \*p < 0.05, \*\*p < 0.01, \*\*\*p < 0.001 (Student's *t*-test). Scale bar, 50  $\mu$ m.

(B) Cells were seeded at the density 0.5 x10<sup>4</sup> cells/ml and differentiated using 2mM RA. Cells were harvested and subjected to the trypan blue analysis at indicated times. Representative data are shown as mean  $\pm$  s.d. n=3, \*\*p < 0.01, \*\*\*p < 0.001 .

(C) SH-SY5Y cells were subjected to BrdU incorporation along the RA-induced differentiation time course. Immunocytochemistry was conducted at 48 hours and 72 hours. PI was used as a nuclear counterstain (not shown). Scale bar, 100 $\mu$ m.

(D) PCNA negative cells and total cell number were scored in 3 different fields of view at 48h and 72h time points. PCNA negative cells are expressed as a percentage of total cell number at each time point. Data are shown as mean  $\pm$  s.d; n=2.

(E & F) Expression levels of (E) *Nestin* and (F) *GAP43* were analyzed by qRT-PCR in SHSY5Y-WT (WT) and SH-SY5Y-Spy1 (Spy1) along differentiation time-course. Representative data are shown as mean  $\pm$ s.d. n=3; \*p < 0.05 (E) and \*\*\*p < 0.001 (F).

## **Spy1 overexpression promotes self-renewal in neuroblastoma cells**

The pool of multipotent NSCs can be purified from heterogeneous cell population utilizing a neurosphere formation assay. Unlike neural progenitor cells with limited proliferative potential, only highly proliferative multipotent NSCs can retain the ability to self-renew and produce neurospheres that can be passaged in a long term culture (Morshead, Reynolds et al. 1994). Additionally, neurospheres derived through this assay retain the capacity to express GAP43 and glial fibrillary acidic protein (GFAP) upon differentiation conditions (Coleman, Marshall et al. 2004). SH-SY5Y neuroblastoma cells have been previously shown to express markers of typical neural crest stem cells (Biagiotti, D'Amico et al. 2006; Cui, Ma et al. 2006) and neuroblastoma cell lines, in general, contain populations of self renewing, multipotent tumour cells (Walton, Kattan et al. 2004; Mahller, Williams et al. 2009). Interestingly, we found that endogenous levels of Spy1 were significantly elevated in cells cultured as neurospheres when compared to monolayer culture, supporting the endogenous requirement for this protein in maintaining multipotency (Fig. 3A). We investigated the influence of Spy1 overexpression on self-renewal in SH-SY5Y cells cultured as neurospheres. Spy1 overexpressing cells almost doubled the number of neurospheres as compared to controls (Fig.3B). Increases in neurosphere number were significant for neurospheres of a diameter smaller than 100 $\mu$ m; however, there was no significant increases seen for neurospheres larger than 100 $\mu$ m (Fig. 3C), notably cultures were carried out in a flat dish and not in aggregate culture (Kawamura, Izumi et al. 2004). Serial passaging of neurospheres demonstrated that Spy1 overexpressing populations had enhanced longevity over control neurospheres (Fig. 3D).

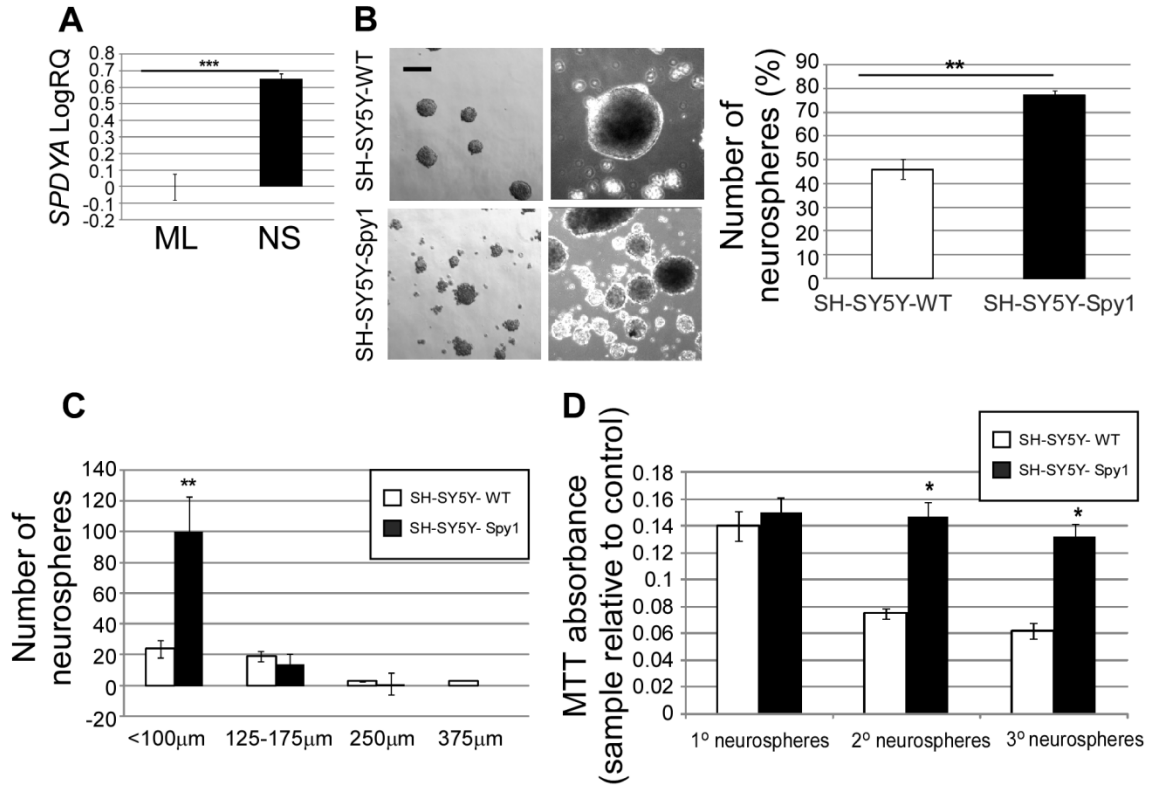


**Figure 3.** Elevated levels of Spy1 protein promote neuroblastoma progenitor self renewal.

(A) SH-SY5Y cells cultured as neurospheres (NS) or in monolayer (ML) were harvested and *SPDYA* expression levels determined by qRT-PCR. Data shown is mean  $\pm$ s.d, \*\*\* $p < 0.001$ . (Student's *t*-test, n=3).

(B-D) SH-SY5Y-WT and SH-SY5Y-Spy1 cells were grown in neurosphere assays.

(B) Morphology of cultures by light microscopy (left panels). Scale bar, 100  $\mu$ m. Spheres were passaged every 6-7 days and the neurosphere formation efficiency was quantified as a number of spheres relative to the total number of the cells seeded (right panel). Representative data are shown as mean  $\pm$ s.d. of triplicates from three independent experiments, \*\* $p < 0.01$  (Student's *t*-test; n=3).

(C) Neurospheres maintained in culture for 14 days were scored according to diameter. Values presented as mean  $\pm$ s.d. of two independent experiments, \*\* $p < 0.01$ . (Student's *t*-test).

(D) Primary, secondary and tertiary neurospheres were subjected to MTT assay. The obtained absorbance at 590nm was corrected for background absorbance. Data shown is mean  $\pm$ s.d, \* $p < 0.05$  (Student's *t*-test; n=2).



## **Spy1 regulation of stemness and neural lineage commitment is controlled by extracellular microenvironment**

Given the environmental differences seen with Spy1 expression in neurosphere culture, corresponding passages of SH-SY5Y-WT or SH-SY5Y-Spy1 cells were cultured either in monolayer or as neurospheres and gene expression was analyzed. Interestingly, expression of the pluripotency marker, *Oct-4* (Fig. 4A) and *BM11*, stem cell marker (Fig. 4B), was significantly elevated by Spy1 when cultured as neurospheres. However, in monolayer cultures, Spy1 expression significantly elevated the expression of glial progenitors and stem-like TIC markers (Fig. 4C-F). Specifically, Spy1 enhanced expression of the glial progenitor marker *OLIG2* (Fig. 4C), the astrocyte-specific marker *GFAP* (Fig. 4E), the TIC marker *CD133* (Fig. 4F) and *Fibronectin*, which has been shown to mediate invasiveness and cell survival in other types of neural derived tumours (Fig. 4D) (Lavial, Bessonard et al.; Yuan, Siegel et al. 2007).

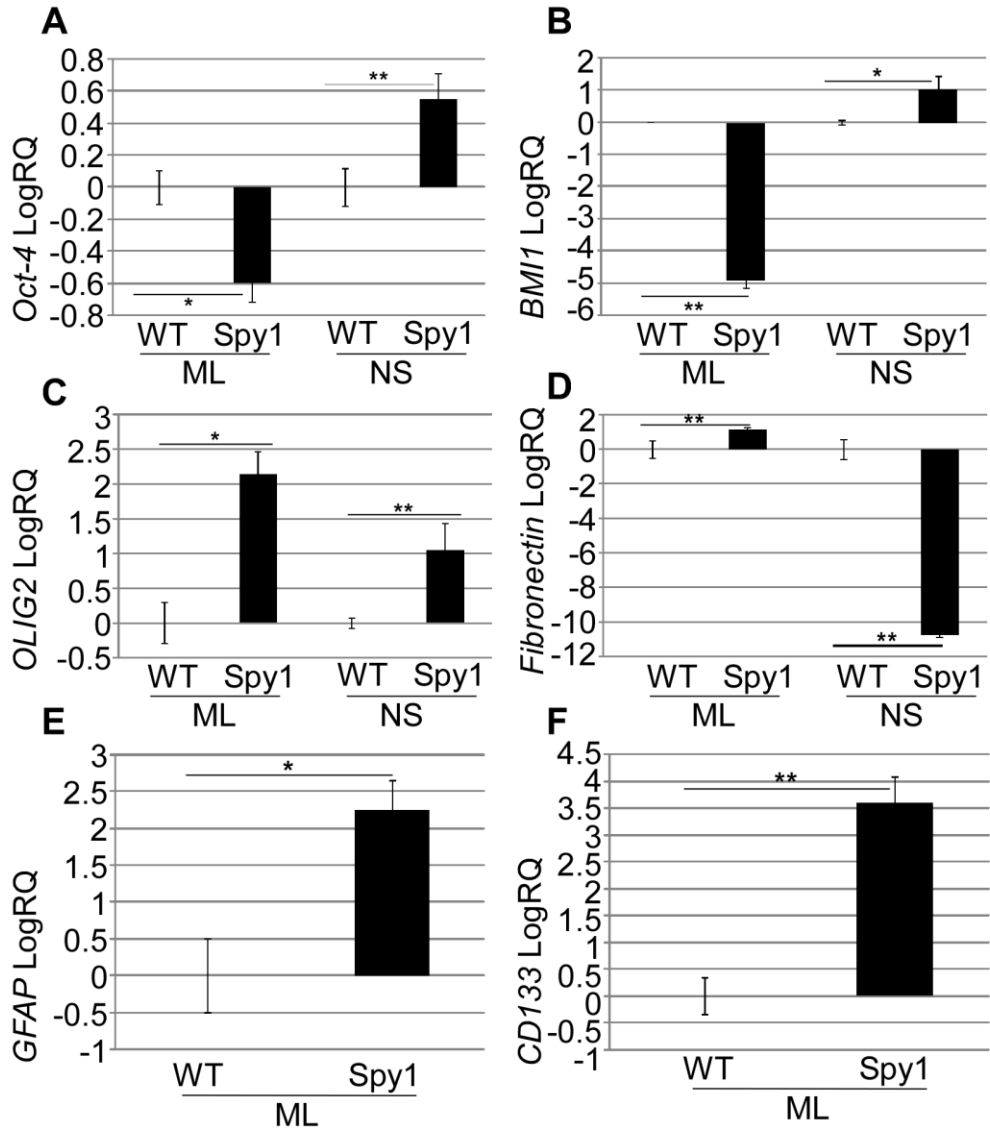


**Figure 4.** Spy1 regulation of stemness and neural lineage commitment is controlled by extracellular microenvironment.

SH-SY5Y control cells (WT) or overexpressing Spy1 (SPY1), cultured in monolayer (ML) or as neurospheres (NS). mRNA levels were analysed using qRT-PCR.

(A-B) Expression levels of *Oct-4* and *BM11*.

(C-D) *OLIG2* and *Fibronectin*.

(E-F) *GFAP* and *CD133*.

Representative data are shown as mean  $\pm$ s.d. of triplicates from three independent experiments, \*p < 0.05, \*\*p < 0.01 (Student's *t*-test).

## DISCUSSION

Inappropriate differentiation of immature cells within the ganglionic lineage are thought to drive neuroblastoma (Anderson 1997; Brodeur 2003; Dyer 2004); Hoehner et al. 1996). Indeed the heterogeneous populations of diverse progenitor cells, seen to exist within the tumour, mirror neural crest plasticity (Ciccarone, Spengler et al. 1989; Ross, Biedler et al. 2003; Ross and Spengler 2007). Multiple studies over the years have attempted to elucidate the molecular basis behind the differentiation processes of neuroblastoma. Diverse agents, growth factors and differentiation protocols have been proposed (Lovat et al. 1997; Chlapek et al. 2010; Truckenmiller et al. 2001; Khan et al. 2001); however, the information about the role of the cell cycle control in neuroblastoma remains insufficient. We report for the first time that a novel G1 phase regulator, Spy1, is implicated in differentiation and self-renewal of neuroblastoma cells.

We utilized the SH-SY5Y cell line of an established N cell phenotype that is blocked at the precursor stage of neuronal development. We find that Spy1 levels are regulated during cell differentiation *in vitro* and altering expression levels of Spy1 prevents functional RA-induced differentiation. Overexpression of Spy1 resulted in enhanced self-renewal and longevity of neuroblastoma cells cultured in a neurosphere formation assay. Spy1 levels were also significantly elevated in self-renewing neurospheres as compared to the populations cultured as a monolayer. Collectively, this suggests a potential role of the Spy1 protein as a stabilizer of proliferation among the populations of higher hierarchy, namely progenitors and tumour initiating cells. Spy1 has demonstrated roles in spinal cord regeneration and was found to possess stem-like qualities in the developing mammary gland, supporting a general role for Spy1 in select

populations of adult stem or progenitor cells (Golipour, Myers et al. 2008; Huang, Liu et al. 2009)). Dobashi *et. al.* demonstrated that a decrease in CDK2 kinase activity must occur in order to support functional differentiation (Dobashi, Kudoh et al. 1995) and others have demonstrated that p27<sup>Kip1</sup> levels accumulate during neuronal cell differentiation (Sasaki, Tamura et al. 2000). Interestingly, suppression of CDK2 activity is required for reduced proliferation and survival of the primary neural crest derived tumour and its inhibition was demonstrated to be synthetic lethal in MYCN overexpressing neuroblastoma (Molenaar, Ebus et al. 2009; (Afanasyeva, Mestdagh et al. 2011). Moreover, high expression of the Skp2 component of the SCF<sup>Skp2</sup> ligase was included in the genetic signature of aggressive stages of neuroblastoma. Skp2 overexpression correlated with p27<sup>Kip1</sup> protein downregulation and poor patient prognosis (Westermann et al. 2007; Muth et al. 2010). The phosphorylated Thr-187 residue of p27<sup>Kip1</sup> is required for its ubiquitination by SCF<sup>Skp2</sup> complex and its subsequent proteolysis (Carrano, Eytan et al. 1999; Tsvetkov, Yeh et al. 1999). Hence, Spy1-mediated CDK2 activity may affect the outcome of patients with Skp2 overexpression.

Interestingly, we observed a difference in gene expression when cells were grown in neurosphere culture versus the general population of cells grown in monolayer culture. In neurospheres, Spy1-induced expression of the progenitor and multipotency markers BMI1 and Oct-4, respectively. Both BMI1 and Oct-4 were shown to exert their functions in the other neural tumours by preventing cellular differentiation and contributing to their growth and progression (Abdouh, Facchino et al. 2009; Ma, Qi et al. 2009)). Hence, this data supports a hypothesis that Spy1 may function in promoting the growth of highly undifferentiated cells in neuroblastoma. When cells were in monolayer, however, Spy1 promoted expression of glial progenitors such as *GFAP* and *OLIG2*. SH-

SY5Y cells were demonstrated previously to contain a minute pool of highly clonogenic S cells (Biagiotti, D'Amico et al. 2006) that are also characterized by expression of glial markers (Ross and Spengler 2007). Thus, forced expression of Spy1 can be speculated to contribute to the expansion of self-renewing cell populations within the heterogeneous tumour. However, careful analysis is required to determine if Spy1 manipulation affects specific subpopulations differently and whether its role in altering potential of downstream progenitors is possible. While the data support a potential role for Spy1 in the arrested differentiation phenotype and maintaining neuroblastoma stem-like TIC population, further study involving cell lines of a different genetic background, primary tumour samples and, finally, an *in vivo* xenograft model is required for firm conclusions.

## REFERENCES

- Abdouh, M., S. Facchino, et al. (2009). "BMI1 sustains human glioblastoma multiforme stem cell renewal." *J Neurosci* **29**(28): 8884-96.
- Afanasyeva, E. A., P. Mestdagh, et al. (2011). "MicroRNA miR-885-5p targets CDK2 and MCM5, activates p53 and inhibits proliferation and survival." *Cell Death Differ* **18**(6): 974-84.
- Anderson, D. J. (1997). "Cellular and molecular biology of neural crest cell lineage determination." *Trends Genet* **13**(7): 276-80.
- Barnes, E. A., L. A. Porter, et al. (2003). "Human Spyl1 promotes survival of mammalian cells following DNA damage." *Cancer Res* **63**(13): 3701-7.
- Biagiotti, T., M. D'Amico, et al. (2006). "Cell renewing in neuroblastoma: electrophysiological and immunocytochemical characterization of stem cells and derivatives." *Stem Cells* **24**(2): 443-53.
- Brodeur, G. M. (2003). "Neuroblastoma: biological insights into a clinical enigma." *Nat Rev Cancer* **3**(3): 203-16.
- Brodeur, G. M., A. T. Look, et al. (2001). "Biological aspects of neuroblastomas identified by mass screening in Quebec." *Med Pediatr Oncol* **36**(1): 157-9.
- Cheng, A., W. Xiong, et al. (2005). "Identification and comparative analysis of multiple mammalian Speedy/Ringo proteins." *Cell Cycle* **4**(1): 155-65.
- Ciccarone, V., B. A. Spengler, et al. (1989). "Phenotypic diversification in human neuroblastoma cells: expression of distinct neural crest lineages." *Cancer Res* **49**(1): 219-25.
- Cournoyer, S., C. Nyalendo, et al. (2012). "Genotype analysis of tumour-initiating cells expressing CD133 in neuroblastoma." *Genes Chromosomes Cancer* **51**(8): 792-804.
- Cuende, J., S. Moreno, et al. (2008). "Retinoic acid downregulates Rael leading to APC(Cdh1) activation and neuroblastoma SH-SY5Y differentiation." *Oncogene* **27**(23): 3339-44.
- Cui, H., J. Ma, et al. (2006). "Bmi-1 regulates the differentiation and clonogenic self-renewal of I-type neuroblastoma cells in a concentration-dependent manner." *J Biol Chem* **281**(45): 34696-704.
- Dinarina, A., L. H. Perez, et al. (2005). "Characterization of a new family of cyclin-dependent kinase activators." *Biochem J* **386**(Pt 2): 349-55.
- Dobashi, Y., T. Kudoh, et al. (1995). "Constitutive overexpression of CDK2 inhibits neuronal differentiation of rat pheochromocytoma PC12 cells." *J Biol Chem* **270**(39): 23031-7.
- Dyer, M. A. (2004). "Mouse models of childhood cancer of the nervous system." *J Clin Pathol* **57**(6): 561-76.
- Gastwirt, R. F., C. W. McAndrew, et al. (2007). "Speedy/RINGO regulation of CDKs in cell cycle, checkpoint activation and apoptosis." *Cell Cycle* **6**(10): 1188-93.

- Golipour, A., D. Myers, et al. (2008). "The Spy1/RINGO family represents a novel mechanism regulating mammary growth and tumorigenesis." *Cancer Res* **68**(10): 3591-600.
- Huang, Y., Y. Liu, et al. (2009). "Peripheral nerve lesion induces an up-regulation of Spy1 in rat spinal cord." *Cell Mol Neurobiol* **29**(3): 403-11.
- Ireland, C. M. (1989). "Activated N-ras oncogenes in human neuroblastoma." *Cancer Res* **49**(20): 5530-3.
- Kaneko, Y., N. Kanda, et al. (1987). "Different karyotypic patterns in early and advanced stage neuroblastomas." *Cancer Res* **47**(1): 311-8.
- Kawamura, K., H. Izumi, et al. (2004). "Induction of centrosome amplification and chromosome instability in human bladder cancer cells by p53 mutation and cyclin E overexpression." *Cancer Res* **64**(14): 4800-9.
- Kerosuo, L., K. Piltti, et al. (2008). "Myc increases self-renewal in neural progenitor cells through Miz-1." *J Cell Sci* **121**(Pt 23): 3941-50.
- Kranenburg, O., V. Scharnhorst, et al. (1995). "Inhibition of cyclin-dependent kinase activity triggers neuronal differentiation of mouse neuroblastoma cells." *J Cell Biol* **131**(1): 227-34.
- Kushner, B. H., F. Gilbert, et al. (1986). "Familial neuroblastoma. Case reports, literature review, and etiologic considerations." *Cancer* **57**(9): 1887-93.
- Ma, Y., X. Qi, et al. (2009). "Identification of candidate genes for human pituitary development by EST analysis." *BMC Genomics* **10**: 109.
- Mahller, Y. Y., J. P. Williams, et al. (2009). "Neuroblastoma cell lines contain pluripotent tumour initiating cells that are susceptible to a targeted oncolytic virus." *PLoS One* **4**(1): e4235.
- Maris, J. M., M. D. Hogarty, et al. (2007). "Neuroblastoma." *Lancet* **369**(9579): 2106-20.
- Maris, J. M. and K. K. Matthay (1999). "Molecular biology of neuroblastoma." *J Clin Oncol* **17**(7): 2264-79.
- Marshall, G. P., 2nd, H. H. Ross, et al. (2008). "Production of neurospheres from CNS tissue." *Methods Mol Biol* **438**: 135-50.
- Matsuo, T., P. Seth, et al. (2001). "Increased expression of p27Kip1 arrests neuroblastoma cell growth." *Med Pediatr Oncol* **36**(1): 97-9.
- Matsuo, T. and C. J. Thiele (1998). "p27Kip1: a key mediator of retinoic acid induced growth arrest in the SMS-KCNR human neuroblastoma cell line." *Oncogene* **16**(25): 3337-43.
- McAndrew, C. W., R. F. Gastwirt, et al. (2007). "Spy1 enhances phosphorylation and degradation of the cell cycle inhibitor p27." *Cell Cycle* **6**(15): 1937-45.
- Mei, Y., Z. Wang, et al. "Regulation of neuroblastoma differentiation by forkhead transcription factors FOXO1/3/4 through the receptor tyrosine kinase PDGFRA." *Proc Natl Acad Sci U S A* **109**(13): 4898-903.



- Molenaar, J. J., M. E. Ebus, et al. (2009). "Inactivation of CDK2 is synthetically lethal to MYCN over-expressing cancer cells." *Proc Natl Acad Sci U S A* **106**(31): 12968-73.
- Ohnishi, T., N. Arita, et al. (1997). "Fibronectin-mediated cell migration promotes glioma cell invasion through chemokinetic activity." *Clin Exp Metastasis* **15**(5): 538-46.
- Porter, L. A., M. Kong-Beltran, et al. (2003). "Spy1 interacts with p27Kip1 to allow G1/S progression." *Mol Biol Cell* **14**(9): 3664-74.
- Reynolds, B. A. and R. L. Rietze (2005). "Neural stem cells and neurospheres--re-evaluating the relationship." *Nat Methods* **2**(5): 333-6.
- Ross, R. A., J. L. Biedler, et al. (2003). "A role for distinct cell types in determining malignancy in human neuroblastoma cell lines and tumours." *Cancer Lett* **197**(1-2): 35-9.
- Ross, R. A. and B. A. Spengler (2007). "Human neuroblastoma stem cells." *Semin Cancer Biol* **17**(3): 241-7.
- Ross, R. A., B. A. Spengler, et al. (1995). "Human neuroblastoma I-type cells are malignant neural crest stem cells." *Cell Growth Differ* **6**(4): 449-56.
- Sasaki, K., S. Tamura, et al. (2000). "Expression and role of p27(kip1) in neuronal differentiation of embryonal carcinoma cells." *Brain Res Mol Brain Res* **77**(2): 209-21.
- Schwab, M., K. Alitalo, et al. (1983). "Amplified DNA with limited homology to myc cellular oncogene is shared by human neuroblastoma cell lines and a neuroblastoma tumour." *Nature* **305**(5931): 245-8.
- Takenobu, H., O. Shimozato, et al. (2011). "CD133 suppresses neuroblastoma cell differentiation via signal pathway modification." *Oncogene* **30**(1): 97-105.
- Tanaka, T., D. J. Slamon, et al. (1988). "Expression of Ha-ras oncogene products in human neuroblastomas and the significant correlation with a patient's prognosis." *Cancer Res* **48**(4): 1030-4.
- Vangipuram, S. D., Z. J. Wang, et al. "Resistance of stem-like cells from neuroblastoma cell lines to commonly used chemotherapeutic agents." *Pediatr Blood Cancer* **54**(3): 361-8.
- Walton, J. D., D. R. Kattan, et al. (2004). "Characteristics of stem cells from human neuroblastoma cell lines and in tumours." *Neoplasia* **6**(6): 838-45.
- Yuan, L., M. Siegel, et al. (2007). "Transglutaminase 2 inhibitor, KCC009, disrupts fibronectin assembly in the extracellular matrix and sensitizes orthotopic glioblastomas to chemotherapy." *Oncogene* **26**(18): 2563-73.
- Zha, Y., E. Ding, et al. "Functional dissection of HOXD cluster genes in regulation of neuroblastoma cell proliferation and differentiation." *PLoS One* **7**(8): e40728.

**CHAPTER 5**  
**DISCUSSION & FUTURE DIRECTIONS**

This work is the first to demonstrate a mechanistic role of a novel cell cycle regulator Spy1 (Spdya; Speedy; Spdy1; Spy1A; RINGO) in fate decisions in the nervous system and in neural cell derived malignancies. We show that Spy1 is present in the neurogenic sites of the adult mammalian brain characterized by populations of multipotent and self-renewing stem cells. Spy1 is co-expressed with Nestin and glial fibrillary acidic protein (GFAP) markers within the subventricular zone (SVZ). Both markers were reported previously to label the populations of B-type multipotent and self-renewing stem cells (Doetsch, Caille et al. 1999). We demonstrate that the forced expression of Spy1 in primary neural culture affects the differentiation commitment, reducing neurite outgrowth and levels of neuronal markers and subsequently increasing self-renewing capacity. These data suggest that Spy1-mediated effects play a role in fate determination in neural systems.

According to abundant literature, neural stem cells residing in the niche of the SVZ have been speculated to serve as a source of brain tumours and (Gilbertson and Rich 2007; Lim, Cha et al. 2007). The subtypes of human glioma proposed by The Cancer Genome Atlas (TCGA) research network reflect characteristics of normal neural stem cells (Verhaak, Hoadley et al. 2010). The TCGA work suggested that multiple populations, possibly at a different commitment level, lay at the source of brain tumour formation (Verhaak, Hoadley et al. 2010). Our data shows that in comparison to normal tissue and benign tumours Spy1 levels are significantly upregulated in the most aggressive forms of human glial tumours, including anaplastic astrocytoma and glioblastoma multiforme (GBM). Depletion of Spy1 levels in human glioblastoma cell lines results in significant decline of proliferation and reduction of self-renewal and stemness marker expression. These data support the hypothesis that Spy1 effects on cell

fate may regulate the self-renewing capacity of the populations of brain tumour initiating cells (BTICs).

Mechanistically the tumour aggressiveness was shown to be associated with pools of expansive, symmetrically self-renewing cancer stem cells (Sugiarto, Persson et al. 2011; Boman, Wicha et al. 2007). Our data demonstrate that Spy1 is involved in the mode of division control in CD133 enriched glioma cell lines and the downregulation of Spy1 levels causes significant increase in a fraction of cells dividing symmetrically in comparison to control or Cyclin E1 knockdown cells. The decrease in Spy1 levels affects the even distribution of Numb in CD133+ cells. Numb is regulated by Musashi1 (Toda, Iizuka et al. 2001), a well established BTIC marker (Sakakibara, Nakamura et al. 2002; Muto, Imai et al. 2012) that can be activated by Spy1 RINGO/CDK (Arumugam, MacNicol et al. 2012). Hence, Spy1-mediated effects in NSCs as well as in the populations of BTIC may rely on Msi1 activation by Spy1-CDK2. Further investigation of this pathway, however, is required to support this model in human glioma.

Spy1 has been shown to activate CDKs using an unconventional mechanism that is insensitive to well established inhibitory mechanisms (Cheng, Xiong et al. 2005; Dinarina, Perez et al. 2005). Furthermore, Spy1 can bind directly to the CDK inhibitor p27 and promotes degradation of this essential tumour suppressor (Porter, Kong-Beltran et al. 2003; McAndrew, Gastwirt et al. 2007). It is known that Spy1 is capable of bypassing established checkpoints and preventing apoptosis (Barnes, Porter et al. 2003; Gastwirt, McAndrew et al. 2007). Whether these mechanisms participate in driving brain tumourigenesis is currently unknown. Our lab has developed a host of mutants that are unable to bind directly to CDK2 and/or p27 (Al Sorkhy, Ferraiuolo et al. 2012). It is an important next step to test the ability of these mutants in driving fate decisions in neural

cells. It is possible that mechanistically Spy1 can have different effects depending on the commitment of the cell type in question. For example, in stem cell populations the demonstrated effects of Spy1 on symmetric vs. asymmetric division may play a prominent role, in progenitor cells the activation of CDK2 may predominantly prevent differentiation from occurring and in more differentiated populations the roles of Spy1 in overriding checkpoint arrest and apoptosis may play a role on the predominate.

Another important next step is to demonstrate whether Spy1 function is essential in primary glioma obtained from patients. Primary tumour cells demonstrate significant advantage over common cell lines as they are not subjected to selective pressure of tissue culture. Primary cells retain the original neoplastic characteristics and closely mimic the phenotype and genetic/genomic signatures of the particular human brain tumour subtype upon ectopic xenotransplantation in mice.

It is also important to determine whether Spy1 expression is capable of initiating the development of neural tumours. For this we will use a conditional inducible mouse model existing in our lab to allow for cell type and developmental stage specific expression of Spy1 within the brain. We will initially utilize the Nestin promoter to target induction to self-renewing populations of stem cells. This model is essential to address the role of Spy1 in diverse populations of neural stem cells and progenitor cells. This model will also allow us to test whether Spy1 can contribute to tumorigenic events occurring at select developmental time points when the level of commitment within the self-renewing pools of progenitors varies.

This mouse model will also be an important first step in mapping the specific neural stem and progenitor populations that are sensitive to Spy1-mediated effects. *In vitro* analysis of cells obtained at different developmental time points can specify whether

increased Spy1 protein levels cause perturbation in the mode of division. Additionally, microarray analysis can be utilized to determine whether Spy1-driven tumours fall under one specific glioma subtype. This data can also be used to generate gene expression signatures specific for tumours derived from Nestin+ stem cells at different developmental stages. It would be tremendously interesting to determine if the age of onset affects the subtype of the tumour.

This study demonstrated that forced expression of Spy1 also inhibits differentiation in neuroblastoma cells of an established neuronal phenotype. As in human glioma, Spy1 overexpression results in increased levels of self-renewal and upregulation of glial lineage markers that characterize highly clonogenic subpopulations of crest derived cells within neuroblastoma tumours (Corvi, Amler et al. 1994; Mahller, Williams et al. 2009). The amplification of the 2p24 locus including MYCN is a signature genomic aberration of neuroblastoma and was reported previously to confer self-renewal potential and selective advantage to tumour cells (Mahller, Williams et al. 2009; Reiter and Brodeur 1996; Brodeur 2003). Spy1 was demonstrated previously to act downstream of c-Myc, another oncogene from the Myc family (Golipour, Myers et al. 2008). Murine mammary cell lines overexpressing Spy1 and the xenotransplantation of these cells resulted in precocious mammary development and tumourigenesis (Golipour, Myers et al. 2008). Whether the observed changes in neuroblastoma cells are due solely to Spy1-mediated cell cycle effects or if there is a potential Myc- driven molecular pathway involved, remains to be determined. Besides the mechanistic background, it is of highest importance to utilize xenograft mouse models to address if Spy1 overexpression drives clonal expansion, commitment resistance and neuroblastoma tumourigenicity *in vivo*.

To summarize, the data obtained in this study supports the hypothesis that Spy1 is involved in regulation of cell fate decisions in neural systems and that Spy1 expression correlates with clonality of tumour cell lines and overall tumour aggressiveness. During normal development Spy1 downregulation is coincident with an established window of neurogenesis at early postnatal stages, while in the adult brain Spy1 positive cells are found in the regions characterized by sustained self-renewing potential. Consistently with the evolution process observed among *Speedy/RINGO* genes (Chauhan, Zheng et al. 2012), their well conserved function in vertebrates versus the complete absence in yeast or *D. melanogaster* suggests that Spy1 is necessary in aiding more sophisticated molecular mechanisms that have been developed in the higher hierarchy organisms. One such example is the complex machinery involved in the cell cycle checkpoint control, progression through the cell cycle and cell activation out of quiescent state. In the circumstances of DNA damage the Spy1 protein is initially downregulated to allow for p53 mediated checkpoint activation (unpublished data), however Spy1 levels reestablish as the damage persists. In the face of the global CDK2 inhibition caused by DNA damage Spy1 can be potentially responsible for the active pool of CDK2 that is eventually required for DNA damage repair. Consequently, as the quiescent state of cell cycle is maintained by high levels of cell cycle inhibitors (Qiu, Takagi et al. 2004), the activation of progenitor or stem cells requires a mechanism that can override this restraint. CDK2 in complex with Spy1 is resistant to p21- mediated inhibition and Spy1/CDK2 promotes p27 degradation. Thus in the face of mobilization signal Spy1 levels are speculated to increase in quiescent cells and stimulate their cell cycle progression. Interestingly, Spy1 levels were found to be rapidly elevated upon injury in glial cells participating in regeneration processes (Huang, Liu et al. 2009). Furthermore, in addition to control of cell activation, a

mechanism simultaneously regulating quiescent state maintenance and senescence suppression was described to involve Notch1 signaling (Sang, Coller et al. 2008). Importantly, forced expression of Spy1 blocks senescence (unpublished data). Therefore, we speculate that tight regulation of Spy1- Notch1 axis is responsible for senescence resistance observed in G0 cells whereas Spy1 upregulation is required for quiescent cell activation.

Importantly, determination of the molecular mechanisms underlying Spy1-mediated effects in collaboration with carefully conducted *in vivo* studies are crucial in addressing the relationship between the role of Spy1 in normal neural systems and during malignant transformation. This may have relevance in cancer initiation and also may serve as an indicator of tumorigenic potential. Resolving the molecular mechanisms driving specific cell populations within nervous system derived tumours is indispensable in designing proper therapeutical anticancer strategies.



## REFERENCES

- Al Sorkhy, M., R. M. Ferraiuolo, et al. (2012). "The cyclin-like protein Spy1/RINGO promotes mammary transformation and is elevated in human breast cancer." *BMC Cancer* **12**: 45.
- Arumugam, K., M. C. MacNicol, et al. (2012). "Ringo/cyclin-dependent kinase and mitogen-activated protein kinase signaling pathways regulate the activity of the cell fate determinant Musashi to promote cell cycle re-entry in *Xenopus* oocytes." *J Biol Chem* **287**(13): 10639-49.
- Barnes, E. A., L. A. Porter, et al. (2003). "Human Spy1 promotes survival of mammalian cells following DNA damage." *Cancer Res* **63**(13): 3701-7.
- Boman, B. M., M. S. Wicha, et al. (2007). "Symmetric division of cancer stem cells--a key mechanism in tumor growth that should be targeted in future therapeutic approaches." *Clin Pharmacol Ther* **81**(6): 893-8.
- Brodeur, G. M. (2003). "Neuroblastoma: biological insights into a clinical enigma." *Nat Rev Cancer* **3**(3): 203-16.
- Chauhan, S., X. Zheng, et al. (2012). "Evolution of the Cdk-activator Speedy/RINGO in vertebrates." *Cell Mol Life Sci* **69**(22): 3835-50.
- Cheng, A., W. Xiong, et al. (2005). "Identification and comparative analysis of multiple mammalian Speedy/Ringo proteins." *Cell Cycle* **4**(1): 155-65.
- Corvi, R., L. C. Amler, et al. (1994). "MYCN is retained in single copy at chromosome 2 band p23-24 during amplification in human neuroblastoma cells." *Proc Natl Acad Sci U S A* **91**(12): 5523-7.
- Dinarina, A., L. H. Perez, et al. (2005). "Characterization of a new family of cyclin-dependent kinase activators." *Biochem J* **386**(Pt 2): 349-55.
- Doetsch, F., I. Caille, et al. (1999). "Subventricular zone astrocytes are neural stem cells in the adult mammalian brain." *Cell* **97**(6): 703-16.
- Gastwirt, R. F., C. W. McAndrew, et al. (2007). "Speedy/RINGO regulation of CDKs in cell cycle, checkpoint activation and apoptosis." *Cell Cycle* **6**(10): 1188-93.
- Gilbertson, R. J. and J. N. Rich (2007). "Making a tumour's bed: glioblastoma stem cells and the vascular niche." *Nat Rev Cancer* **7**(10): 733-6.
- Golipour, A., D. Myers, et al. (2008). "The Spy1/RINGO family represents a novel mechanism regulating mammary growth and tumorigenesis." *Cancer Res* **68**(10): 3591-600.
- Lim, D. A., S. Cha, et al. (2007). "Relationship of glioblastoma multiforme to neural stem cell regions predicts invasive and multifocal tumor phenotype." *Neuro Oncol* **9**(4): 424-9.
- Mahller, Y. Y., J. P. Williams, et al. (2009). "Neuroblastoma cell lines contain pluripotent tumor initiating cells that are susceptible to a targeted oncolytic virus." *PLoS One* **4**(1): e4235.
- McAndrew, C. W., R. F. Gastwirt, et al. (2007). "Spy1 enhances phosphorylation and degradation of the cell cycle inhibitor p27." *Cell Cycle* **6**(15): 1937-45.
- Muto, J., T. Imai, et al. (2012). "RNA-binding protein Musashi1 modulates glioma cell growth through the post-transcriptional regulation of Notch and PI3 kinase/Akt signaling pathways." *PLoS ONE* **7**(3): e33431.
- Porter, L. A., M. Kong-Beltran, et al. (2003). "Spy1 interacts with p27Kip1 to allow G1/S progression." *Mol Biol Cell* **14**(9): 3664-74.

- Qiu, J., Y. Takagi, et al. (2004). "Regenerative response in ischemic brain restricted by p21cip1/waf1." *J Exp Med* **199**(7): 937-45.
- Reiter, J. L. and G. M. Brodeur (1996). "High-resolution mapping of a 130-kb core region of the MYCN amplicon in neuroblastomas." *Genomics* **32**(1): 97-103.
- Sakakibara, S., Y. Nakamura, et al. (2002). "RNA-binding protein Musashi family: roles for CNS stem cells and a subpopulation of ependymal cells revealed by targeted disruption and antisense ablation." *Proc Natl Acad Sci U S A* **99**(23): 15194-9.
- Sang, L., H. A. Coller, et al. (2008). "Control of the reversibility of cellular quiescence by the transcriptional repressor HES1." *Science* **321**(5892): 1095-100.
- Sugiarto, S., A. I. Persson, et al. (2011). "Asymmetry-defective oligodendrocyte progenitors are glioma precursors." *Cancer Cell* **20**(3): 328-40.
- Toda, M., Y. Iizuka, et al. (2001). "Expression of the neural RNA-binding protein Musashi1 in human gliomas." *Glia* **34**(1): 1-7.

## APENDIX A. Detailed protocols.

### I. Tissue Microarray Immunofluorescent Staining protocol

#### *De-paraffinization*

Before deparaffinization in xylene, tissue (microarray) section slides shall be baked in oven at 60°C for 30 minutes on a vertical rack to melt the extra layer of coated paraffin. Trial slides do not have paraffin coating so it can be deparaffinized without baking. All of our tissue (microarray) section slides, unless otherwise specified, were baked at 60°C for two hours after sectioning and are stored at 4°C.

1. Immerse slide in xylene for 10 minutes. Repeat once in new xylene for 10 minutes.
2. Immerse array slide in 100% ethanol for 5 minutes.
3. Immerse in 95% ethanol for 5 minutes.
4. Immerse in 70% ethanol for 5 minutes.
5. Rinse for 5 minutes in water or PBS buffer.

#### *Immunostaining using fluorescent probes*

1. Deparaffinize and dry array slide as referred to in protocol of deparaffinization.
2. Rinse array slide twice with PBST for 5 min each in a Coplin jar.
3. Antigen retrieval (formalin-fixed, paraffin-embedded tissue sections).  
Boiling Bath. Heat the buffer (1mM EDTA, pH 8.0 or 0.01M sodium citrate buffer, pH 6.0) to about 95°C, and then put array slides in the buffer for 10~15 minutes. **Do NOT let the medium boil when you have array slide in. Avoid the slide drying during the procedure.**
4. Rinse array slide in PBST for 5 minutes

5. Apply the blocking antibody (normal goat serum- 150ul/10ml), incubate for 40 minutes at room temperature (RT), and throw off residual fluid (don't wash.).
6. Apply the primary antibody 60 minutes at RT (Spy1 Novus 1:50) usually 200ul volume to cover all the cores.
9. Rinse array slide twice for 5 minutes each in a Coplin jar on the orbital rotator.
10. Incubate array slide with a fluorophore-conjugated secondary antibody at 20~37°C (in a humidity chamber) for 20 minutes (Alexa488 1:1200)
11. Rinse array slide twice in PBST for 5 minutes each in a Coplin jar on the orbital rotator.
12. Incubate array slide with TOTO-3 nuclear stain (0.75ul:1000) in PBST at RT 30 min.
13. Rinse array slide 3 times in PBST for 5 minutes each in a Coplin jar on the orbital rotator.
14. Dehydration and transparency of array slide.
  1. Immerse in 70% ethanol for 5 minutes.
  2. Immerse in 95% ethanol for 5 minutes.
  3. Immerse array slide in 100% ethanol for 5 minutes.
  4. Immerse slide in xylene for 10 minutes. Repeat once in new xylene for 10 minutes
15. Mount array slides with the Vectashield mounting media and cover with a square or rectangular cover slip no.1.
16. The TMA slide is being placed in the slide scanner. **The edges and surface of the cover slip have to be clean and dry in order to place the slide in the slide scanner.**

The fluorescent signal for the secondary antibody fluorophore and nuclear stain is detected and quantified by ScanArray Express software (Perkin Elmer Inc.)

17. The mean the fluorophore signal intensity values are normalized to the mean of the nuclear stain signal.

## II. Magnetic bead labeling

**Buffer 1:** 0.1 M sodium phosphate buffer, pH 7.4–8.0 or 0.1 M sodium borate buffer, pH 7.6–9.5.

**Buffer 2:** Ca<sup>2+</sup> and Mg<sup>2+</sup> free phosphate buffered saline (PBS) supplemented with 0.1% bovine serum albumin (BSA) and 2 mM EDTA, pH 7.4. **Note:** BSA can be replaced by human serum albumin (HSA) or fetal calf serum (FCS). EDTA can be replaced by sodium citrate.

This protocol describes coupling 100µg of CD133 antibody (Biorbyt) to 500µl (2x 10<sup>8</sup>) of beads.

1. The beads are resuspended in by vortexing for 30 seconds followed by rotation for 5 minutes.
2. 500µl of beads are transferred to the magnet vial.
3. 1ml of Buffer 1. is added and beads are resuspended.
4. Vial is placed in a magnet for 1 minute and the liquid is pipetted out.
5. Step 3 and 4 are repeated.
6. Add 500µl of Buffer1. for 1 minute, pipette out the liquid.
7. Remove the vial from the magnet.
8. Resuspend the beads in 400µl and add 100µl of the CD133 antibody.
9. Incubate the mix for 15 minutes at room temperature.
10. Add BSA to 0.01–0.1% w/v.
11. Close the tube tightly and seal around with parafilm.

12. Incubate on a rotator to ensure constant movement of beads and buffer for 16-24 hours at room temperature.
13. Place the tube on the magnet for 1 minute, pipette the liquid out, take the tube out of the magnet.
14. Add 1ml of Buffer 2 and incubate on a rotator for 5 minutes.
15. Repeat steps 13 and 14 twice.
16. Suspend the labelled beads in 500µl Buffer 2.
17. Store sealed with parafilm at 4°C.

### **III. Magnetic bead sorting**

**Buffer 2:** Ca<sup>2+</sup> and Mg<sup>2+</sup> free phosphate buffered saline (PBS) supplemented with 0.1% bovine serum albumin (BSA) and 2 mM EDTA, pH 7.4. **Note:** BSA can be replaced by human serum albumin (HSA) or fetal calf serum (FCS). EDTA can be replaced by sodium citrate.

1. Prior to CD133 enrichment, cells should be cultured in SFM-N2 media for 48 hours.
2. Cells are detached from culture dishes by gentle rinsing (CD133 is sensitive to Trypsin-EDTA).
3. Transfer the cells to a conical tube, record the number of ml's the cells are suspended and vortex on medium for 2-3 seconds.
4. Take 50µl for cell count and spin the rest down for 5-8 minutes (depending on the volume) at 1000 rpm.
5. Count the cells in meantime and multiply the number of ml's the cells were collected in.
6. Discard the media and suspend the cells in Buffer 2 to obtain 2.5x 10<sup>6</sup> cells/ml.
7. Obtain the vial with labelled beads from the fridge.
8. The beads are settle at the bottom, pipette to resuspend starting from pipetting the liquid supernatant to the bead pellet.
9. Obtain 25µl of beads per every 2.5x 10<sup>6</sup> cells suspended in Buffer 2.
10. Add the beads to the cells in the buffer.

11. Close the tube tightly and transfer on ice to the rotator in 4 C cold room for 20 minute incubation.
12. Place the vial in the magnet for 2 minutes, pipette the liquid containing large portion of cells out- these are your CD133- cells. Place them in a conical tube, spin down for 5 minutes, 1000 rpm. Resuspend the pellet in SFM-N2 media and place in the ultra low attachment dish or in MaxGel™ coated plates.
13. Remove the vial from the magnet, add 1 ml of Buffer 2.
14. Place the vial in the magnet, incubate for 1 min.
15. Repeat steps 13. and 14. three times.
16. Suspend the beads with CD133+ cells in SFM-N2 and place in the ultra low attachment dish or in MaxGel™ coated plates.

#### **IV. Primary neural cell extraction**

Prior to tissue dissection the working area has to be sterilized and dissecting instruments have to be autoclaved.

1. Mice are humanely euthanized in CO<sub>2</sub> chamber or by Pentobarbital overdose.
2. The top of the head is shaved and swabbed with Betadine followed by 95% ethanol.
3. Make a midline incision in the skin along the full length of the skull.
4. Cut skin at both sides below ears to expose the skull.
5. Using scissors cut the skull at the sides and peel it off with forceps.
6. To cut the spinal cord, cranial nerves and blood vessels connected to the base of the brain, slide the forceps under the base of the brain.
7. With the same forceps transfer the brain to 60mm dish containing media with 3% P/S solution.
8. Slice the brain in the coronal fashion and under the dissecting microscope remove the area around the lateral ventricles.
9. Transfer the tissue to a separate dish with media with 3% P/S solution.
10. Using a scalpel blade no. 11 chop the tissue to 1mm<sup>3</sup> cubes.

11. Transfer the minced tissue to a round bottom 5ml polypropylene tube with a sterile Pasteur pipette.
12. Spin down for 1 minute at 250g to remove the P/S media.
13. Remove the supernatant and add 1 ml of Trypsin- 0.05% EDTA.
14. Place the tube in the 37°C water bath for 5-10 minutes.
15. Remove the tube and triturate tissue- Trypsin mix gently to disrupt the tissue particles.
16. If visible particle still remain, add 1ml of Trypsin- 0.5% EDTA and incubate in the 37°C water bath for additional 5-10 minutes.
16. Repeat the step 15.
17. Centrifuge for 5 minutes at 250g.
18. Remove the supernatant, add 2ml of media containing 10% FBS and incubate for 5 minutes.
19. Centrifuge for 5 minutes at 500g.
20. Remove the supernatant and add 2ml SFM-N2.
21. Repeat steps 19 and 20 and triturate to obtain single cell suspension.
22. Plate cells in the ultra low attachment plates at the density of  $5 \times 10^4$ .

## **V. Cell pair assay**

1. Circular, glass, non-coated, baked cover slips are placed in the wells of a 6-well plate.
2. MaxGel™ ECM (Sigma) is diluted in serum free media in the ratio 1:4, and kept chilled at all times.
3. Add 10ul of diluted MaxGel™ per each cover slip and spread using a pipette tip.
4. Place the plate containing now coated cover slips in the incubator 37°C, 5%CO<sub>2</sub> for 2 hours.
5. After the incubation, remove the excess of MaxGel™ and allow for the cover slips to dry for ½ hour under the laminar flow with the plate lid open.
6. In meantime, wash the cells required for the assay and detach them from their culture plate using Trypsin- 0.05-0.25% EDTA.



7. Count the cells and seed  $0.5-1 \times 10^3$  cells in a drop of media (SFM-N2) onto the dry, coated cover slips.
8. Every cover slip is inspected carefully for single cell suspension right after seeding as well as in 3 hours after.
9. The cells are incubated in a drop over night at  $37^{\circ}\text{C}$ ,  $5\% \text{CO}_2$ .
10. Depending on the population doubling time the cover slips should be examined for mitotic pairs.
11. Mitotic pairs on cover slips are fixed with 4% PFA for 15 minutes at room temperature.
12. The cover slips can be stored till stained at  $4^{\circ}\text{C}$  in 1% PFA/PBS (if staining for CD133, immunocytochemistry has to be performed right away without the fixation step).

## VITA AUCTORIS

NAME: Dorota Lubanska

PLACE OF BIRTH: Turek, Poland

YEAR OF BIRTH: 1981

EDUCATION: I High School. Cyprian Norwid, Bydgoszcz,  
Poland, 2000

Karol Marcinkowski Poznan University of  
Medical Sciences, M.Sc.,Poznan, Poland, 2006

University of Windsor, Ph.D., Windsor, ON,  
2013